Energy Storage Materials

Large-Scale Giant Architectonic Electrodes Designated with Complex Geometrics and Super Topographic Surfaces for Fully Cycled Dynamic LIB Modules

--Manuscript Draft--

Manuscript Number:	ENSM_2019_704R1
Article Type:	Research Paper
Section/Category:	Electrochemical energy storage
Keywords:	Super architectonics, capacity storage; super-surface topographies, anode/cathode; complex geometrics, lithium-ion batteries (LIBs); fully cycled dynamics; electric vehicles (EVs)
Corresponding Author:	Sherif A. El-Safty National Institute for Materials Science (NIMS) Tsukuba, Ibaraki JAPAN
First Author:	Hesham Khalifa
Order of Authors:	Hesham Khalifa
	Sherif A. El-Safty, Professor
	Mohamed A. Shenashen, Associate Professor
	Abdullah Reda
	Ahmed Elmarakbi, Prof.
Manuscript Region of Origin:	Asia Pacific
Abstract:	Abstract: Given exceptional specific discharge capacity, excellent energy density, high rate capability, fast charge capacity, and long-term cycling stability, large-scale giant porous complex super-architectonics (GPS) integrated into anode/cathode complex geometrics improve the full-model lithium ion batteries (LIBs). We examine the integration of a series of anode and cathode (GPS) super-architectonics into half- and full-cell LIB models to allow non-prescriptive charge/discharge cycles, and to achieve spatial rate performance capabilities. As a distinguishable GPS model, the super-architectonics included multi-directional orientation geometrics, building-blocks egress/ingress pathways, and giant loophole-on-surface topographies of ripples, irregular bumps, undulations, and anticlines offer a set of fully functional multi-axial/dimension GPS cathode- and anode-electrode geometrics and multi-gate-in-transports of electron/Li+ ions in diverse pathways. Our precisely defined GPS-modulated LIB models generate high-power and volumetric-energy density, excellent long-term cycling durability without deterioration in its capacity under a high energy density, and a comparable high tap density. GPS-integrated LIB modules provide superior durability (i.e., maintaining high specific capacity ~77.5% within long-term life period of 2000 cycles) and average Coulombic efficacy of ~99.6% at 1 C. Powerful and robust super-architectonic GPS building-blocks-in full-scale LIB designs offer outstanding specific energy density of ≈179 Wh kg–1 for a future market of LIB-EVs with longest driving range. The key leap super-surface topographies of LIB-GPS modules are critical in creating ever-changing charge/discharge cycles, “fully cycled dynamics,” affordable on-/off-site storage, and super-large door-in transport of Li+-ion/electron, thereby highlighting its promising storage modules and rechargeable lithium batteries.
Suggested Reviewers:	Madhavi Srinivasan Madhavi@ntu.edu.sg
	Jaephil Cho jpcho@unist.ac.kr
Opposed Reviewers:	
Response to Reviewers:	Manuscript Number: ENSM_2019_704 Large-Scale Giant Architectonic Mesosponginess and Complex Superstructures

Integrated Anode/Cathode Full-Scale LIBs

Reviewer #1:
This work developed a giant porous complex superstructures as a concept, to integrate LMPO and TiO2 as cathode and anode for LIBs. The work is interesting, while the novelty and battery performance is not very well presented. please carefully consider the following comments:
Q1.What is the determined step that forms the "GPS" structure, in both anode and cathode?
A1. We thank the reviewer for this valuable comment.
Per of the reviewer comment, intensive discussion related to the "GPS" structure has been carried out in the experimental part, and results and discussion part, Please see additional information in blue font as follows:
(a)New section has been added to Results and Discussion part including:
•Control synthesis of complex super-architectonics (GPS) cathode-/anode-geometrics (Please see pages 12- 14)
(b)New sections have been added to experimental part including:
•Configuration of super-architectonics-integrated GPS-LIB CR2032 coin-cell models and pouch-type modules (Please see pages 8, and 9)
•Architectonic anode/cathode GPS-LIB CR2032 coin-cell models (Please see pages 9-11), and
•Architectonics-integrated into bundled layer-by-layer pouch and 18650-cylindrical GPS-LIB-types (Please see pags 11, and 12)
Q2.More detailed information should be provided in the experiment, for example the loading of active materials, the tap-density of the active materials, the areal density of active materials on the electrodes on both anode and cathode, for both half-cell and full-cells. Because these are very important parameters for the overall performance of the batteries. Moreover, these should be carefully compared with the industrial standard.
A2- We thank the reviewer for his constructive comment. Per of these valuable notes, experimental and sets are carefully revised as can be seen in the supporting information and the entire manuscript. Please see this modification and additive to the following part of experimental section and supporting information as follows:
(a) New sections have been added to experimental part including:
•Configuration of super-architectonics-integrated GPS-LIB CR2032 coin-cell models and pouch-type modules (Please see pages 8, and 9)
•Architectonic anode/cathode GPS-LIB CR2032 coin-cell models (Please see pages 9-11), and
•Architectonics-integrated into bundled layer-by-layer pouch and 18650-cylindrical GPS-LIB-types (Please see pags 11, and 12)
(b) New sections have been added to supporting information part including:
•S1-C- GPS super architectonics built-in 2032 coin-cell LIBs (Please see pages S5)
•S1-D. The mass fraction analysis of GPS super architectonic cell components (Please see page S5 and S6)
•S11. Super architectonic specific energy density of GPS-modulated full-scale LIB-model (Please see pages S 21-S23)
•S12. Optimization of full cell based (N/P)Cap balancing capacity ratio (Please see page S24)
•S13. The mass loading, areal capacity density and N/P capacity-ratio of GPS-MSTO@C//LMPO@C anode//cathode full-scale pouch LIB-model (Please see page S25)
•S15. A comparison between the GPS-SSF@C half-scale LIB and the other reported LiMnPO4 cathodes (Please see page S 27)
• S16. A comparison between the GPS-MSTO@C half-scale LIB and the other reported TiO2 anodes(Please see page S 28)
•S17. A comparison between the GPS-SSF@C//MSTO@C full-cell LIB electrode system and the other reported LiMnPO4//TiO2 full cells (Please see page S 29)
•S 18. Tap density of the LiMnPO4@C cathode (Please see page S 30)

S1-C- GPS super architectonics built-in 2032 coin-cell LIBs
GPS super architectonic half-scale anode or cathode LIBs are explored by using CR2032-coin cells. For precision accuracy and possible control of electrochemical experiments, the designated GPS super architectonics built-in MSTO@C-anode and SSF@C-cathode half-cell and MSTO@C//SSF@C anode//cathode full-cell LIBs are

arranged and oriented in CR2032-coin cells under specific protocols (see supporting information, Figure S1).
Moreover, the configuration of stacked-layers-in pouch LIBs-type along full-scale ordered sets of GPS super architectonic MSTO@C//SSF@C anode//cathode geometrics is the key broadening of the design LIB-modules, as shown in supporting information S1-D, Fig.S11..

On the base of the experimental sets of GPS super architectonic MSTO@C GPS-anode//SSF@C GPS-cathode pouch LIB-model, the optimized loading amount (mass/coverage area, mg/cm2) is of 13.3 and 7.14 mg/cm2 for SSF@C GPS-cathode and MSTO@C GPS-anode geometrics, respectively. Accordingly, the areal discharge capacities of SSF@C P-cathode and MSTO@C N-anode electrodes are 0.85 Ah/cm2 and 0.89 Ah/cm2, respectively. The similarity in the areal discharge capacity' value (in Ah) of P-cathode and N-anode electrodes indicates that the finest mass (N:P)Cap balancing capacity ratio is 1.05:1. The significant control of (N:P)Cap ratio is mainly dependent of the optimal tradeoff LIB manufacturing rapports between (i) the safety betterment (i.e., at which the increase of loading mass of N-electrode to offer (N:P)Cap ratio of >1 :1 is essential), and (ii) the specific energy density (at which rational mass balancing (N:P)Cap ratio is of 1:1).

S1-D. The mass fraction analysis of GPS super architectonic cell components
The mass fraction analysis of individual cell components in the pouch full-cell model can be seen in schematic diagram as seen in Fig. (S2). The GPS super architectonic working electrodes are prepared by mixing each active material of GPS-TO@C anode composite and GPS-LMPO@C cathode materials with carbon black, and polyvinylidene fluoride (PVDF) as a binder in a weight ratio of 80:15:5. Based on the mass fraction of a cathode material in a GPS super architectonic sets of bundled layer-by-layer pouch models is approximately 44%, leading to determine of the specific energy density for the GPS-LMPO@C//TO@C full-scale LIB, which is practically equal to 178.8 Wh kg-1 (see supporting information S13- B).

Fig. S2 Schematic diagram of mass fraction of individual components used in the GPS super architectonic pouch model

S11. Super architectonic specific energy density of GPS-modulated full-scale LIB-model
The calculation and quantification methods for specific energy density of GPS-(MSTO@C N-anode// GPS-LMPO@C P-cathode full-scale LIBs are carried out based on the expected theoretical model and real experiment sets of the super-architectonic contents of the LMPO@C and MSTO@C P-cathode and N-anode electrodes-modulated into full-scale LIBs. Here, we provide intensive studies based on the theoretical and practical or experimental models as follows:
A- Theoretical calculation of GPS specific energy density:
In the designed integrated super-architectonic built into the GPS-full-scale LIB, the nominal open circuit voltage (VOC) along P-cathode and N-anode electrodes-modulated CR2032 coin cells can be detected according to the equations:
VOC = V+ - V-
VOC = 4.1 V – 1.76 V =2.34 V,
Where V+ represents the potential of half-cell of GPS-LMPO@C P-electrode that equalized to 4.1 V, and V- is the potential of GPS-MSTO@C N-electrode that equalized to 1.76 V.
Faraday's law is used to calculate the theoretical specific cell capacity of a cell in mAhg−1.
Qtheoretical = (nF) / (3600*Mw)
Where, F is the Faraday constant, n is the number of charge carrier, and Mw is the molecular weight of the architect materials electrode surfaces. The Qtheoretical for GPS-LMPO cathode-base electrode is found to be 171 mAh g-1. Where, Mw of GPS-LMPO is 156.85 g mol-1, n=1 and Li+=1. F=96 485.3329 sA mol-1. In addition, Qtheoretical for common-used anodic electrode is as follows: nano-sized TiO2= 335 mAh/g [Ref-S1- Ref-S3].

S11- A- (i) The contribution of each component of LMPO@C and MSTO@C super-architectonics built-in full cell specific capacity:

According to TG and EDS analyses, the relative composition contents of in cathode- and anode-based GPS super-architectonics are determined. The obtained results indicated the carbon content to be ~ 4.3 wt % in the LMPO@C compositions.
-Therefore, the theoretical specific capacity of LMPO@C P-electrode can be calculated as follows: ~ (335 mAh/g * 0.043 + 171 mAh/g * 0.9996) ~ 185.33 mAh/g.

S11- A- (ii) N-, and P-electrode cell capacity balancing
In fact, a significant effect of the N/P ratio on the electrochemical response is an important factor in full cell efficiency. The lithium plating during charging is firmly attached to N/P ratio. The lithium coating causes irreversibility and is assembled during cycling, ultimately reducing the loss of capacity, mechanical swelling and possibly a short inner circuit. To avoid the danger of metallic lithium plating, this is considered as retrospective aging process and safety, one should control the mass balancing capacity ratio of P- or N-electrode materials. The cell capacity is controlled by the key value of specific capacity of each of the P- or N-electrode materials presented in the LIB full cell [Ref-S4 -Ref. S6]. In this study, in order to reconcile these two contrast options, the LIB-Model is designed to extend 3D super-scalable full-scale GPS-LMPO@C//MSTO@C cathode//anode stacked layers pouch LIB-model under optimized mass loading and ((N:P)Cap capacity ratio ≈ 1.02 – 1.1 :1.
-Assuming an ideal N / P ratio for positive and negative electrode materials in a manner commensurate with its conceptual strength, the ideal capacity ratio for the full scale model (GPS-LMPO@C//MSTO@C) is as follows: 171 Ah kg−1/335 Ah kg−1 = 0.51
-Based on the calculation, for an ideal battery with 171 Ah of capacity, 1 kg of LiMnPO4@C and 0.51 kg MSTO@C are required for design.
-The combined mass fraction of both P- and N-electrodes in the practical pouch LIB cell key-component constitutes (i.e., conductive electrolyte, polymeric membrane separator, current electrodes and package cortices, see Figures S1, is 34%, leading to that the full scale GPS-LIB with a specific capacity of ((171 Ah)/(1 kg+0.51 kg))/1.34 is about 84.5 Ah .kg-1.
The theoretical mode of calculated specific energy of GPS-LMPO@C//MSTO@C battery can be quantified as equal to (2.34 V *84.5 Ah kg-1)= 197.7 Wh kg-1.

S11- B - Practical method-based experimental sets of super-architectonics built-in LIBs
In galvanostatic cycling test (i.e., only at constant current), the graphically specific energy of super-architectonic built into the GPS-full-scale LIB can be detected from the charge–discharge voltage-capacity profile at 1C as follows:
-The specific energy for the GPS-LMPO@ C cathode (Wh/kg) is = the average working voltage of the super-architectonics built-in LIBs in (V) x maximum discharge capacity delivered by cell (Ahkg-1).
-The specific capacity delivered by cell (Ahkg-1) at 1C = 156.3 Ahkg-1.
-The specific energy for the GPS-cathode (Wh/kg) = 2.6 V x 156.3 Ahkg-1 =406.4 Wh/kg.
-Thus, the specific energy density of full-cell super-architectonic built into the GPS-full-scale LIB (Whkg-1) = the estimated mass fraction of a cathode active material in a LIB cell (in pouch-type, mass fraction is 44% (see S1)) x Specific Energy for the cathode (Whkg-1).

-Therefore, practical value of the specific energy density of the GPS-LMPO@C//MSTO@C full-scale LIB is 178.8 Whkg-1.

S11-C- Key difference between experimental and theoretical calculations of specific energy density of full-scale GPS-LIBs
For both the intensive determination of specific energy density for the super-architectonic built into the GPS-full-scale LIB, the practical and theoretical values are of 178.8 Whkg-1 (practically) and 197.7 Whkg-1 (theoretically), respectively. The low value of specific energy density in a practical determination may attributed to
(i)the Li+-ions can’t be completely removed from the N-electrode and P-electrode surface topographies, and
(ii) non-usable cutoff voltage profiles to clean-up N-electrode and P-electrode surface topographies to remove the rest Li+ ion on the interlay complex super-architectonics, constraining the perfect charge-discharge rate.
The proposed GPS-MSTO@C//LMPO@C full-scale battery system integrates the latest advances in Li-battery technology to create a battery that delivers outstanding

electrochemical performance.

S12. Optimization of full cell based (N/P)Cap balancing capacity ratio
As we mentioned before, The (N/P)Cap ratio of positive and negative electrode materials has significant effect on the efficiency of the full cell, as the formation of lithium plating/deposition along anode surfaces during a charging procedure firmly related to N/P ratio. As a side reaction, the lithium plating caused at anode N-electrode lead to the irreversible capacity. The accumulation of undesirable anode Li deposition during multiple cycles of charge-discharge voltage profiles leads to mechanical swelling, and possibly internal short-circuit along the anode surfaces. The electro-deposition during charging would intensively lead to capacity loss, and short-life cycle of LIBs. In this regards, to avoid the adverse effect of lithium metal plating, a slight oversizing of the mass loading capacity of anode ((N:P)Cap capacity balancing ratio ≈1.02–1.1: 1) is furthermore required for both battery safety and life-cycle [Ref-S5-S8]. Thus, an optimal tradeoff relationship between both key parameters is required as follows:
(i)safety betterment (i.e., which can be achieved by increasing the mass of N-electrode with (N:P)Cap ratio of >1:1), and
(ii)high specific energy storage (i.e., which can be achieved at equal capacities of N- and P-electrode, (N:P)Cap ratio of 1:1).
The current design configuration of the proposed GPS-MSTO@C (anode) // LMPO@-C (cathode) sets into bundled layer-by-layer pouch models under optimized (N:P)Cap ratio of ≈ 1.05 – 1.1 :1.
S13. The mass loading, areal capacity density and N/P capacity-ratio of GPS-MSTO@C//LMPO@C anode//cathode full-scale pouch LIB-model
Full-scale GPS-TO@C//LMPO@C sets of bundled layer-by-layer pouch models has dimensions of 35 mm (width), 55 mm (length) and ~ 3mm (thickness) and the stacking sequence of electrodes can be seen in following configuration
SS cathode | [DS anode| DS cathode|] DS anode | SS cathode
where SS=single side, DS = double sided, | = separator and [] = repeatable unit
The weight fraction calculation for sets of bundled layer-by-layer pouch model components were explained (Figure S2), and the required active mass of the GPS-LMPO@C-cathode and GPS-MSTO@C-anode are 2.79 g and 1.43 g respectively. In this large-scale design, well-packed and dense GPS-MSTO@C-anode (8-layers/14-sides, loaded on Cu-foil (8μm))// GPS-LMPO@C-cathode (7-layers/14-sides, loaded on Al-foil (12μm)) coin cells are contiguously connected into a series of the built-in stack layer configuration of pouch LIB-types. These designable optimizations may provide a compact LIB coin-cell module in pouch modes with a permanent flexible transport of electron/Li+ ion during lithiation and delithiation cycling. The optimal electrode features in the super-architectonics built-in full-cell LIBs can be summarized as follows:
•The area for cathode and anode is selected with the following dimensions of (3*5=15 cm2) and (3*4.75 = 14.3 cm2), respectively.
•The total area of the cathode and anode coverage the pouch LIB cells are 210 and 200 cm2; respectively.
•The mass stacking is 13.3 and 7.14 mg/cm2 for cathode and anode, respectively.
•The areal discharge capacities are 0.85 Ah/cm2 and 0.89 Ah/cm2, of cathode and anode electrodes, respectively.
•The areal discharge capacity of N- and P-electrodes is determined at specific (N:P)Cap capacity ratio of 1.05:1.

S15. A comparison between the GPS-SSF@C half-scale LIB and the other reported LiMnPO4 cathodes
To show evidence of the effectiveness of the super-architectonic GPS-LMPO@C and GPS-MSTO@C anode geometrics, building-blocks-in a wide-range of egress/ingress

egress/ingress hierarchy, and super topographic-surface heterogeneity, roughness and anisotropy on the GPS-designated LIBs, we offer intensive studies of the key parameters in terms of rate capability, Coulombic efficiency, reversible capacity and long-term cycle stability of our GPS LIBs and other reported LIB designs, as one can see in Table S1-S3.

Table S1 A comparison between the GPS-LMPO (with SSF@C geometrics) half-scale LIB and normal and conventional LMPO cathode-LIBs

Cathode material	Nominal Voltage (V)	Cycles	Specific Capacity mA h g-1	Coulombic efficiency	Ref
LiMnPO4@C	4.1	retained ~100% of its reversible capacity after 100 cycles	155	At 0.5C	Not mentioned21
LiMnPO4@C	4.1	capacity retained 120 mAhg-1 after 50 cycles	153.4 at 0.1C	Not mentioned	37
LiMnPO4@C	4.1	capacity retained 89.1 mAhg-1 after 500 cycles	147.9 at 1C	Not mentioned	Ref-10
LiMnPO4	4.1	capacity retained 125 mAhg-1 after 30 cycles	133 at 0.1 C	Not mentioned	17
LiMnPO4@C (GPS-SSF@C)	4.1	Retains ~100% after 100 cycles	133 at 1C	~100%	Current Work

S16. A comparison between the GPS-MSTO@C half-scale LIB and the other reported TiO2 anodes

Table S2 A comparison between the GPS-MSTO@C half-scale LIB and the other reported TiO2 anodes.

Anode material	Nominal Voltage (V)	Cycles	Specific Capacity mA h g-1	Coulombic efficiency	Ref
Rutile TiO2	1.7	retained 50% of its reversible capacity after 100 cycles	250	At 0.1C~ 100% after 100 cycles	Ref [S11]
Rutile TiO2	1.5	retained 77% of its reversible capacity after 40 cycles	223 at 0.1C	Not mentioned after 100 cycles	Ref [S12]
Anatase TiO2	1.73	76% of its initial capacity after 30 cycles at 0.2C~ 300	Not mentioned		Ref [S13]
P25, a commercial titania powder from Degussa	1.76	1% of its initial capacity after 30 cycles at 0.2C	95	Not mentioned	Ref [S13, S14]
TiO2	1.74	70% of its initial capacity after 100 cycles at 0.2C	270	Not mentioned	Ref [S15]
TiO2	0.85	5% of its initial capacity after 30 cycles	310~100%		Ref [S16]
TiO2@C (GPS-MSTO@C)	1.78	7% of its initial capacity after 100 cycles at 1C	231	Not mentioned	Current Work

S17. A comparison between the GPS-SSF@C//MSTO@C full-cell LIB electrode system and the other reported LiMnPO4//TiO2 full cells

Table S3 A comparison between the GPS-SSF@C//MSTO@C full-cell LIB electrode system and the other reported LiFePO4//TiO2 and LiMnPO4//TiO2 full cells.

Cathode material	Anode material	Nominal Voltage (V)	Cycles	Specific Capacity mA h g-1	Coulombic efficiency	Ref
LiFePO4	Anatase TiO2 hollow nanofibers	1.4	retained 88% of its reversible capacity after 300 cycles	103	> 99 %	Ref [S17]
LiFePO4	Rutile TiO2	1.8	retained 50% of its reversible capacity after 40 cycles	150	Not mentioned	Ref [S18]
LiFePO4	Anatase TiO2	1.68	1% of its initial capacity after 300 cycles at 20C	160	Not mentioned	Ref [S19]
LiFePO4	anatase/graphene	1.67	00127~ 100%			Ref [S20]
LiFePO4	spinel Li4Ti5O12/C	1.8	Retain 98.1% after 400 cycles	167	~100%	Ref [S21]
LiFePO4	spinel Li4Ti5O12	1.65	Retain 98.9% after 100 cycles	150	~100%	Ref [S22]
LiMnPO4	Li4Ti5O12	2.5	Retain ~100% after 300 cycles at C/2	105	~100%	Ref [S23]
LiMnPO4@C (GPS-SSF@C)	TiO2@C (GPS-MSTO@C)	2.6	Retains 77.5% after 2000 cycles at 1C	156.3	~100%	Current Work

S 18. Tap density of the super-architectonic GPS-LiMnPO4@C cathode geometrics
Due to the increasing demand and the urgent need of the LIBs in the field of consumer electronics and EVs, an important characteristic is the tap density being exploited. The tap density was mainly influenced by the material morphology, particle size and the distribution of powder particles. Design of spherical particles was used to increase the tap-density. Developing new LMPO structures with both high rate performance and high tap density is challenging and appealing for the preparation of cathode materials [Ref-S24, Ref-S25].
To calculate the tap density of GPS-LMPO@C modulated LIBs, we used ZS-102 tap density meter (Liaoning Institute of Research Tools Co., Ltd.) to measure the tap density of the super-architectonics built-in LIB models. In such super-architectonic LIB models or modules, the optimal carbon content should not be more than 5%. The carbon content of SSF@C composites is found in the optimal range of about 4% (lower than 5%) [Ref-S26].
A powerful tool to develop the super architectonic engineering design of GPS-MSTO@C anodic and GPS-LMPO@C of geometric-SSF@C, -CSN@C and -NR@C cathode electrodes can be achieved by a rational mass-loading control. The high-density GPS SSF@C super-architectonics modulated LIBs shows excellent high rate performance, a high tap density (~1.51 g cm-3) compared to 1.24 and 1.02 g cm-3 of GPS-CSN@C, and GPS-NR@C cathode geometrics, respectively. The finding indicates the effect of GPS complex super-architectonic SSF@C in its excellent electrochemical performance, particularly during the Li+-insertion (cathodic, reduction, lithiation) /extraction (anodic, oxidation, delithiation) processes. Together, the GPS-SSF@C super-architectonics can be a potential candidate for high-performance LIBs.

Q3.From Fig. 7, the capacity of anode is almost double of the cathode in the full-cell configuration, isn't it a "waste" for the whole cell and decreasing the energy density?
A3- We thank the reviewer for this comment. Per of your comment and avoid of any waste or decrease of the full cell energy density due to cell configuration, the key design configuration of built-in ordered set of full-scale super architectonic complexity GPS-SSF@C//MSTO@C cathode//anode hierarchy giant mesosponginess building blocks are fabricated in stacked layers pouch LIBs-type based on balancing between anode and cathode capacities under optimized mass loading (balancing N/P ratio), leading to contiguous charge/discharge rate, and a high energy density overcomes the energy-density limit required in the EV driving range. Please see this modification and additive to the following part of Results and discussion section, and supporting information as follows:
(a) New parts have been added to results and discussion part including:
•GPS cathode- and anode-electrode-geometrics-integrated full-scale LIBs (Please see pages 27- 33)
(b) New sections have been added to supporting information part including:
•S12. Optimization of full cell based (N/P)Cap balancing capacity ratio (Please see page S24)
•S13. The mass loading, areal capacity density and N/P capacity-ratio of GPS-MSTO@C//LMPO@C anode//cathode full-scale pouch LIB-model (Please see page S25)

In Results and Discussion:
GPS cathode- and anode-electrode-geometrics-integrated full-scale LIBs
We designed fully functional multi-axial/dimension GPS cathode- and anode-electrode geometrics into the precisely defined full-cell LIB pattern model. In GPS-modulated LIB designs, we used MSTO@C GPS anode//SSF@C GPS cathode as the preferred N-electrode and P-electrode surface topographies, respectively (Fig. 7 and Scheme 3). The GPS complex architectonic SSF@C-cathode//MSTO@C-anode LIB surface topographies are specified into CR2032 coin-cell types (see supporting information S1). This GPS full-cell LIB design sheds light on the key influences of vast super architectonic complexity, geometrics, vacancies and surface topographies on the sets of bundled layer-by-layer pouch models and on large-scale LIB module configurations. These key factors of super-architectonic GPS-modulated LIB significantly affect the non-prescriptive cycle usages, heavily interior Li+ ion loads, spatial rate performance capabilities, specific energy density and high Coulombic efficiency. To approve our engineering perspective of proposed GPS- SSF@C// GPS-MSTO@C full scale LIBs, we offer comprehensive comparison studies between the GPS-modulated-LIB and

other designated LiFePO4//TiO2 and LiMnPO4//TiO2 LIB cells that previously reported, (see supporting information S17).
To calculate the super-architectonic GPS cell-energy density of full-scale LIB modules, the bundled layers of MSTO@C GPS anode//SSF@C GPS cathode electrodes are specified in pouch-LIB-model (see supporting information S14). The multiple bundled layers of incorporated amounts of GPS-MSTO@C (N-electrode anode) // GPS-SSF@C (P-electrode cathode) are 8-//7- layers, and along 14 surface topographic sides. These 8-anode//7-cathode surface topographic layers are substantially decorated with the 8 μm-Cu-foil and 12 μm-Al-foil platform electrodes, respectively. The GPS average working potential of GPS-MSTO@C (N-electrode anode) // GPS-SSF@C (P-electrode cathode) full-scale battery is 3.8 V, enabling highly practical specific energy-density of 178.8 Whkg-1, in agreement to theoretical value of 197.7 Whkg-1 for a full-scale GPS-LMPO@C//MSTO@C battery, (see more details studies of supporting information S11 A, B and C). The slight decrease of the practical energy density compared with its theoretical value of GPS-MSTO@C (N-electrode anode) // GPS-SSF@C (P-electrode cathode) full-scale LIB may be due to the difficulty to remove Li+ ions completely during the fully-dynamic extraction. The full delithiation process of the occupant/truck Li+ ion loads from the interfacial-scale of fully-accessed pocket storage requires cutoff voltage >3.0V.
Aiming to explore the safety and large timescale LIB-EV driving ranges with high power density, a model of full-scale GPS-MSTO@C (N-electrode anode) // GPS-SSF@C (P-electrode cathode) pouch LIBs is fabricated under optimization control of the mass-loading of N-anode and P-cathode electrodes and their ratio of capacity (i.e., balancing capacity of (N/P)Cap ratio). A set of full experiments is carried out for controlling a pouch model with optimal (N/P)Cap ratio, which leads to outstanding trade–off performance variability (see supporting information S12 - S14, and experimental section). Accordingly, the optimal accuracy of the mass-fraction of SSF@C GPS cathode components formulated in a pouch LIB model is about 44%, leading to specific energy density of the GPS-TO@C//LMPO@C full-scale LIB of 178.8 Whkg-1.
For reliable structural design of large scale LIB modules, the volumetric energy density is ideal parameter of LIB engineering perspective (see supporting S14). The structural GPS-building-blocks-in 18650-cylinder and bundled-layers of pouch models offer volumetric energy density of MSTO@C GPS-anode//LMPO@C GPS-cathode full-scale CR2032 LIB-module of 435.63 Wh/L and 247.68 Wh/L, respectively. Although, the GPS-modulated 18650-cylinders produce highly recognizable value, the bundled layer-by-layer pouch models represent the practical and optimal engineering designs for a wide range of electrochemical performances.
The mutual balancing capacity of (N/P)Cap ratio of super-architectonic GPS-MSTO@C (N-electrode anode) // GPS-SSF@C (P-electrode cathode) LIB-modules offers areal discharge capacity of 0.89 and 0.85 Ah/cm2, respectively. The optimization of areal discharge capacity performance super-architectonic built-in pouch LIB models would be a more rational choice for the most effective solutions in terms of high specific energy density yet with large safety factors of the proposed super-architectonic GPS-built-in pouch LIB models. Such super-architectonic GPS-built-in LIBs are promising to enhance betterment of safety factor issues for GPS-LIB-powered engineering modules.
The stability of the super-architectonic built-in SSF@C GPS-cathode // MSTO@C GPS-anode full-scale geometric and surface topographic LIB models is investigated by studying its discharge cycle performance as shown in Fig. 7(a). The architectonic GPS-modulated-LIB model retains 90.0 % of its first cycle discharge capacity after 100 cycles at 1 C. Figure 7(a) shows the typical first cycle of charging/discharging voltage patterns of full-scale GPS-modulated-LIB model cycles at C-rate range from 0.1 C to 20 C by applying a voltage range from 1.5V to 3.8V. The results reveal that the values of super-architectonic GPS-modulated LIB discharging capacities decrease with C-rate upsurge (i.e., from 0.1 to 20 C). The super-architectonic GPS-modulated LIB full-cell is maintained the discharge capacity of 108.3 mAhg–1 at 20 C for its initial performance value.
The super-architectonic GPS-modulated LIB capability rates are investigated at the voltage range from 1.5 to 3.8 V and the C-rate range from 0.1 C – to 5 C, then back to C-rate of 0.1 C and 10 C, and finally back to 1 C and 20 C, with continuous operation of cycling variation up to 100 cycles at each recorded C-rate (Figure 7c). The super-architectonic specific capacity of the full-cell SSF@C GPS-cathode//MSTO@C GPS-anode geometrics and surface topographies is decreased with an increase in the current rate. Feasible discharge capacity of a multiple cycles and C-rates indicates the

superstructure effect on the overall scales of GPS-modulated-LIBs. The complex super-architectonics of SSF@C GPS-cathode // MSTO@C GPS-anode full-scale models or modules create ever-changing charge/discharge contributory usage of cycles, “fully cycled dynamics,” affordable on-off-site storage modules, and super-large gate-in-transport of electron/Li+-ion trails. Our finding indicates that the GPS P-cathode/N-anode electrodes integrated into full-scale CR2032 coin-cells are potential candidates to achieve the high power energy modules for LIB-EVs.

Fig. 7& Scheme 3

Super-architectonic GPS Coulombic efficacy (CE) of full-scale SSF@C GPS-cathode // MSTO@C GPS-anode models describes the charge efficiency, by which Li+ ions/electrons are transferred into powerful GPS multiple orientations and super-surface topographies of our distinguishable super-architectonic batteries. CE is the effective ratio between the total values of extracted and inserted charging from the distinct super-architectonic GPS-battery over one-full-cycle. For developing a scalar optimization perspective of GPS-modulated LIB-EVs, we investigate a fast-charging pattern of architectonic bundled-layers of GPS-MSTO@C (N-electrode anode) // GPS-SSF@C (P-electrode cathode) pouch models by applying constant current and voltage (named as CC-CV) protocol. A set of fast-charging experiments is recorded for GPS-modulated-LIB pouch models at different C-rate values, ranging from 1C to 10C, and temperature between 25oC to 35oC (see supporting information S19 & Figure S13). The CC-charging timescale decays with an increase of the charging rate in the applying range from 1C to 5C. The CC-charging timescale dependent sets at C-rate > 5C are not recognizable conditions. Therefore, the CV-charging timescale dependent sets are efficient, reliable, and quantifiable at the range of C-rate variabilities (see Fig. S13). The formation of long, stable static-flat plateau of CV-charging timescale (i.e. approximately 10 to 12 minutes) at C-rate > 5C is recognizable with a contribution of the surface-elevated temperature at 35oC as a maximal value. The fast CV-charging timescale ≥ 5 minutes can be optimized at C-rate range of from 1C to 4C, respectively. Under an ever-increasing demand on reliable and fast time-scale charge capacity, the super-architectonic GPS-MSTO@C (N-electrode anode) // GPS-SSF@C (P-electrode cathode) pouch models and modules are powerful in Li+ ion diffusion regimes, and improving hovering electron density for high-speed discharging and charging rates. The multi-criteria optimization of outstanding cycle performance, long-term stability, and Coulombic efficacy of full-scale super-architectonic GPS-MSTO@C (N-electrode anode) // GPS-SSF@C (P-electrode cathode) models and modules is studied at C-rate of 1C within 2000 cycles between 1.5V and 3.8 V vs. Li/Li+ (Fig. 7d). Note, the magnification of the first 200 cycles of the charging/discharging performance is recorded in Figure 7e. The super-architectonic GPS-modulated LIB model retains 77.5% specific discharging capacity from its original value of 156.3 mAhg–1 after 2000 cycles, and Coulombic efficacy of approximately 99.6% at C-rate of 1C, and at 25oC. For a wide range of charging/discharging cycles (i.e., >2000 cycles), the super-architectonic full-scale GPS-modulated LIB model is attained approximately 100% of its Coulombic efficacy. In general, the complex super-architectonic full-scale GPS-modulated LIB models demonstrate an outstanding structural design stability, high specific charging/discharging capacity, high rate capability, high-speed discharging and charging rates and long cycle life (see Scheme 3 and Figure 7).

Scheme 3A shows the simulated 3D projection of robust full-scale design optimization of GPS SSF@C GPS-cathode // MSTO@C GPS-anode full-scale architectonics after discharge capacity cycles. The systematic projection represents the powerful structural stability of super-architectonic GPS-building-blocks-in a wide-range of 3D distinguishable orientation geometrics, egress/ingress vacancy models, and super topographic-surfaces after a number of charging/discharging cycles (i.e.≥ 2000) (Scheme 3B). The super-architectonic SSF@C GPS-cathode // MSTO@C GPS-anode platform electrodes provide built-in full-cell GPS-integrated LIBs with four key features.

First, multi-dimensional electron/Li+-ion mobility is occurred as a result of including many GPS-building-blocks-in egress/ingress pathways along the upper, middle, and lower multi-zone crystal surface geometrics, as well as along the frontal edge/apex/central crystal sites. For instance, the SSF@C GPS-cathode with a top-upper square-based pyramid structure offers four-facet exposure surfaces that enable the diffusion of electrons/Li ions along the central site crystals, multi-edges, vertices, kinks, steps, and upper-top-zone surfaces (Scheme 3B).

Second, GPS-heavily interior loads, movements and diffusions of Li+ ion along the axial directions and axis of coordinates (i.e. lateral, vertical, circular, zigzag, and longitudinal axes) ensured the mobility of electrons/Li+ ions along the peripheral top

electrode surfaces.

Third, the super-architectonic diffusion gates into the interlaid-complex vacancies, such as caves, holes, nests, windows, canals, ridges, cavities, and pipes may create GPS-modulated LIBs with superb specific capacities, high energy density, high-speed discharging/discharging rates, and extended long-term power stability.

Fourth, the loophole-on-surfaces with different topographies and curvatures including ripples, winglets, protuberances, irregular bumps, V-hooks, undulations, and anticlines are key roles in retaining LIBs, ensuring the continuous function and stability of electron/Li+-ion transport pathways after 2000 cycles, and assuring the simultaneous diffusion of Li+-ions during the lithiation/delithiation (discharging/charging) cycling processes for SSF@C GPS-cathode // MSTO@C GPS-anode full-scale architectonics.

The super-architectonic built-in SSF@C GPS-cathode // MSTO@C GPS-anode full-scale LIB model shows its excellent Li+-ion egress/ingress capacity with high rate velocity, on-/off-site storage modules, and super-large door-in transport of Li+-ion/electron during discharging (insertion, lithiation) and charging (delithiation, extraction) processes. Furthermore, the super-architectonic GPS proximity of Li+ ion accessible loophole-on-surfaces and open-gate-in-transports is one of the most effective solutions to avoid geometric and surface topographic polarization and to boost the fully-cycled dynamics during discharge (insertion, lithiation) / charge (delithiation, extraction) processes. These GPS tectonic-power-driven SSF@C GPS-cathode // MSTO@C GPS-anode geometrics offer highly reversible capacity rate of LIBs, and structural stability to withstand under high-temperature environments.

Fig. 7(a) Cycling performance of powerful complex super-architectonic full-scale SSF@C GPS-cathode // MSTO@C GPS-anode LIB-modulated LIB models for first 100 cycles. (b) Behavior of specific discharge capacity in mAhg-1 versus current C-rates at 0.1C, 0.2C, 0.5C, 1C, 2C, 5C, 10C and 20C, in potential region from 1.5 to 3.8V vs. Li/Li+ for SSF@C//MSTO@C full-scale LIB-model. (c) Performance and behavior of the rate capability of SSF@C GPS-cathode // MSTO@C GPS-anode LIB-modulated LIB models over a range from 1.5 to 3.8V at various current rates from 0.1C to 20C. (d) Long term cycling performance (stability) and coulombic efficacy for SSF@C GPS-cathode // MSTO@C GPS-anode LIB-modulated LIB models, at rate of 1C up to 2000 cycles, in a voltage range from 1.5 to 3.8V at 25oC. The magnification of first 200 cycles is exhibited in Fig. 7(e).

In Supporting Information:

S12. Optimization of full cell based (N/P)Cap balancing capacity ratio

As we mentioned before, The (N/P)Cap ratio of positive and negative electrode materials has significant effect on the efficiency of the full cell, as the formation of lithium plating/deposition along anode surfaces during a charging procedure firmly related to N/P ratio. As a side reaction, the lithium plating caused at anode N-electrode lead to the irreversible capacity. The accumulation of undesirable anode Li deposition during multiple cycles of charge-discharge voltage profiles leads to mechanical swelling, and possibly internal short-circuit along the anode surfaces. The electro-deposition during charging would intensively lead to capacity loss, and short-life cycle of LIBs. In this regards, to avoid the adverse effect of lithium metal plating, a slight oversizing of the mass loading capacity of anode ((N:P)Cap capacity balancing ratio ≈1.02–1.1: 1) is furthermore required for both battery safety and life-cycle [Ref-S5-S8]. Thus, an optimal tradeoff relationship between both key parameters is required as follows:

(iii)safety betterment (i.e., which can be achieved by increasing the mass of N-electrode with (N:P)Cap ratio of >1:1), and

(iv)high specific energy storage (i.e., which can be achieved at equal capacities of N- and P-electrode, (N:P)Cap ratio of 1:1).

The current design configuration of the proposed GPS-MSTO@C (anode) // LMPO@-C (cathode) sets into bundled layer-by-layer pouch models under optimized (N:P)Cap ratio of ≈ 1.05 – 1.1 :1.

S13. The mass loading, areal capacity density and N/P capacity-ratio of GPS-MSTO@C//LMPO@C anode//cathode full-scale pouch LIB-model

Full-scale GPS-TO@C//LMPO@C sets of bundled layer-by-layer pouch models has dimensions of 35 mm (width), 55 mm (length) and ~ 3mm (thickness) and the stacking

sequence of electrodes can be seen in following configuration
SS cathode | [DS anode| DS cathode|] DS anode | SS cathode
where SS=single side, DS = double sided, | = separator and [] = repeatable unit
The weight fraction calculation for sets of bundled layer-by-layer pouch model components were explained (Figure S2), and the required active mass of the GPS-LMPO@C-cathode and GPS-MSTO@C-anode are 2.79 g and 1.43 g respectively. In this large-scale design, well-packed and dense GPS-MSTO@C-anode (8-layers/14-sides, loaded on Cu-foil (8μm))// GPS-LMPO@C-cathode (7-layers/14-sides, loaded on Al-foil (12μm)) coin cells are contiguously connected into a series of the built-in stack layer configuration of pouch LIB-types. These designable optimizations may provide a compact LIB coin-cell module in pouch modes with a permanent flexible transport of electron/Li+ ion during lithiation and delithiation cycling. The optimal electrode features in the super-architectonics built-in full-cell LIBs can be summarized as follows:
•The area for cathode and anode is selected with the following dimensions of (3*5=15 cm2) and (3*4.75 = 14.3 cm2), respectively.
•The total area of the cathode and anode coverage the pouch LIB cells are 210 and 200 cm2; respectively.
•The mass stacking is 13.3 and 7.14 mg/cm2 for cathode and anode, respectively.
•The areal discharge capacities are 0.85 Ah/cm2 and 0.89 Ah/cm2, of cathode and anode electrodes, respectively.
•The areal discharge capacity of N- and P-electrodes is determined at specific (N:P)Cap capacity ratio of 1.05:1.
Q4.A "fast charge" mode should be tested to see the battery performance, especially the full-cell configuration.
A4- We appreciate the reviewer comment and thank him for this nice view. Per of this important comment the fast charge is highlighted in the manuscript and new section was added to supporting information as follows:

(a) In the results and discussion:
•The following results was added (Please see page 30)
The fast CV-charging timescale ≥ 5 minutes can be optimized at C-rate range of from 1C to 4C, respectively. Under an ever-increasing demand on reliable and fast time-scale charge capacity, the super-architectonic GPS-MSTO@C (N-electrode anode) // GPS-SSF@C (P-electrode cathode) pouch models and modules are powerful in Li+ ion diffusion regimes, and improving hovering electron density for high-speed discharging and charging rates.

(b) New sections have been added to supporting information part including:
•S19. Fast charge process for GPS-LIBs (Please see pages S31, and S32)
S19. Fast charge process for GPS-LIBs
Developing fast-charging protocols for LIBs is a key issue for a wider deployment of EVs and portable electrical devices. Fast-charging of LIBs was investigated with different protocols namely the normal constant current / constant voltage (CC-CV) method and ohmic-drop compensation ODC method. The ODC method can be carried out with an extended constant current period as a result of the high limit voltage based on the ohmic-drop compensation principle.

Herein, fast charge of the GPS-modulated-LIB pouch models can be determined by CC-CV method under specific conditions. In this CC-CV protocol, the charging C-rate is usually increased; leading to the total charging time is decreased. Indeed, at higher C-rate the CC stages are extremely short compared to shorter one. This latter phenomenon is related to the larger contribution of the ohmic drop when the current C-rate increases. Under this basic observation with most of designated LIBs, the fast battery charging process is performed absolutely at CV stage when the C-rate becomes too high (see Figure S13).

Our designed 3D super-scalable GPS-TO@C//LMPO@C anode//cathode full-scale sets of bundled layer-by-layer pouch models was fast charged using CC-CV protocol for C-rate ranging from 1C to 10C. The fast-charging pattern of architectonic bundled layer-by-layer GPS-MSTO@C (N-electrode anode) // GPS-SSF@C (P-electrode cathode) pouch models is applied a constant current and voltage (named as CC-CV) protocol. A set of fast-charging experiments is recorded for GPS-modulated-LIB pouch models at different C-rate values, ranging from 1C to 10C, and at a range of

temperature of 25-35 oC (see Figure S13). The CC-charging timescale decays with increasing of the charging rate in the applying range of 1C to 5C. The CC-charging-depended timescale sets at C-rate > 5C is not recognizable conditions; thereby the CV-charging-depended timescale sets are efficient, reliable, quantifiable means at a range of C-rate variability (see Fig. S13). The formation of long, stable static-flat plateau of CV-charging timescale (i.e. 10-12 minutes) at C-rate > 5C is recognizable with a contribution of the surface-elevated temperature at 35 oC as a maximal value.

The fast CV-charging timescale ≥ 5 minutes can be optimized at C-rate range of 1C-4C, respectively. Under an ever increasing demand on reliable, fast time-scale charge capacity, the super-architectonic GPS-MSTO@C (N-electrode anode) // GPS-SSF@C (P-electrode cathode) pouch models and modules are powerful Li-ion diffusion regimes, and improving hovering electron density for high-speed discharging and charging rates (see Figure S13).

Fig. S13. Schematic diagram of charging time of GPS-modulated-LIB pouch models until 100% of (SOC) state-of-charge using normal CC-CV method. CC stages are in the blue color while CV stages are in the red color. Green color-bar shows the maximum outer surface temperatures elevation of the cell.

5.There are some spell error or typos throughout the manuscript, for example
(1)there should be space between number and unit;
(2)some the temperature unit in "Fabrication of LMPO@C cathodes and MSTO@C anode architectonic mesosponginess";
(3)"power" should be "powder" in "The power MSTO@C (anode) and SSF@C, CSN@C, and NR@C (cathodes) built-up electrode sets in the half-cell anode or cathode";
(4)please double-check other parts

We appreciate the reviewer comment. Per of this comment the whole manuscript and supporting information sections were revised thoroughly and modified to avoid all of these typo.

Reviewer #2:
We really would like to acknowledge the reviewer comments and efforts.
This manuscript reported that the design porous structure materials can be used as electrode materials for Lithium ion battery. It is very interesting topic. But I did not think it is good study.
Q1- First of all, the porous materials is not good for electrode as the coulomb efficiency must be very low. In the manuscript it is not any things about CE.
A1- We appreciate and thank the reviewer for his comment. Per of this comment more information and discussion related to the material merits have been added, also we have shadow a light on the CE for GPS-full scale LIB; Please see this additive to the main text, and supporting information as following:
(a) New parts have been added to results and discussion part including:
•Control synthesis of complex super-architectonics (GPS) cathode-/anode-geometrics (Please see pages 12- 14)
•Material super-architectonics merits (Please see pages 16, 17)
•Modification in “GPS cathode geometrics for half-cell GPS-modulated LIB models” section (Please see pages 19- 23)
•GPS cathode- and anode-electrode-geometrics-integrated full-scale LIBs (Please see pages 27- 32)
(b) New sections have been added to supporting information part including:
•S S11. Super architectonic specific energy density of GPS-modulated full-scale LIB-model (Please see pages S 21-S23)
•S12. Optimization of full cell based (N/P)Cap balancing capacity ratio (Please see page S24)
•S13. The mass loading, areal capacity density and N/P capacity-ratio of GPS-MSTO@C//LMPO@C anode//cathode full-scale pouch LIB-model (Please see page S25)
•S15. A comparison between the GPS-SSF@C half-scale LIB and the other reported LiMnPO4 cathodes (Please see page S 27)

	• S16. A comparison between the GPS-MSTO@C half-scale LIB and the other reported TiO2 anodes(Please see page S 28) •S17. A comparison between the GPS-SSF@C//MSTO@C full-cell LIB electrode system and the other reported LiMnPO4//TiO2 full cells (Please see page S 29) A combination of the finite GPS perspective and topographic space volumes, in general, offers GPS electrodes with fully-access-surfaces, free-space dynamic environments, and multi-scale building-blocks egress/ingress pathways including; (i)multi-diffusive open-pore hole systems, connective meso-macroscopic windows along the entire and randomly dispersed NRs, CNS sheets and layers, and SSF-tower-star complex, (ii)GPS building architects "block-by-block" with a large density of exposed active facets surface (containing numerous sites of connective multi-diffusible dimensions of the exposed bubbly meso-macro-free spaces open-pore system), and (iii)multi-vast-mouth vacancies in highly-dense mesopores and mesogrooves, inter-trapped free occupation mesocage cavities, ridge-gate windows, cave nests, and intra-formational smooth shell/belt-walled/rounded fence-rims along the GPS surfaces. These vast free surface-volume spaces can accommodate and enhance the multicentral dimensionality diffusion of Li+-ions through their discharge (insertion, lithiation)/charge(delithiation, extraction) processes and their transfer along the electrolyte/electrode interfaces (Scheme 2). Regarding to CE (Please see pages 30, and 31) as follows: Super-architectonic GPS Coulombic efficacy (CE) of full-scale SSF@C GPS-cathode // MSTO@C GPS-anode models describes the charge efficiency, by which Li+ ions/electrons are transferred into powerful GPS multiple orientations and super-surface topographies of our distinguishable super-architectonic batteries. CE is the effective ratio between the total values of extracted and inserted charging from the distinct super-architectonic GPS-battery over one-full-cycle. For developing a scalar optimization perspective of GPS-modulated LIB-EVs, we investigate a fast-charging pattern of architectonic bundled-layers of GPS-MSTO@C (N-electrode anode) // GPS-SSF@C (P-electrode cathode) pouch models by applying constant current and voltage (named as CC-CV) protocol. A set of fast-charging experiments is recorded for GPS-modulated-LIB pouch models at different C-rate values, ranging from 1C to 10C, and temperature between 25oC to 35oC (see supporting information S19 & Figure S13). The CC-charging timescale decays with an increase of the charging rate in the applying range from 1C to 5C. The CC-charging timescale dependent sets at C-rate > 5C are not recognizable conditions. Therefore, the CV-charging timescale dependent sets are efficient, reliable, and quantifiable at the range of C-rate variabilities (see Fig. S13). The formation of long, stable static-flat plateau of CV-charging timescale (i.e. approximately 10 to 12 minutes) at C-rate > 5C is recognizable with a contribution of the surface-elevated temperature at 35oC as a maximal value. The fast CV-charging timescale ≥ 5 minutes can be optimized at C-rate range of from 1C to 4C, respectively. Under an ever-increasing demand on reliable and fast time-scale charge capacity, the super-architectonic GPS-MSTO@C (N-electrode anode) // GPS-SSF@C (P-electrode cathode) pouch models and modules are powerful in Li+ ion diffusion regimes, and improving hovering electron density for high-speed discharging and charging rates. The multi-criteria optimization of outstanding cycle performance, long-term stability, and Coulombic efficacy of full-scale super-architectonic GPS-MSTO@C (N-electrode anode) // GPS-SSF@C (P-electrode cathode) models and modules is studied at C-rate of 1C within 2000 cycles between 1.5V and 3.8 V vs. Li/Li+ (Fig. 7d). Note, the magnification of the first 200 cycles of the charging/discharging performance is recorded in Figure 7e. The super-architectonic GPS-modulated LIB model retains 77.5% specific discharging capacity from its original value of 156.3 mAhg–1 after 2000 cycles, and Coulombic efficacy of approximately 99.6% at C-rate of 1C, and at 25oC. For a wide range of charging/discharging cycles (i.e., >2000 cycles), the super-architectonic full-scale GPS-modulated LIB model is attained approximately 100% of its Coulombic efficacy. In general, the complex super-architectonic full-scale GPS-modulated LIB models demonstrate an outstanding structural design stability, high specific charging/discharging capacity, high rate capability, high-speed discharging and charging rates and long cycle life (see Scheme 3 and Figure 7). Q2- Second the tap density of porous structure will be low. It is not any discussion about it. A2- We appreciate and thank the reviewer for his comment. Per of this comment the

	tap density is added; Please see this additive to the supporting information (S.18, Please see page S30) as follows: S 18. Tap density of the super-architectonic GPS-LiMnPO4@C cathode geometrics Due to the increasing demand and the urgent need of the LIBs in the field of consumer electronics and EVs, an important characteristic is the tap density being exploited. The tap density was mainly influenced by the material morphology, particle size and the distribution of powder particles. Design of spherical particles was used to increase the tap-density. Developing new LMPO structures with both high rate performance and high tap density is challenging and appealing for the preparation of cathode materials [Ref-S24, Ref-S25]. To calculate the tap density of GPS-LMPO@C modulated LIBs, we used ZS-102 tap density meter (Liaoning Institute of Research Tools Co., Ltd.) to measure the tap density of the super-architectonics built-in LIB models. In such super-architectonic LIB models or modules, the optimal carbon content should not be more than 5%. The carbon content of SSF@C composites is found in the optimal range of about 4% (lower than 5%) [Ref-S26]. A powerful tool to develop the super architectonic engineering design of GPS-MSTO@C anodic and GPS-LMPO@C of geometric-SSF@C, -CSN@C and -NR@C cathode electrodes can be achieved by a rational mass-loading control. The high-density GPS SSF@C super-architectonics modulated LIBs shows excellent high rate performance, a high tap density (~1.51 g cm-3) compared to 1.24 and 1.02 g cm-3 of GPS-CSN@C, and GPS-NR@C cathode geometrics, respectively. The finding indicates the effect of GPS complex super-architectonic SSF@C in its excellent electrochemical performance, particularly during the Li+-insertion (cathodic, reduction, lithiation) /extraction (anodic, oxidation, delithiation) processes. Together, the GPS-SSF@C super-architectonics can be a potential candidate for high-performance LIBs. Q3- Third it is not good writing. In the main text, the advantages of the structure was listed, but there is not experimental supported, such the Li ion transfer number and the exchange current density. A3- We appreciate this valuable comment. Per of this comment, the specific energy density, N-, and P-electrode cell capacity balancing, experimental and theoretical calculations of specific energy density, Optimization of full cell based (N/P)Cap balancing capacity ratio, and estimation of volumetric energy density have been highlighted and added; Please see this additive to the supporting information (S.11- S 16) as follows: •S11. Super architectonic specific energy density of GPS-modulated full-scale LIB-model (Please see pages S 21-S23) Theoretical calculation of GPS specific energy density: (Please see page S21) S11- A- (i) The contribution of each component of LMPO@C and MSTO@C super-architectonics built-in full cell specific capacity: (Please see page S21) S11- A- (ii) N-, and P-electrode cell capacity balancing: (Please see page S22) •S11- B - Practical method-based experimental sets of super-architectonics built-in LIBs (Please see page S22) •S11-C- Key difference between experimental and theoretical calculations of specific energy density of full-scale GPS-LIBs (Please see page S23) •S12. Optimization of full cell based (N/P)Cap balancing capacity ratio (Please see page S24) •S13. The mass loading, areal capacity density and N/P capacity-ratio of GPS-TO@C//LMPO@C anode//cathode full-scale pouch LIB-model (Please see page S25) •S14. GPS volumetric energy density of super-architectonics built-in LIB-designs (Please see page S26) Q4- Fourth, the quality of image is too poor. A4- We thank the reviewer for his comment. All figures have been provided with high quality. Q5- Fifth the capacitance of porous materials is not compared with the normal or commercialization or theoretical capacity. A5- We would like to thank reviewer for this comment. Per of this comment please see this additive in supporting information as following:

S13(A,B and C) and comparisons S17-S19,
•S11. Calculating processes of specific energy density of GPS-(MSTO@C// LMPO@C) full-scale LIB-model (Please see page S20- S22); which includ The contribution of each component of LMPO@C and MSTO@C architectural-design building-blocks-in full cell specific capacity: (Please see page S20), (ii) N-, and P-electrode cell capacity balancing (Please see page S21), B - Practical method-based experimental sets of architectural-design building-blocks-in LIBs (Please see page 22), and C- Key difference between experimental and theoretical calculations of specific energy density of full-scale LIBs (Please see page 22)
•S11. Super architectonic specific energy density of GPS-modulated full-scale LIB-model (Please see pages S 21-S23) Including:
Theoretical calculation of GPS specific energy density: (Please see page S21)
S11- A- (i) The contribution of each component of LMPO@C and MSTO@C super-architectonics built-in full cell specific capacity: (Please see page S21)
S11- A- (ii) N-, and P-electrode cell capacity balancing: (Please see page S22)
S11- B - Practical method-based experimental sets of super-architectonics built-in LIBs (Please see page S22)
S11-C- Key difference between experimental and theoretical calculations of specific energy density of full-scale GPS-LIBs (Please see page S23)
•S15. A comparison between the GPS-SSF@C half-scale LIB and the other reported LiMnPO4 cathodes (Please see page S 27)
• S16. A comparison between the GPS-MSTO@C half-scale LIB and the other reported TiO2 anodes(Please see page S 28)
•S17. A comparison between the GPS-SSF@C//MSTO@C full-cell LIB electrode system and the other reported LiMnPO4//TiO2 full cells (Please see page S 29)

S11. Super architectonic specific energy density of GPS-modulated full-scale LIB-model
The calculation and quantification methods for specific energy density of GPS-(MSTO@C N-anode// GPS-LMPO@C P-cathode full-scale LIBs are carried out based on the expected theoretical model and real experiment sets of the super-architectonic contents of the LMPO@C and MSTO@C P-cathode and N-anode electrodes-modulated into full-scale LIBs. Here, we provide intensive studies based on the theoretical and practical or experimental models as follows:
A- Theoretical calculation of GPS specific energy density:
In the designed integrated super-architectonic built into the GPS-full-scale LIB, the nominal open circuit voltage (VOC) along P-cathode and N-anode electrodes-modulated CR2032 coin cells can be detected according to the equations:
VOC = V+ - V-
VOC = 4.1 V – 1.76 V =2.34 V,
Where V+ represents the potential of half-cell of GPS-LMPO@C P-electrode that equalized to 4.1 V, and V- is the potential of GPS-MSTO@C N-electrode that equalized to 1.76 V.
Faraday's law is used to calculate the theoretical specific cell capacity of a cell in mAhg−1.
Qtheoretical = (nF) / (3600*Mw)
Where, F is the Faraday constant, n is the number of charge carrier, and Mw is the molecular weight of the architect materials electrode surfaces. The Qtheoretical for GPS-LMPO cathode-base electrode is found to be 171 mAh g-1. Where, Mw of GPS-LMPO is 156.85 g mol-1, n=1 and Li+=1. F=96 485.3329 sA mol-1. In addition, Qtheoretical for common-used anodic electrode is as follows: nano-sized TiO2= 335 mAh/g [Ref-S1- Ref-S3].

S11- A- (i) The contribution of each component of LMPO@C and MSTO@C super-architectonics built-in full cell specific capacity:
According to TG and EDS analyses, the relative composition contents of in cathode- and anode-based GPS super-architectonics are determined. The obtained results indicated the carbon content to be ~ 4.3 wt % in the LMPO@C compositions.
-Therefore, the theoretical specific capacity of LMPO@C P-electrode can be calculated as follows: ~ (335 mAh/g * 0.043 + 171 mAh/g * 0.9996) ~ 185.33 mAh/g.

S11- A- (ii) N-, and P-electrode cell capacity balancing
In fact, a significant effect of the N/P ratio on the electrochemical response is an important factor in full cell efficiency. The lithium plating during charging is firmly

attached to N/P ratio. The lithium coating causes irreversibility and is assembled during cycling, ultimately reducing the loss of capacity, mechanical swelling and possibly a short inner circuit. To avoid the danger of metallic lithium plating, this is considered as retrospective aging process and safety, one should control the mass balancing capacity ratio of P- or N-electrode materials. The cell capacity is controlled by the key value of specific capacity of each of the P- or N-electrode materials presented in the LIB full cell [Ref-S4 -Ref. S6]. In this study, in order to reconcile these two contrast options, the LIB-Model is designed to extend 3D super-scalable full-scale GPS-LMPO@C//MSTO@C cathode//anode stacked layers pouch LIB-model under optimized mass loading and ((N:P)Cap capacity ratio ≈ 1.02 – 1.1 :1.
-Assuming an ideal N / P ratio for positive and negative electrode materials in a manner commensurate with its conceptual strength, the ideal capacity ratio for the full scale model (GPS-LMPO@C//MSTO@C) is as follows: 171 Ah kg−1/335 Ah kg−1 = 0.51
-Based on the calculation, for an ideal battery with 171 Ah of capacity, 1 kg of LiMnPO4@C and 0.51 kg MSTO@C are required for design.
-The combined mass fraction of both P- and N-electrodes in the practical pouch LIB cell key-component constitutes (i.e., conductive electrolyte, polymeric membrane separator, current electrodes and package cortices, see Figures S1, is 34%, leading to that the full scale GPS-LIB with a specific capacity of ((171 Ah)/(1 kg+0.51 kg))/1.34 is about 84.5 Ah .kg-1.
The theoretical mode of calculated specific energy of GPS-LMPO@C//MSTO@C battery can be quantified as equal to (2.34 V *84.5 Ah kg-1)= 197.7 Wh kg-1.

S11- B - Practical method-based experimental sets of super-architectonics built-in LIBs
In galvanostatic cycling test (i.e., only at constant current), the graphically specific energy of super-architectonic built into the GPS-full-scale LIB can be detected from the charge–discharge voltage-capacity profile at 1C as follows:
-The specific energy for the GPS-LMPO@ C cathode (Wh/kg) is = the average working voltage of the super-architectonics built-in LIBs in (V) x maximum discharge capacity delivered by cell (Ahkg-1).
-The specific capacity delivered by cell (Ahkg-1) at 1C = 156.3 Ahkg-1.
-The specific energy for the GPS-cathode (Wh/kg) = 2.6 V x 156.3 Ahkg-1 =406.4 Wh/kg.
-Thus, the specific energy density of full-cell super-architectonic built into the GPS-full-scale LIB (Whkg-1) = the estimated mass fraction of a cathode active material in a LIB cell (in pouch-type, mass fraction is 44% (see S1)) x Specific Energy for the cathode (Whkg-1).

-Therefore, practical value of the specific energy density of the GPS-LMPO@C//MSTO@C full-scale LIB is 178.8 Whkg-1.

S11-C- Key difference between experimental and theoretical calculations of specific energy density of full-scale GPS-LIBs
For both the intensive determination of specific energy density for the super-architectonic built into the GPS-full-scale LIB, the practical and theoretical values are of 178.8 Whkg-1 (practically) and 197.7 Whkg-1 (theoretically), respectively. The low value of specific energy density in a practical determination may attributed to
(iii)the Li+-ions can’t be completely removed from the N-electrode and P-electrode surface topographies, and
(iv) non-usable cutoff voltage profiles to clean-up N-electrode and P-electrode surface topographies to remove the rest Li+ ion on the interlay complex super-architectonics, constraining the perfect charge-discharge rate.
The proposed GPS-MSTO@C//LMPO@C full-scale battery system integrates the latest advances in Li-battery technology to create a battery that delivers outstanding electrochemical performance.

S15. A comparison between the GPS-SSF@C half-scale LIB and the other reported LiMnPO4 cathodes
To show evidence of the effectiveness of the super-architectonic GPS-LMPO@C and GPS-MSTO@C anode geometrics, building-blocks-in a wide-range of egress/ingress egress/ingress hierarchy, and super topographic-surface heterogeneity, roughness and

anisotropy on the GPS-designated LIBs, we offer intensive studies of the key parameters in terms of rate capability, Coulombic efficiency, reversible capacity and long-term cycle stability of our GPS LIBs and other reported LIB designs, as one can see in Table S1-S3.

Table S1 A comparison between the GPS-LMPO (with SSF@C geometrics) half-scale LIB and normal and conventional LMPO cathode-LIBs

Cathode material	Nominal Voltage (V)	Cycles	Specific Capacity mA h g-1	Coulombic efficiency	Ref
LiMnPO4@C	4.1	retained ~100% of its reversible capacity after 100 cycles	155		
At 0.5C	Not mentioned		21		
LiMnPO4@C	4.1	capacity retained 120 mAhg-1 after 50 cycles	153.4 at 0.1C	Not mentioned	37
LiMnPO4@C	4.1	capacity retained 89.1 mAhg-1 after 500 cycles	147.9 at 1C	Not mentioned	Ref-10
LiMnPO4	4.1	capacity retained 125 mAhg-1 after 30 cycles	133 at 0.1 C	Not mentioned	17
LiMnPO4@C (GPS-SSF@C)	4.1	Retains ~100% after 100 cycles	133 at 1C	~100%	Current Work

S16. A comparison between the GPS-MSTO@C half-scale LIB and the other reported TiO2 anodes

Table S2 A comparison between the GPS-MSTO@C half-scale LIB and the other reported TiO2 anodes.

Anode material	Nominal Voltage (V)	Cycles	Specific Capacity mA h g-1	Coulombic efficiency	Ref
Rutile TiO2	1.7	retained 50% of its reversible capacity after 100 cycles	250		
At 0.1C	~ 100% after 100 cycles		Ref [S11]		
Rutile TiO2	1.5	retained 77% of its reversible capacity after 40 cycles	223 at 0.1C	Not mentioned after 100 cycles	Ref [S12]
Anatase TiO2	1.73	76% of its initial capacity after 30 cycles at 0.2C	~ 300	Not mentioned	Ref [S13]
P25, a commercial titania powder from Degussa	1.76	1% of its initial capacity after 30 cycles at 0.2C	95	Not mentioned	Ref [S13, S14]
TiO2	1.74	70% of its initial capacity after 100 cycles at 0.2C	270	Not mentioned	Ref [S15]
TiO2	0.85	5% of its initial capacity after 30 cycles	310	~100%	Ref [S16]
TiO2@C (GPS-MSTO@C)	1.78	7% of its initial capacity after 100 cycles at 1C	231	Not mentioned	Current Work

S17. A comparison between the GPS-SSF@C//MSTO@C full-cell LIB electrode system and the other reported LiMnPO4//TiO2 full cells

Table S3 A comparison between the GPS-SSF@C//MSTO@C full-cell LIB electrode system and the other reported LiFePO4//TiO2 and LiMnPO4//TiO2 full cells.

Cathode material	Anode material	Nominal Voltage (V)	Cycles	Specific Capacity mA h g-1	Coulombic efficiency	Ref
LiFePO4	Anatase TiO2 hollow nanofibers	1.4	retained 88% of its reversible capacity after 300 cycles	103	> 99 %	Ref [S17]
LiFePO4	Rutile TiO2	1.8	retained 50% of its reversible capacity after 40 cycles	150	Not mentioned	Ref [S18]
LiFePO4	Anatase TiO2	1.68	1% of its initial capacity after 300 cycles at 20C	160	Not mentioned	Ref [S19]
LiFePO4	anatase/graphene	1.67	00127~ 100%			Ref [S20]
LiFePO4	spinel Li4Ti5O12/C	1.8	Retain 98.1% after 400 cycles	167	~100%	Ref [S21]
LiFePO4	spinel Li4Ti5O12	1.65	Retain 98.9% after 100 cycles	150	~100%	Ref [S22]
LiMnPO4	Li4Ti5O12	2.5	Retain ~100% after 300 cycles at C/2	105	~100%	Ref [S23]

	LiMnPO4@C (GPS-SSF@C)TiO2@C (GPS-MSTO@C)2.6Retains 77.5% after 2000 cycles at 1C156.3~100%Current Work Reviewer #3: We really would like to acknowledge the reviewer comments and efforts. Per of this respectful vision, we thoroughly amended our manuscript taking all points raised in our consideration This work realizes the coupling of a series of super hierarchy and interlay-complex superstructures of anode and cathode (GPS), which were fabricated with irregular surface ripples, bumps, undulations, and anticlines and integrated into half- and full-cell LIB models to allow non-prescriptive cycle usages, loading, diffusion, and interaction and to achieve excellent rate capabilities. After integrating GPS cathode- and anode-electrode geometrics into precisely defined LIB pattern models, the LIBs showed an outstanding long-term cycling performance for 2000 cycles at 1C. In my opinion, this work displays an effective method for the construction of highly efficient electrode materials but overall I suggest some questions should be addressed in the manuscript. Q1. The English needs a lot of edition throughout the paper. The authors should pay attention to the use of the article, conjunction, and comma. There are some syntax errors in sentences or phrases; several sentences are contextually incorrect. Some examples are below: "These GPS configurations preserve the multi-scale and interior space complexities as well as the vortex flow dynamics that are connectively arranged in lateral/longitudinal exposure modulates …" "These intrinsic features may lead to create ageless reachable LIBs …" "The orientation of SSF@C-electrode superstructure along vertical, lateral and longitudinal axes, which had upper-top-capped pyramidal prisms makes the charge/discharge rate more facile." "Accordingly, we studied the temperature dependence functionality of these cathodes versus their electrical conductivity …" A1- We appreciate the reviewer comment. Per of this comment the whole manuscript carefully revised and covered all of these comments, in addition, the language of the manuscript and supporting is revised by English Company. Q2. Some phrases are used in a non-standard manner, for example, multi-gate-in-transport, land energy density, power electron density, spatial rate performance capabilities, electronic surfaces, capability performance rates, and C-shell dresser. A2- Thanks for this comment. Per of this comment the manuscript was revised and improved, please see modification in the revised form with blue font. Q3. The format of chemical formula should be detailedly checked throughout the manuscript. A3- Thanks for this observation. Per of this comment the chemical formula was revised and modified. Q4. What's the tap density of GPS materials? Then, a table should be added to compare with other reported values in literatures. A3- We appreciate the reviewer comment. Per of this comment, the following modification has been done as follows: •S15. A comparison between the GPS-SSF@C half-scale LIB and the other reported LiMnPO4 cathodes (Please see page S 27) • S16. A comparison between the GPS-MSTO@C half-scale LIB and the other reported TiO2 anodes(Please see page S 28) •S17. A comparison between the GPS-SSF@C//MSTO@C full-cell LIB electrode system and the other reported LiMnPO4//TiO2 full cells (Please see page S 29) •S 18. Tap density of the LiMnPO4@C cathode (Please see page S 30) S15. A comparison between the GPS-SSF@C half-scale LIB and the other reported LiMnPO4 cathodes

To show evidence of the effectiveness of the super-architectonic GPS-LMPO@C and GPS-MSTO@C anode geometrics, building-blocks-in a wide-range of egress/ingress egress/ingress hierarchy, and super topographic-surface heterogeneity, roughness and anisotropy on the GPS-designated LIBs, we offer intensive studies of the key parameters in terms of rate capability, Coulombic efficiency, reversible capacity and long-term cycle stability of our GPS LIBs and other reported LIB designs, as one can see in Table S1-S3.

Table S1 A comparison between the GPS-LMPO (with SSF@C geometrics) half-scale LIB and normal and conventional LMPO cathode-LIBs

Cathode material	Nominal Voltage (V)	Cycles	Specific Capacity mA h g-1	Coulombic efficiency	Ref
LiMnPO4@C	4.1	retained ~100% of its reversible capacity after 100 cycles	155	At 0.5C	Not mentioned21
LiMnPO4@C	4.1	capacity retained 120 mAhg-1 after 50 cycles	153.4 at 0.1C	Not mentioned37	
LiMnPO4@C	4.1	capacity retained 89.1 mAhg-1 after 500 cycles	147.9 at 1C	Not mentionedRef-10	
LiMnPO4	4.1	capacity retained 125 mAhg-1 after 30 cycles	133 at 0.1 C	Not mentioned17	
LiMnPO4@C (GPS-SSF@C)	4.1	Retains ~100% after 100 cycles	133 at 1C	~100%	Current Work

S16. A comparison between the GPS-MSTO@C half-scale LIB and the other reported TiO2 anodes

Table S2 A comparison between the GPS-MSTO@C half-scale LIB and the other reported TiO2 anodes.

Anode material	Nominal Voltage (V)	Cycles	Specific Capacity mA h g-1	Coulombic efficiency	Ref
Rutile TiO2	1.7	retained 50% of its reversible capacity after 100 cycles	250	At 0.1C	~ 100% after 100 cyclesRef [S11]
Rutile TiO2	1.5	retained 77% of its reversible capacity after 40 cycles	223 at 0.1C	Not mentioned after 100 cyclesRef [S12]	
Anatase TiO2	1.737	6% of its initial capacity after 30 cycles at 0.2C	~ 300	Not mentioned	Ref [S13]
P25, a commercial titania powder from Degussa	1.76	1% of its initial capacity after 30 cycles at 0.2C	95	Not mentioned	Ref [S13, S14]
TiO2	1.747	0% of its initial capacity after 100 cycles at 0.2C	270	Not mentioned	Ref [S15]
TiO2	0.85	5% of its initial capacity after 30 cycles	310	~100%	Ref [S16]
TiO2@C (GPS-MSTO@C)	1.7	87% of its initial capacity after 100 cycles at 1C	231	Not mentioned	Current Work

S17. A comparison between the GPS-SSF@C//MSTO@C full-cell LIB electrode system and the other reported LiMnPO4//TiO2 full cells

Table S3 A comparison between the GPS-SSF@C//MSTO@C full-cell LIB electrode system and the other reported LiFePO4//TiO2 and LiMnPO4//TiO2 full cells.

Cathode material	Anode material	Nominal Voltage (V)	Cycles	Specific Capacity mA h g-1	Coulombic efficiency	Ref
LiFePO4	Anatase TiO2 hollow nanofibers	1.4	retained 88% of its reversible capacity after 300 cycles	103	> 99 %	Ref [S17]
LiFePO4	Rutile TiO2	1.8	retained 50% of its reversible capacity after 40 cycles	150	Not	

	mentionedRef [S18] LiFePO4Anatase TiO21.681% of its initial capacity after 300 cycles at 20C160Not mentionedRef [S19] LiFePO4anatase/graphene1.6700127~ 100%Ref [S20] LiFePO4spinel Li4Ti5O12/C1.8Retain 98.1% after 400 cycles167~100%Ref [S21] LiFePO4spinel Li4Ti5O121.65Retain 98.9% after 100 cycles150~100%Ref [S22] LiMnPO4Li4Ti5O122.5Retain ~100% after 300 cycles at C/2105~100%Ref [S23] LiMnPO4@C (GPS-SSF@C)TiO2@C (GPS-MSTO@C)2.6Retains 77.5% after 2000 cycles at 1C156.3~100%Current Work S 18. Tap density of the super-architectonic GPS-LiMnPO4@C cathode geometrics Due to the increasing demand and the urgent need of the LIBs in the field of consumer electronics and EVs, an important characteristic is the tap density being exploited. The tap density was mainly influenced by the material morphology, particle size and the distribution of powder particles. Design of spherical particles was used to increase the tap-density. Developing new LMPO structures with both high rate performance and high tap density is challenging and appealing for the preparation of cathode materials [Ref-S24, Ref-S25]. To calculate the tap density of GPS-LMPO@C modulated LIBs, we used ZS-102 tap density meter (Liaoning Institute of Research Tools Co., Ltd.) to measure the tap density of the super-architectonics built-in LIB models. In such super-architectonic LIB models or modules, the optimal carbon content should not be more than 5%. The carbon content of SSF@C composites is found in the optimal range of about 4% (lower than 5%) [Ref-S26]. A powerful tool to develop the super architectonic engineering design of GPS-MSTO@C anodic and GPS-LMPO@C of geometric-SSF@C, -CSN@C and -NR@C cathode electrodes can be achieved by a rational mass-loading control. The high-density GPS SSF@C super-architectonics modulated LIBs shows excellent high rate performance, a high tap density (~1.51 g cm-3) compared to 1.24 and 1.02 g cm-3 of GPS-CSN@C, and GPS-NR@C cathode geometrics, respectively. The finding indicates the effect of GPS complex super-architectonic SSF@C in its excellent electrochemical performance, particularly during the Li+-insertion (cathodic, reduction, lithiation) /extraction (anodic, oxidation, delithiation) processes. Together, the GPS-SSF@C super-architectonics can be a potential candidate for high-performance LIBs. Q5. More evidences should be provided to confirm the pyramid structure. A5- Thank you so much for this nice vision and constructive comment. Per of this comment further information and discussion related to the material control is added. New section has been added to Results and Discussion part “Control synthesis of complex super-architectonics (GPS) cathode-/anode-geometrics (Please see pages 12- 14)” as follows: Control synthesis of complex super-architectonics (GPS) cathode-/anode-geometrics Control synthesis of large-scale giant porous complex super-architectonics (GPS) is mainly composition- and time-dependent protocol that enabled well-defined growth GSP reaction kinetics to build up block-by-block hierarchy. As a result, super-architectonics are fabricated with structural GPS-building-blocks-in a wide-range of (i) distinguishable geometrics in 3-dimesnional (3D) and multi-directional orientations (lateral, vertical, circular, zigzag, and longitudinal), (ii) egress/ingress models such as caves, channels and grooves, and (iii) giant topographic-surfaces including ripples, winglets, protuberances, irregular bumps, V-hooks, undulations, and anticlines. Accordingly, well-designed super-architectonics (GPS) LMPO@C-cathodes, including three variable geometrics solanum star-shaped flower (SSF@C), mesocave nanorods (NRs@C), and axially edged stack sheets (CSN@C) are successfully fabricated under our protocol synthesis. The anode-based GPS anatase MSTO@C architectonic geometrics and super surface topographies are fabricated with multi-layered shells dressed mesosphere core and vertically oriented along its central axes. The structurally-shaped architectonics of MSTO@C GPS-anode are attained the interior space complexities and vortex flow dynamics under our realistic synthesis conditions. The simple synthesis protocol provides a powerful tool to develop the architectonic

	engineering design of GPS-MSTO@C anodic and GPS-LMPO@C of geometric-SSF@C, -CSN@C and -NR@C cathode electrodes in a rational mass-loading control. These GPS electrode geometrics integrated into CR2032 coin cells are the key enabling fabrication of low-cost super-architectonics built-in LIB-models and modules with ever-decreasing timescale of discharge capacity and path-dependent battery with high-energy density. In this regards, the complex super architectonic LMPO-GPS geometrics, namely, SSF, CSN, and NR, are then tailored by varying the manganese anions (i.e., chloride, sulfate, and nitrate, respectively) and by controlling the time-dependent particle-to-particle growth under the optimization conditions, such as pH solution, growth-assisted agent, and high-temperature treatment. For a thorough grasp of the LiMnPO4 crystals building-growth approach with various 3D-morphological structures, a sensible explanation can be determined as follows: First, nucleation-directing agents such as ethylene glycol and H3PO4, to some extent, affect the particle-to-particle growth direction. Second, the potential decrease in the power strength of precursor manganese-anions (i.e., NO3-, SO42-, and Cl-) plays an extreme role in the kinetic- and thermodynamic-control growth-path mechanism, leading to the structural optimization of GPS morphology, and the modulation of 3D GPS multidirectional geometrics. Third, the environment synthesis conditions provide large surface scales of ripples, irregular bumps, undulations, anticlines, and active top-zone Mn2+/Mn3+ espoused surface for a facile lithiation/delithiation process. Consequently, the decrease in the reduction power of manganese-anions was in this order NO3- > SO42- > Cl-, leading to pronounced changes in complex super-architectonic (GPS) geometrics in this sequence of NRs - CSN- SSF structures, respectively. The addition of manganese sources with (i) NO3- , (ii) SO42-, and (iii) Cl- anion species with similarly well-controlled synthesis condition and composition guides fabricating of (i) 1D-model open-top mesopore NRs, passing through (ii) axially-edged plate sheets stacked circularly around central axis and concentrically formed a cylinder sphere-hole-like cage nest (CSN) structure, to (iii) 3D solanum star-shaped flowers with multi-branchlet nanorods spreading out from central core in to lateral and axial directions (SSF) structure, respectively. The mechanistic formation of NRs, CSN nd SSF geometrics is evidenced from the microscopic patterns, including a top- and plane-view (FE-SEM) field emission scanning electron microscope and (HR-TEM) a high-resolution transmission electron microscopy (Figs. 1, 2, S2, and S3). Furthermore, facile electron/Li+ ion mobility and highly conductive surfaces for MSTO-anode and SSF-, CSN- and NR-cathode composites are improved by well-ordered and sustainable modification by ~5nm C-shell dressers along entirely giant surface ripples, irregular bumps, undulations, and anticlines. These giant topographic surfaces affect high rate performance and tap density, and cyclic stability characteristics of half- or full-scale GPS-LIBs (see supporting information S1-S19). The integration of GPS interlay-complex architectonic anode/cathode geometrics into half-/full-scale LIBs may allow multi-gate-in-transport electron/ion mobility in building-blocks egress/ingress paths. These diverse pathways, including the upper, middle, and lower multi-zone crystal patterns, and for evaluating the frontal edge/apex/central/corner access sites are given their potentials in the design of GPS-LIB models and modules with superb specific capacities, high energy density, facile discharge–discharge rates, and extended long-term power stability. The GPS complex architectonic anode/cathode surface topographies that have irregular ripples, bumps, undulations and anticlines significantly affect electrochemical performance of both half- and full-cell LIB designs in terms of non-prescriptive cycle usages, heavily interior Li+ ion loads, and spatial rate performance capabilities (Scheme 1). Q6. Please pay more attention to the references. There are several ill-formed abbreviations of journal names. A6- Thanks for this observation. Per of this important comment, references have carefully revised and modified. Finally, we would like to thank the reviewers for their valuable comments that improved the manuscript thoroughly. We would like to emphasize that all comments have been considered and notified in our manuscript. Please see our response and the accordance change in the entire manuscript (blue color).

NATIONAL INSTITUTE FOR MATERIALS SCIENCE
Sengen 1-2-1, Tsukuba, Ibaraki 305-0047, JAPAN

Dear Prof. H.M. Cheng
Chief Editor: Energy Storage Materials

Nov. 8th, 2019

Revision Manuscript: ENSM_2019_704
Title: "Large-Scale Giant Architectonic Electrodes Designated with Complex Geometrics and Super Topographic Surfaces for Fully Cycled Dynamic LIB Modules".
Corresponding Author: Prof. Sherif A. A. El-Safty

Dear Professor,
Thank you so much for accepting submission of our manuscript to your respected reviewers.
I do appreciate your effort and selection of the appropriate Reviewers, whom they offered us great opinions to modify our work. Indeed, I acknowledge their efforts and thank them for allotment a time to consider the quality of our manuscript.

The revised version has been modified based on the reviewer's comments. I would like to refine that the current version has been carefully revised and made significant adjustments without affecting the main essence of the manuscript. This revision improved the current version to be appropriate for the journal and readers. Based on these procedures, the authors participating in this edition have been updated.

Therefore, significant changes in the revised manuscript can be highlighted as follows:

1. We have modified the manuscript' text, supporting, figures& schemes thoroughly, but the core goal of our manuscript was attained.
2. We recovered all points raised either through practically experimental sets in our laboratory and theoretical studies of half-and full-scale LIBs coin-cell designs, modes, and modules.
3. New sections have been added to the manuscript including:

➢ **In the Experimental part:**

- Configuration of super-architectonics-integrated GPS-LIB CR2032 coin-cell models and pouch-type modules (**Please see pages 8, 9**)
- Architectonic anode/cathode GPS-LIB CR2032 coin-cell models (**Please see pages 9- 11**)
- Architectonics-integrated into bundled layer-by-layer pouch and 18650-cylindrical GPS-LIB-types (**Please see pages 11, 12**)

➢ **In the Results and Discussion part:**

- *Control synthesis of complex super-architectonics (GPS) cathode-/anode-geometrics (**Please see pages 12- 14**)*
- *GPS cathode- and anode-electrode-geometrics-integrated full-scale LIBs (**Please see pages 27- 33**)*

➢ **In the supporting information part:**

- *S11. Super architectonic specific energy density of GPS-modulated full-scale LIB-model (**Please see pages S 21-S23**)*
- *S12. Optimization of full cell based (N/P)Cap balancing capacity ratio (**Please see page S24**)*
- *S13. The mass loading, areal capacity density and N/P capacity-ratio of GPS-MSTO@C//LMPO@C anode//cathode full-scale pouch LIB-model (**Please see page S25**)*
- S14. GPS volumetric energy density of super-architectonics built-in LIB-designs *(**Please see page S26**)*
- *S15. A comparison between the GPS-SSF@C half-scale LIB and the other reported LiMnPO4 cathodes (**Please see page S 27**)*
- *S16. A comparison between the GPS-MSTO@C half-scale LIB and the other reported TiO_2 anodes(**Please see page S 28**)*
- *S17. A comparison between the GPS-SSF@C//MSTO@C full-cell LIB electrode system and the other reported $LiMnPO_4$//TiO_2 full cells (**Please see page S 29**)*
- *S 18. Tap density of the LiMnPO4@C cathode (**Please see page S 30**)*

- *S19. Fast charge process for GPS-LIBs (**Please see pages S31, and S32**)*

4. The language of the manuscript has been carefully revised.

Please have a look to these highlights in the supplementary or text for quick and easy action

Moreover, per of the journal instructions, the following files were attached as separate files:

a. A response to the comments made by the reviewers.
b. Revised manuscript-text, as word file, with changes in a blue color font.
c. A version of our complete revised supplementary including figures.
d. Cover letter to Editor addressing the changes

Hopefully, this revised version would be in a level to deserve your consideration.

Sincerely yours

Sherif A. El-Safty, PhD, FRSC

Research Manager, Center for Functional Materials
National Institute for Materials Science (NIMS)
Sengen 1-2-1, Tsukuba, Ibaraki, 305-0047, JAPAN
Tel: +81-29-859-2135
E-mail: sherif.elsafty@nims.go.jp
https://samurai.nims.go.jp/profiles/sherif_elsafty

Professor of Nanomaterials
University of Sunderland
Faculty of Engineering and Advanced Manufacturing
St Peter's Campus, Sunderland, SR6 0DD, United Kingdom
E-mail: sherif.el-safty@sunderland.ac.uk

Manuscript Number: ENSM_2019_704

Large-Scale Giant Architectonic Mesosponginess and Complex Superstructures Integrated Anode/Cathode Full-Scale LIBs

Reviewer #1:

This work developed a giant porous complex superstructures as a concept, to integrate LMPO and TiO2 as cathode and anode for LIBs. The work is interesting, while the novelty and battery performance is not very well presented. please carefully consider the following comments:

Q1. What is the determined step that forms the "GPS" structure, in both anode and cathode?

A1. *We thank the reviewer for this valuable comment.*

Per of the reviewer comment, intensive discussion related to the "GPS" structure has been carried out in the experimental part, and results and discussion part, Please see additional information in blue font as follows:

(a) New section has been added to Results and Discussion part including:

- *Control synthesis of complex super-architectonics (GPS) cathode-/anode-geometrics (**Please see pages 12- 14**)*

(b) New sections have been added to experimental part including:

- *Configuration of super-architectonics-integrated GPS-LIB CR2032 coin-cell models and pouch-type modules (**Please see pages 8, and 9**)*
- *Architectonic anode/cathode GPS-LIB CR2032 coin-cell models (**Please see pages 9-11**), and*
- *Architectonics-integrated into bundled layer-by-layer pouch and 18650-cylindrical GPS-LIB-types (**Please see pags 11, and 12**)*

Q2. More detailed information should be provided in the experiment, for example the loading of active materials, the tap-density of the active materials, the areal density of active materials on the electrodes on both anode and cathode, for both half-cell and full-cells. Because these are very important parameters for the overall performance of the batteries. Moreover, these should be carefully compared with the industrial standard.

A2- *We thank the reviewer for his constructive comment. Per of these valuable notes, experimental and sets are carefully revised as can be seen in the supporting information and the entire manuscript. Please see this modification and additive to the following part of experimental section and supporting information as follows:*

(a) New sections have been added to experimental part including:

- *Configuration of super-architectonics-integrated GPS-LIB CR2032 coin-cell models and pouch-type modules (**Please see pages 8, and 9**)*
- *Architectonic anode/cathode GPS-LIB CR2032 coin-cell models (**Please see pages 9-11**), and*
- *Architectonics-integrated into bundled layer-by-layer pouch and 18650-cylindrical GPS-LIB-types (**Please see pags 11, and 12**)*

(b) New sections have been added to supporting information part including:

- *S1-C- GPS super architectonics built-in 2032 coin-cell LIBs (**Please see pages S5**)*
- *S1-D. The mass fraction analysis of GPS super architectonic cell components (**Please see page S5 and S6**)*
- *S11. Super architectonic specific energy density of GPS-modulated full-scale LIB-model (**Please see pages S 21-S23**)*
- *S12. Optimization of full cell based (N/P)Cap balancing capacity ratio (**Please see page S24**)*
- *S13. The mass loading, areal capacity density and N/P capacity-ratio of GPS-MSTO@C//LMPO@C anode//cathode full-scale pouch LIB-model (**Please see page S25**)*
- *S15. A comparison between the GPS-SSF@C half-scale LIB and the other reported LiMnPO4 cathodes (**Please see page S 27**)*
- *S16. A comparison between the GPS-MSTO@C half-scale LIB and the other reported TiO_2 anodes(**Please see page S 28**)*
- *S17. A comparison between the GPS-SSF@C//MSTO@C full-cell LIB electrode system and the other reported $LiMnPO_4$//TiO_2 full cells (**Please see page S 29**)*
- *S 18. Tap density of the LiMnPO4@C cathode (**Please see page S 30**)*

S1-C- GPS super architectonics built-in 2032 coin-cell LIBs

GPS super architectonic half-scale anode or cathode LIBs are explored by using CR2032-coin cells. For precision accuracy and possible control of electrochemical experiments, the designated GPS super architectonics built-in MSTO@C-anode and SSF@C-cathode half-cell and MSTO@C//SSF@C anode//cathode full-cell LIBs are arranged and oriented in CR2032-coin cells under specific protocols (see supporting information, Figure S1).

Moreover, the configuration of stacked-layers-in pouch LIBs-type along full-scale ordered sets of GPS super architectonic MSTO@C//SSF@C anode//cathode geometrics is the key broadening of the design LIB-modules, as shown in supporting information S1-D, Fig.S11..

On the base of the experimental sets of GPS super architectonic MSTO@C GPS-anode//SSF@C GPS-cathode pouch LIB-model, the optimized loading amount (mass/coverage area, mg/cm^2) is of 13.3 and 7.14 mg/cm^2 for SSF@C GPS-cathode and MSTO@C GPS-anode geometrics, respectively. Accordingly, the areal discharge capacities of SSF@C P-cathode and MSTO@C N-anode electrodes are 0.85 Ah/cm^2 and 0.89 Ah/cm^2, respectively. The similarity in the areal discharge capacity' value (in Ah) of P-cathode and N-anode electrodes indicates that the finest mass $(N:P)_{Cap}$ balancing capacity ratio is 1.05:1. The significant control of $(N:P)_{Cap}$ ratio is mainly dependent of the optimal tradeoff LIB manufacturing rapports between (i) the safety betterment (i.e., at which the increase of loading mass of N-electrode to offer $(N:P)_{Cap}$ ratio of >1 :1 is essential), and (ii) the specific energy density (at which rational mass balancing $(N:P)_{Cap}$ ratio is of 1:1).

S1-D. The mass fraction analysis of GPS super architectonic cell components

The mass fraction analysis of individual cell components in the pouch full-cell model can be seen in schematic diagram as seen in Fig. (S2). The GPS super architectonic working electrodes are prepared by

mixing each active material of GPS-TO@C anode composite and GPS-LMPO@C cathode materials with carbon black, and polyvinylidene fluoride (PVDF) as a binder in a weight ratio of 80:15:5. Based on the mass fraction of a cathode material in a GPS super architectonic sets of bundled layer-by-layer pouch models is approximately 44%, leading to determine of the specific energy density for the GPS-LMPO@C//TO@C full-scale LIB, which is practically equal to 178.8 Wh kg^{-1} (see supporting information S13- B).

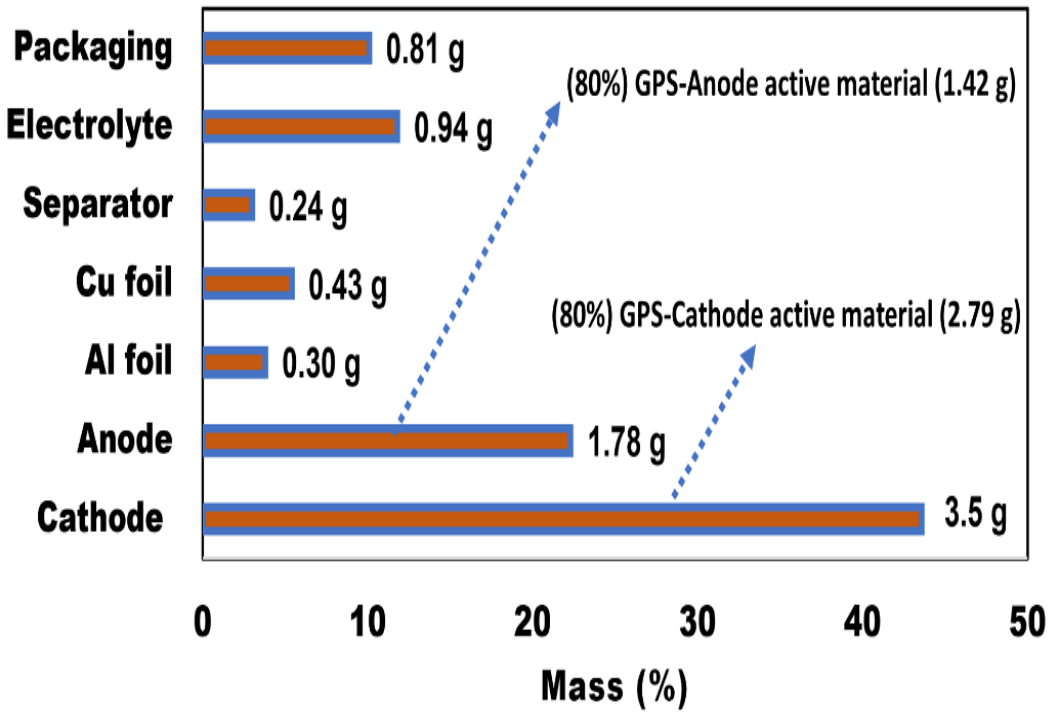

Fig. S2 Schematic diagram of mass fraction of individual components used in the GPS super architectonic pouch model

S11. Super architectonic specific energy density of GPS-modulated full-scale LIB-model

The calculation and quantification methods for specific energy density of GPS-(MSTO@C N-anode// GPS-LMPO@C P-cathode full-scale LIBs are carried out based on the expected theoretical model and real experiment sets of the super-architectonic contents of the LMPO@C and MSTO@C P-cathode and N-anode electrodes-modulated into full-scale LIBs. Here, we provide intensive studies based on the theoretical and practical or experimental models as follows:

A- Theoretical calculation of GPS specific energy density:

In the designed integrated super-architectonic built into the GPS-full-scale LIB, the nominal open circuit voltage (V_{OC}) along P-cathode and N-anode electrodes-modulated CR2032 coin cells can be detected according to the equations:

$$V_{OC} = V_{+} - V_{-}$$

$$V_{OC} = 4.1\ V - 1.76\ V = 2.34\ V,$$

Where V_{+} represents the potential of half-cell of GPS-LMPO@C P-electrode that equalized to 4.1 V, and V_{-} is the potential of GPS-MSTO@C N-electrode that equalized to 1.76 V.

Faraday's law is used to calculate the theoretical specific cell capacity of a cell in $mAhg^{-1}$.

$$Q_{theoretical} = (nF) / (3600*M_w)$$

Where, F is the Faraday constant, n is the number of charge carrier, and M_w is the molecular weight of the architect materials electrode surfaces. The $Q_{theoretical}$ for GPS-LMPO cathode-base electrode is found to be 171 mAh g^{-1}. Where, M_w of GPS-LMPO is 156.85 g mol^{-1}, n=1 and Li^+=1. F=96 485.3329 sA mol^{-1}. In addition, $Q_{theoretical}$ for common-used anodic electrode is as follows: nano-sized TiO_2= 335 mAh/g [Ref-S1-Ref-S3].

S11- A- (i) The contribution of each component of LMPO@C and MSTO@C super-architectonics built-in full cell specific capacity:

According to TG and EDS analyses, the relative composition contents of in cathode- and anode-based GPS super-architectonics are determined. The obtained results indicated the carbon content to be ~ 4.3 wt % in the LMPO@C compositions.

- Therefore, the theoretical specific capacity of LMPO@C P-electrode can be calculated as follows: ~ (335 mAh/g * 0.043 + 171 mAh/g * 0.9996) ~ 185.33 mAh/g.

S11- A- (ii) N-, and P-electrode cell capacity balancing

In fact, a significant effect of the N/P ratio on the electrochemical response is an important factor in full cell efficiency. The lithium plating during charging is firmly attached to N/P ratio. The lithium coating causes irreversibility and is assembled during cycling, ultimately reducing the loss of capacity, mechanical swelling and possibly a short inner circuit. To avoid the danger of metallic lithium plating, this is considered as retrospective aging process and safety, one should control the mass balancing capacity ratio of P- or N-electrode materials. The cell capacity is controlled by the key value of specific capacity of each of the P- or N-electrode materials presented in the LIB full cell [Ref-S4 -Ref. S6]. In this study, in order to reconcile these two contrast options, the LIB-Model is designed to extend 3D super-scalable full-scale GPS-LMPO@C//MSTO@C cathode//anode stacked layers pouch LIB-model under optimized mass loading and $((N:P)_{Cap}$ capacity ratio ≈ 1.02 – 1.1 :1.

- Assuming an ideal N / P ratio for positive and negative electrode materials in a manner commensurate with its conceptual strength, the ideal capacity ratio for the full scale model (GPS-LMPO@C//MSTO@C) is as follows: 171 Ah kg^{-1}/335 Ah kg^{-1} = 0.51
- Based on the calculation, for an ideal battery with 171 Ah of capacity, 1 kg of $LiMnPO_4$@C and 0.51 kg MSTO@C are required for design.
- The combined mass fraction of both P- and N-electrodes in the practical pouch LIB cell key-component constitutes (i.e., conductive electrolyte, polymeric membrane separator, current electrodes and package cortices, **see Figures S1**, is 34%, leading to that the full scale GPS-LIB with a specific capacity of ((171 Ah)/(1 kg+0.51 kg))/1.34 is about 84.5 Ah .kg^{-1}.

The theoretical mode of calculated specific energy of GPS-LMPO@C//MSTO@C battery can be quantified as equal to (2.34 V *84.5 Ah kg^{-1})= 197.7 Wh kg^{-1}.

S11- B - Practical method-based experimental sets of super-architectonics built-in LIBs

In galvanostatic cycling test (i.e., only at constant current), the graphically specific energy of super-architectonic built into the GPS-full-scale LIB can be detected from the charge–discharge voltage-capacity profile at 1C as follows:

- The specific energy for the GPS-LMPO@ C cathode (Wh/kg) is = the average working voltage of the super-architectonics built-in LIBs in (V) x maximum discharge capacity delivered by cell (Ahkg^{-1}).

- The specific capacity delivered by cell ($Ahkg^{-1}$) at 1C = 156.3 $Ahkg^{-1}$.
- The specific energy for the GPS-cathode (Wh/kg) = 2.6 V x 156.3 $Ahkg^{-1}$ =406.4 Wh/kg.
- Thus, the specific energy density of full-cell super-architectonic built into the GPS-full-scale LIB ($Whkg^{-1}$) = the estimated mass fraction of a cathode active material in a LIB cell (in pouch-type, mass fraction is 44% (see S1)) x Specific Energy for the cathode ($Whkg^{-1}$).

- **Therefore, practical value of the specific energy density of the GPS-LMPO@C//MSTO@C full-scale LIB is 178.8 $Whkg^{-1}$.**

S11-C- Key difference between experimental and theoretical calculations of specific energy density of full-scale GPS-LIBs

For both the intensive determination of specific energy density for the super-architectonic built into the GPS-full-scale LIB, the practical and theoretical values are of ***178.8 $Whkg^{-1}$ (practically) and 197.7 $Whkg^{-1}$ (theoretically)***, respectively. The low value of specific energy density in a practical determination may attributed to

(i) the Li^+-ions can't be completely removed from the N-electrode and P-electrode surface topographies, and

(ii) non-usable cutoff voltage profiles to clean-up N-electrode and P-electrode surface topographies to remove the rest Li^+ ion on the interlay complex super-architectonics, constraining the perfect charge-discharge rate.

The proposed GPS-MSTO@C//LMPO@C full-scale battery system integrates the latest advances in Li-battery technology to create a battery that delivers outstanding electrochemical performance.

S12. Optimization of full cell based $(N/P)_{Cap}$ balancing capacity ratio

As we mentioned before, The $(N/P)_{Cap}$ ratio of positive and negative electrode materials has significant effect on the efficiency of the full cell, as the formation of lithium plating/deposition along anode surfaces during a charging procedure firmly related to N/P ratio. As a side reaction, the lithium plating caused at anode N-electrode lead to the irreversible capacity. The accumulation of undesirable anode Li deposition during multiple cycles of charge-discharge voltage profiles leads to mechanical swelling, and possibly internal short-circuit along the anode surfaces. The electro-deposition during charging would intensively lead to capacity loss, and short-life cycle of LIBs. In this regards, to avoid the adverse effect of lithium metal plating, a slight oversizing of the mass loading capacity of anode ($(N:P)_{Cap}$ capacity balancing ratio ≈1.02–1.1: 1) is furthermore required for both battery safety and life-cycle [Ref-S5-S8]. Thus, an optimal tradeoff relationship between both key parameters is required as follows:

(i) safety betterment (i.e., which can be achieved by increasing the mass of N-electrode with $(N:P)_{Cap}$ ratio of >1:1), and

(ii) high specific energy storage (i.e., which can be achieved at equal capacities of N- and P-electrode, $(N:P)_{Cap}$ ratio of 1:1).

The current design configuration of the proposed GPS-MSTO@C (anode) // LMPO@-C (cathode) sets into bundled layer-by-layer pouch models under optimized $(N:P)_{Cap}$ ratio of ≈ 1.05 – 1.1 :1.

S13. The mass loading, areal capacity density and N/P capacity-ratio of GPS-MSTO@C//LMPO@C anode//cathode full-scale pouch LIB-model

Full-scale GPS-TO@C//LMPO@C sets of bundled layer-by-layer pouch models has dimensions of 35 mm (width), 55 mm (length) and ~ 3mm (thickness) and the stacking sequence of electrodes can be seen in following configuration

SS cathode | [DS anode| DS cathode|] DS anode | SS cathode

where SS=single side, DS = double sided, | = separator and [] = repeatable unit

The weight fraction calculation for sets of bundled layer-by-layer pouch model components were explained (Figure S2), and the required active mass of the GPS-LMPO@C-cathode and GPS-MSTO@C-anode are 2.79 g and 1.43 g respectively. In this large-scale design, well-packed and dense GPS-MSTO@C-anode (8-layers/14-sides, loaded on Cu-foil (8μm))// GPS-LMPO@C-cathode (7-layers/14-sides, loaded on Al-foil (12μm)) coin cells are contiguously connected into a series of the built-in stack layer configuration of pouch LIB-types. These designable optimizations may provide a compact LIB coin-cell module in pouch modes with a permanent flexible transport of electron/Li^+ ion during lithiation and delithiation cycling. The optimal electrode features in the super-architectonics built-in full-cell LIBs can be summarized as follows:

- The area for cathode and anode is selected with the following dimensions of (3*5=15 cm^2) and (3*4.75 = 14.3 cm^2), respectively.
- The total area of the cathode and anode coverage the pouch LIB cells are 210 and 200 cm^2; respectively.
- The mass stacking is 13.3 and 7.14 mg/cm^2 for cathode and anode, respectively.
- The areal discharge capacities are 0.85 Ah/cm^2 and 0.89 Ah/cm^2, of cathode and anode electrodes, respectively.
- The areal discharge capacity of N- and P-electrodes is determined at specific $(N:P)_{Cap}$ capacity ratio of 1.05:1.

S15. A comparison between the GPS-SSF@C half-scale LIB and the other reported $LiMnPO_4$ cathodes

To show evidence of the effectiveness of the super-architectonic GPS-LMPO@C and GPS-MSTO@C anode geometrics, building-blocks-in a wide-range of egress/ingress egress/ingress hierarchy, and super topographic-surface heterogeneity, roughness and anisotropy on the GPS-designated LIBs, we offer intensive studies of the key parameters in terms of rate capability, Coulombic efficiency, reversible capacity and long-term cycle stability of our GPS LIBs and other reported LIB designs, as one can see in Table S1-S3.

Table S1 A comparison between the GPS-LMPO (with SSF@C geometrics) half-scale LIB and normal and conventional LMPO cathode-LIBs

Cathode material	Nominal Voltage (V)	Cycles	Specific Capacity mA h g^{-1}	Coulombic efficiency	Ref
$LiMnPO_4$@C	4.1	retained ~100% of its reversible capacity after 100 cycles	155 At 0.5C	Not mentioned	**21**
$LiMnPO_4$@C	4.1	capacity retained 120 $mAhg^{-1}$ after 50 cycles	153.4 at 0.1C	Not mentioned	**37**
$LiMnPO_4$@C	4.1	capacity retained 89.1 $mAhg^{-1}$ after 500 cycles	147.9 at 1C	Not mentioned	**Ref-10**
$LiMnPO_4$	4.1	capacity retained 125 $mAhg^{-1}$ after 30 cycles	133 at 0.1 C	Not mentioned	**17**
$LiMnPO_4$@C (GPS-SSF@C)	4.1	Retains ~100% after 100 cycles	133 at 1C	~100%	**Current Work**

S16. A comparison between the GPS-MSTO@C half-scale LIB and the other reported TiO_2 anodes

Table S2 A comparison between the GPS-MSTO@C half-scale LIB and the other reported TiO_2 anodes.

Anode material	Nominal Voltage (V)	Cycles	Specific Capacity mA h g^{-1}	Coulombic efficiency	Ref
Rutile TiO_2	1.7	retained 50% of its reversible capacity after 100 cycles	250 At 0.1C	~ 100% after 100 cycles	**Ref [S11]**
Rutile TiO_2	1.5	retained 77% of its reversible capacity after 40 cycles	223 at 0.1C	Not mentioned after 100 cycles	**Ref [S12]**
Anatase TiO_2	1.73	76% of its initial capacity after 30 cycles at 0.2C	~ 300	Not mentioned	**Ref [S13]**
P25, a commercial titania powder from Degussa	1.7	61% of its initial capacity after 30 cycles at 0.2C	95	Not mentioned	**Ref [S13, S14]**
TiO_2	1.74	70% of its initial capacity after 100 cycles at 0.2C	270	Not mentioned	**Ref [S15]**
TiO_2	0.8	55% of its initial capacity after 30 cycles	310	~100%	**Ref [S16]**
TiO_2@C (GPS-MSTO@C)	1.7	87% of its initial capacity after 100 cycles at 1C	231	Not mentioned	**Current Work**

S17. A comparison between the GPS-SSF@C//MSTO@C full-cell LIB electrode system and the other reported $LiMnPO_4$//TiO_2 full cells

Table S3 A comparison between the GPS-SSF@C//MSTO@C full-cell LIB electrode system and the other reported $LiFePO_4$//TiO_2 and $LiMnPO_4$//TiO_2 full cells.

Cathode material	Anode material	Nominal Voltage (V)	Cycles	Specific Capacity mA h g^{-1}	Coulombic efficiency	Ref
$LiFePO_4$	Anatase TiO_2 hollow nanofibers	1.4	retained 88% of its reversible capacity after 300 cycles	103	> 99 %	**Ref [S17]**
$LiFePO_4$	Rutile TiO_2	1.8	retained 50% of its reversible capacity after 40 cycles	150	Not mentioned	**Ref [S18]**
$LiFePO_4$	Anatase TiO_2	1.6	81% of its initial capacity after 300 cycles at 20C	160	Not mentioned	**Ref [S19]**
$LiFePO_4$	anatase/graphene	1.6	700	127	~ 100%	**Ref [S20]**
LiFePO4	spinel $Li_4Ti_5O_{12}$/C	1.8	Retain 98.1% after 400 cycles	167	~100%	**Ref [S21]**
$LiFePO_4$	spinel $Li_4Ti_5O_{12}$	1.65	Retain 98.9% after 100 cycles	150	~100%	**Ref [S22]**
$LiMnPO_4$	$Li_4Ti_5O_{12}$	2.5	Retain ~100% after 300 cycles at C/2	105	~100%	**Ref [S23]**
$LiMnPO_4$@C (GPS-SSF@C)	TiO_2@C (GPS-MSTO@C)	2.6	Retains 77.5% after 2000 cycles at 1C	156.3	~100%	**Current Work**

S 18. Tap density of the super-architectonic GPS-$LiMnPO_4$@C cathode geometrics

Due to the increasing demand and the urgent need of the LIBs in the field of consumer electronics and EVs, an important characteristic is the tap density being exploited. The tap density was mainly influenced by the material morphology, particle size and the distribution of powder particles. Design of spherical particles was used to increase the tap-density. Developing new LMPO structures with both high rate performance and high tap density is challenging and appealing for the preparation of cathode materials [Ref-S24, Ref-S25].

To calculate the tap density of GPS-LMPO@C modulated LIBs, we used ZS-102 tap density meter (Liaoning Institute of Research Tools Co., Ltd.) to measure the tap density of the super-architectonics built-in LIB models. In such super-architectonic LIB models or modules, the optimal carbon content should not be more than 5%. The carbon content of SSF@C composites is found in the optimal range of about 4% (lower than 5%) [Ref-S26].

A powerful tool to develop the super architectonic engineering design of GPS-MSTO@C anodic and GPS-LMPO@C of geometric-SSF@C, -CSN@C and -NR@C cathode electrodes can be achieved by a rational mass-loading control. The high-density GPS SSF@C super-architectonics modulated LIBs shows excellent high rate performance, a high tap density (~1.51 g cm^{-3}) compared to 1.24 and 1.02 g cm^{-3} of GPS-CSN@C, and GPS-NR@C cathode geometrics, respectively. The finding indicates the effect of GPS complex super-architectonic SSF@C in its excellent electrochemical performance, particularly during the Li^{+}-insertion (cathodic, reduction, lithiation) /extraction (anodic, oxidation, delithiation) processes. Together, the GPS-SSF@C super-architectonics can be a potential candidate for high-performance LIBs.

Q3. From Fig. 7, the capacity of anode is almost double of the cathode in the full-cell configuration, isn't it a "waste" for the whole cell and decreasing the energy density?

A3- *We thank the reviewer for this comment. Per of your comment and avoid of any waste or decrease of the full cell energy density due to cell configuration, the key design configuration of built-in ordered set of full-scale super architectonic complexity GPS-SSF@C//MSTO@C cathode//anode hierarchy giant mesosponginess building blocks are fabricated in stacked layers pouch LIBs-type based on balancing between anode and cathode capacities under optimized mass loading (balancing N/P ratio), leading to contiguous charge/discharge rate, and a high energy density overcomes the energy-density limit required in the EV driving range. Please see this modification and additive to the following part of Results and discussion section, and supporting information as follows:*

(a) New parts have been added to results and discussion part including:

- *GPS cathode- and anode-electrode-geometrics-integrated full-scale LIBs (**Please see pages 27- 33**)*

(b) New sections have been added to supporting information part including:

- *S12. Optimization of full cell based (N/P)Cap balancing capacity ratio (**Please see page S24**)*
- *S13. The mass loading, areal capacity density and N/P capacity-ratio of GPS-MSTO@C//LMPO@C anode//cathode full-scale pouch LIB-model (**Please see page S25**)*

In Results and Discussion:

GPS cathode- and anode-electrode-geometrics-integrated full-scale LIBs

We designed fully functional multi-axial/dimension GPS cathode- and anode-electrode geometrics into the precisely defined full-cell LIB pattern model. In GPS-modulated LIB designs, we used MSTO@C GPS anode//SSF@C GPS cathode as the preferred N-electrode and P-electrode surface topographies, respectively (Fig. 7 and Scheme 3). The GPS complex architectonic SSF@C-cathode//MSTO@C-anode LIB surface topographies are specified into CR2032 coin-cell types (see supporting information S1). This GPS full-cell LIB design sheds light on the key influences of vast super architectonic complexity, geometrics, vacancies and surface topographies on the sets of bundled layer-by-layer pouch models and on large-scale LIB module configurations. These key factors of super-architectonic GPS-modulated LIB significantly affect the non-prescriptive cycle usages, heavily interior Li^{+} ion loads, spatial rate performance capabilities, specific energy density and high Coulombic efficiency. To approve our engineering

perspective of proposed GPS- SSF@C// GPS-MSTO@C full scale LIBs, we offer comprehensive comparison studies between the GPS-modulated-LIB and other designated $LiFePO_4//TiO_2$ and $LiMnPO_4//TiO_2$ LIB cells that previously reported, (see supporting information S17).

To calculate the super-architectonic GPS cell-energy density of full-scale LIB modules, the bundled layers of MSTO@C GPS anode//SSF@C GPS cathode electrodes are specified in pouch-LIB-model (see supporting information S14). The multiple bundled layers of incorporated amounts of GPS-MSTO@C (N-electrode anode) // GPS-SSF@C (P-electrode cathode) are 8-//7- layers, and along 14 surface topographic sides. These 8-anode//7-cathode surface topographic layers are substantially decorated with the 8 µm-Cu-foil and 12 µm-Al-foil platform electrodes, respectively. The GPS average working potential of GPS-MSTO@C (N-electrode anode) // GPS-SSF@C (P-electrode cathode) full-scale battery is 3.8 V, enabling highly practical specific energy-density of 178.8 $Whkg^{-1}$, in agreement to theoretical value of 197.7 $Whkg^{-1}$ for a full-scale GPS-LMPO@C//MSTO@C battery, (see more details studies of supporting information S11 A, B and C). The slight decrease of the practical energy density compared with its theoretical value of GPS-MSTO@C (N-electrode anode) // GPS-SSF@C (P-electrode cathode) full-scale LIB may be due to the difficulty to remove Li^+ ions completely during the fully-dynamic extraction. The full delithiation process of the occupant/truck Li^+ ion loads from the interfacial-scale of fully-accessed pocket storage requires cutoff voltage >3.0V.

Aiming to explore the safety and large timescale LIB-EV driving ranges with high power density, a model of full-scale GPS-MSTO@C (N-electrode anode) // GPS-SSF@C (P-electrode cathode) pouch LIBs is fabricated under optimization control of the mass-loading of N-anode and P-cathode electrodes and their ratio of capacity (i.e., balancing capacity of $(N/P)_{Cap}$ ratio). A set of full experiments is carried out for controlling a pouch model with optimal $(N/P)_{Cap}$ ratio, which leads to outstanding trade–off performance variability (see supporting information S12 - S14, and experimental section). Accordingly, the optimal accuracy of the mass-fraction of SSF@C GPS cathode components formulated in a pouch LIB model is about 44%, leading to specific energy density of the GPS-TO@C//LMPO@C full-scale LIB of 178.8 $Whkg^{-1}$.

For reliable structural design of large scale LIB modules, the volumetric energy density is ideal parameter of LIB engineering perspective (see supporting S14). The structural GPS-building-blocks-in 18650-cylinder and bundled-layers of pouch models offer volumetric energy density of MSTO@C GPS-anode//LMPO@C GPS-cathode full-scale CR2032 LIB-module of 435.63 Wh/L and 247.68 Wh/L, respectively. Although, the GPS-modulated 18650-cylinders produce highly recognizable value, the bundled layer-by-layer pouch models represent the practical and optimal engineering designs for a wide range of electrochemical performances.

The mutual balancing capacity of $(N/P)_{Cap}$ ratio of super-architectonic GPS-MSTO@C (N-electrode anode) // GPS-SSF@C (P-electrode cathode) LIB-modules offers areal discharge capacity of 0.89 and 0.85 Ah/cm^2, respectively. The optimization of areal discharge capacity performance super-architectonic built-in pouch LIB models would be a more rational choice for the most effective solutions in terms of high specific energy density yet with large safety factors of the proposed super-architectonic GPS-built-in pouch LIB models. Such super-architectonic GPS-built-in LIBs are promising to enhance betterment of safety factor issues for GPS-LIB-powered engineering modules.

The stability of the super-architectonic built-in SSF@C GPS-cathode // MSTO@C GPS-anode full-scale geometric and surface topographic LIB models is investigated by studying its discharge cycle performance as shown in Fig. 7(a). The architectonic GPS-modulated-LIB model retains 90.0 % of its first cycle discharge capacity after 100 cycles at 1 C. Figure 7(a) shows the typical first cycle of charging/discharging

voltage patterns of full-scale GPS-modulated-LIB model cycles at C-rate range from 0.1 C to 20 C by applying a voltage range from 1.5V to 3.8V. The results reveal that the values of super-architectonic GPS-modulated LIB discharging capacities decrease with C-rate upsurge (i.e., from 0.1 to 20 C). The super-architectonic GPS-modulated LIB full-cell is maintained the discharge capacity of 108.3 $mAhg^{-1}$ at 20 C for its initial performance value.

The super-architectonic GPS-modulated LIB capability rates are investigated at the voltage range from 1.5 to 3.8 V and the C-rate range from 0.1 C – to 5 C, then back to C-rate of 0.1 C and 10 C, and finally back to 1 C and 20 C, with continuous operation of cycling variation up to 100 cycles at each recorded C-rate (Figure 7c). The super-architectonic specific capacity of the full-cell SSF@C GPS-cathode//MSTO@C GPS-anode geometrics and surface topographies is decreased with an increase in the current rate. Feasible discharge capacity of a multiple cycles and C-rates indicates the superstructure effect on the overall scales of GPS-modulated-LIBs. The complex super-architectonics of SSF@C GPS-cathode // MSTO@C GPS-anode full-scale models or modules create ever-changing charge/discharge contributory usage of cycles, "fully cycled dynamics," affordable on-off-site storage modules, and super-large gate-in-transport of electron/Li^+-ion trails. Our finding indicates that the GPS P-cathode/N-anode electrodes integrated into full-scale CR2032 coin-cells are potential candidates to achieve the high power energy modules for LIB-EVs.

Fig. 7& Scheme 3

Super-architectonic GPS Coulombic efficacy (CE) of full-scale SSF@C GPS-cathode // MSTO@C GPS-anode models describes the charge efficiency, by which Li^+ ions/electrons are transferred into powerful GPS multiple orientations and super-surface topographies of our distinguishable super-architectonic batteries. CE is the effective ratio between the total values of extracted and inserted charging from the distinct super-architectonic GPS-battery over one-full-cycle. For developing a scalar optimization perspective of GPS-modulated LIB-EVs, we investigate a fast-charging pattern of architectonic bundled-layers of GPS-MSTO@C (N-electrode anode) // GPS-SSF@C (P-electrode cathode) pouch models by applying constant current and voltage (named as CC-CV) protocol. A set of fast-charging experiments is recorded for GPS-modulated-LIB pouch models at different C-rate values, ranging from 1C to 10C, and temperature between 25°C to 35°C (see supporting information S19 & Figure S13). The CC-charging timescale decays with an increase of the charging rate in the applying range from 1C to 5C. The CC-charging timescale dependent sets at C-rate > 5C are not recognizable conditions. Therefore, the CV-charging timescale dependent sets are efficient, reliable, and quantifiable at the range of C-rate variabilities (see Fig. S13). The formation of long, stable static-flat plateau of CV-charging timescale (i.e. approximately 10 to 12 minutes) at C-rate > 5C is recognizable with a contribution of the surface-elevated temperature at 35°C as a maximal value. The fast CV-charging timescale ≥ 5 minutes can be optimized at C-rate range ~~of~~ from 1C to 4C, respectively. Under an ever-increasing demand on reliable and fast time-scale charge capacity, the super-architectonic GPS-MSTO@C (N-electrode anode) // GPS-SSF@C (P-electrode cathode) pouch models and modules are powerful in Li^+ ion diffusion regimes, and improving hovering electron density for high-speed discharging and charging rates.

The multi-criteria optimization of outstanding cycle performance, long-term stability, and Coulombic efficacy of full-scale super-architectonic GPS-MSTO@C (N-electrode anode) // GPS-SSF@C (P-electrode cathode) models and modules is studied at C-rate of 1C within 2000 cycles between 1.5V and 3.8 V vs. Li/Li^+ (Fig. 7d). Note, the magnification of the first 200 cycles of the charging/discharging performance is recorded in Figure 7e. The super-architectonic GPS-modulated LIB model retains 77.5% specific discharging capacity from its original value of 156.3 $mAhg^{-1}$ after 2000 cycles, and Coulombic efficacy of approximately 99.6% at C-rate of 1C, and at 25°C. For a wide range of charging/discharging cycles (i.e.,

>2000 cycles), the super-architectonic full-scale GPS-modulated LIB model is attained approximately 100% of its Coulombic efficacy. In general, the complex super-architectonic full-scale GPS-modulated LIB models demonstrate an outstanding structural design stability, high specific charging/discharging capacity, high rate capability, high-speed discharging and charging rates and long cycle life (see Scheme 3 and Figure 7).

Scheme 3A shows the simulated 3D projection of robust full-scale design optimization of GPS SSF@C GPS-cathode // MSTO@C GPS-anode full-scale architectonics after discharge capacity cycles. The systematic projection represents the powerful structural stability of super-architectonic GPS-building-blocks-in a wide-range of 3D distinguishable orientation geometrics, egress/ingress vacancy models, and super topographic-surfaces after a number of charging/discharging cycles (i.e.≥ 2000) (Scheme 3B). The super-architectonic SSF@C GPS-cathode // MSTO@C GPS-anode platform electrodes provide built-in full-cell GPS-integrated LIBs with four key features.

First, multi-dimensional electron/Li^+-ion mobility is occurred as a result of including many GPS-building-blocks-in egress/ingress pathways along the upper, middle, and lower multi-zone crystal surface geometrics, as well as along the frontal edge/apex/central crystal sites. For instance, the SSF@C GPS-cathode with a top-upper square-based pyramid structure offers four-facet exposure surfaces that enable the diffusion of electrons/Li ions along the central site crystals, multi-edges, vertices, kinks, steps, and upper-top-zone surfaces (Scheme 3B).

Second, GPS-heavily interior loads, movements and diffusions of Li^+ ion along the axial directions and axis of coordinates (i.e. lateral, vertical, circular, zigzag, and longitudinal axes) ensured the mobility of electrons/Li^+ ions along the peripheral top electrode surfaces.

Third, the super-architectonic diffusion gates into the interlaid-complex vacancies, such as caves, holes, nests, windows, canals, ridges, cavities, and pipes may create GPS-modulated LIBs with superb specific capacities, high energy density, high-speed discharging/discharging rates, and extended long-term power stability.

Fourth, the loophole-on-surfaces with different topographies and curvatures including ripples, winglets, protuberances, irregular bumps, V-hooks, undulations, and anticlines are key roles in retaining LIBs, ensuring the continuous function and stability of electron/Li^+-ion transport pathways after 2000 cycles, and assuring the simultaneous diffusion of Li^+-ions during the lithiation/delithiation (discharging/charging) cycling processes for SSF@C GPS-cathode // MSTO@C GPS-anode full-scale architectonics.

The super-architectonic built-in SSF@C GPS-cathode // MSTO@C GPS-anode full-scale LIB model shows its excellent Li^+-ion egress/ingress capacity with high rate velocity, on-/off-site storage modules, and super-large door-in transport of Li^+-ion/electron during discharging (insertion, lithiation) and charging (delithiation, extraction) processes. Furthermore, the super-architectonic GPS proximity of Li^+ ion accessible loophole-on-surfaces and open-gate-in-transports is one of the most effective solutions to avoid geometric and surface topographic polarization and to boost the fully-cycled dynamics during discharge (insertion, lithiation) / charge (delithiation, extraction) processes. These GPS tectonic-power-driven SSF@C GPS-cathode // MSTO@C GPS-anode geometrics offer highly reversible capacity rate of LIBs, and structural stability to withstand under high-temperature environments.

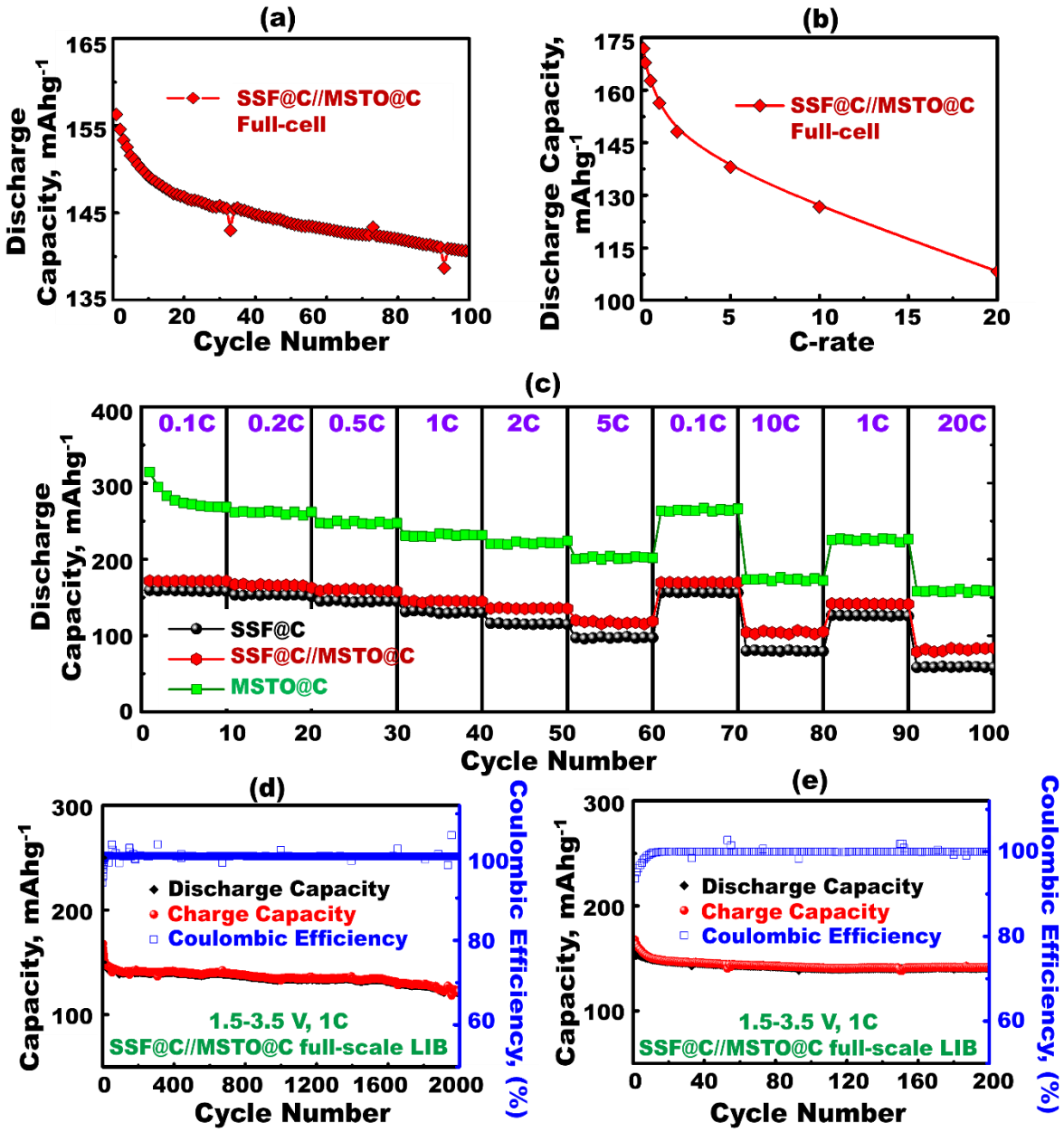

Fig. 7(a) Cycling performance of powerful complex super-architectonic full-scale SSF@C GPS-cathode // MSTO@C GPS-anode LIB-modulated LIB models for first 100 cycles. **(b)** Behavior of specific discharge capacity in $mAhg^{-1}$ versus current C-rates at 0.1C, 0.2C, 0.5C, 1C, 2C, 5C, 10C and 20C, in potential region from 1.5 to 3.8V vs. Li/Li^+ for SSF@C//MSTO@C full-scale LIB-model. **(c)** Performance and behavior of the rate capability of SSF@C GPS-cathode // MSTO@C GPS-anode LIB-modulated LIB models over a range from 1.5 to 3.8V at various current rates from 0.1C to 20C. **(d)** Long term cycling performance (stability) and coulombic efficacy for SSF@C GPS-cathode // MSTO@C GPS-anode LIB-modulated LIB models, at rate of 1C up to 2000 cycles, in a voltage range from 1.5 to 3.8V at 25°C. The magnification of first 200 cycles is exhibited in **Fig. 7(e)**.

In Supporting Information:

S12. Optimization of full cell based $(N/P)_{Cap}$ balancing capacity ratio

As we mentioned before, The $(N/P)_{Cap}$ ratio of positive and negative electrode materials has significant effect on the efficiency of the full cell, as the formation of lithium plating/deposition along anode surfaces during a charging procedure firmly related to N/P ratio. As a side reaction, the lithium plating caused at anode N-electrode lead to the irreversible capacity. The accumulation of undesirable anode Li deposition during multiple cycles of charge-discharge voltage profiles leads to mechanical swelling, and possibly internal short-circuit along the anode surfaces. The electro-deposition during charging would intensively lead to capacity loss, and short-life cycle of LIBs. In this regards, to avoid the adverse effect of lithium metal plating, a slight oversizing of the mass loading capacity of anode ($(N:P)_{Cap}$ capacity balancing ratio ≈1.02–1.1: 1) is furthermore required for both battery safety and life-cycle [Ref-S5-S8]. Thus, an optimal tradeoff relationship between both key parameters is required as follows:

(iii) safety betterment (i.e., which can be achieved by increasing the mass of N-electrode with $(N:P)_{Cap}$ ratio of >1:1), and

(iv) high specific energy storage (i.e., which can be achieved at equal capacities of N- and P-electrode, $(N:P)_{Cap}$ ratio of 1:1).

The current design configuration of the proposed GPS-MSTO@C (anode) // LMPO@-C (cathode) sets into bundled layer-by-layer pouch models under optimized $(N:P)_{Cap}$ ratio of ≈ 1.05 – 1.1 :1.

S13. The mass loading, areal capacity density and N/P capacity-ratio of GPS-MSTO@C//LMPO@C anode//cathode full-scale pouch LIB-model

Full-scale GPS-TO@C//LMPO@C sets of bundled layer-by-layer pouch models has dimensions of 35 mm (width), 55 mm (length) and ~ 3mm (thickness) and the stacking sequence of electrodes can be seen in following configuration

SS cathode | [DS anode| DS cathode|] DS anode | SS cathode

where SS=single side, DS = double sided, | = separator and [] = repeatable unit

The weight fraction calculation for sets of bundled layer-by-layer pouch model components were explained (Figure S2), and the required active mass of the GPS-LMPO@C-cathode and GPS-MSTO@C-anode are 2.79 g and 1.43 g respectively. In this large-scale design, well-packed and dense GPS-MSTO@C-anode (8-layers/14-sides, loaded on Cu-foil (8μm))// GPS-LMPO@C-cathode (7-layers/14-sides, loaded on Al-foil (12μm)) coin cells are contiguously connected into a series of the built-in stack layer configuration of pouch LIB-types. These designable optimizations may provide a compact LIB coin-cell module in pouch modes with a permanent flexible transport of electron/Li^+ ion during lithiation and delithiation cycling. The optimal electrode features in the super-architectonics built-in full-cell LIBs can be summarized as follows:

- The area for cathode and anode is selected with the following dimensions of (3*5=15 cm^2) and (3*4.75 = 14.3 cm^2), respectively.
- The total area of the cathode and anode coverage the pouch LIB cells are 210 and 200 cm^2; respectively.
- The mass stacking is 13.3 and 7.14 mg/cm^2 for cathode and anode, respectively.
- The areal discharge capacities are 0.85 Ah/cm^2 and 0.89 Ah/cm^2, of cathode and anode electrodes, respectively.
- The areal discharge capacity of N- and P-electrodes is determined at specific $(N:P)_{Cap}$ capacity ratio of 1.05:1.

Q4. A "fast charge" mode should be tested to see the battery performance, especially the full-cell configuration.

A4- *We appreciate the reviewer comment and thank him for this nice view. Per of this important comment the fast charge is highlighted in the manuscript and new section was added to supporting information as follows:*

(a) In the results and discussion:

- *The following results was added (**Please see page 30**)*

The fast CV-charging timescale ≥ 5 minutes can be optimized at C-rate range ~~of~~ from 1C to 4C, respectively. Under an ever-increasing demand on reliable and fast time-scale charge capacity, the super-architectonic GPS-MSTO@C (N-electrode anode) // GPS-SSF@C (P-electrode cathode) pouch models and modules are powerful in Li^+ ion diffusion regimes, and improving hovering electron density for high-speed discharging and charging rates.

(b) New sections have been added to supporting information part including:

- *S19. Fast charge process for GPS-LIBs (**Please see pages S31, and S32**)*

S19. Fast charge process for GPS-LIBs

Developing fast-charging protocols for LIBs is a key issue for a wider deployment of EVs and portable electrical devices. Fast-charging of LIBs was investigated with different protocols namely the normal constant current / constant voltage (CC-CV) method and ohmic-drop compensation ODC method. The ODC method can be carried out with an extended constant current period as a result of the high limit voltage based on the ohmic-drop compensation principle.

Herein, fast charge of the GPS-modulated-LIB pouch models can be determined by CC-CV method under specific conditions. In this CC-CV protocol, the charging C-rate is usually increased; leading to the total charging time is decreased. Indeed, at higher C-rate the CC stages are extremely short compared to shorter one. This latter phenomenon is related to the larger contribution of the ohmic drop when the current C-rate increases. Under this basic observation with most of designated LIBs, the fast battery charging process is performed absolutely at CV stage when the C-rate becomes too high (see Figure S13).

Our designed 3D super-scalable GPS-TO@C//LMPO@C anode//cathode full-scale sets of bundled layer-by-layer pouch models was fast charged using CC-CV protocol for C-rate ranging from 1C to 10C. The fast-charging pattern of architectonic bundled layer-by-layer GPS-MSTO@C (N-electrode anode) // GPS-SSF@C (P-electrode cathode) pouch models is applied a constant current and voltage (named as CC-CV) protocol. A set of fast-charging experiments is recorded for GPS-modulated-LIB pouch models at different C-rate values, ranging from 1C to 10C, and at a range of temperature of 25-35 ^oC (see Figure S13). The CC-charging timescale decays with increasing of the charging rate in the applying range of 1C to 5C. The CC-charging-depended timescale sets at C-rate > 5C is not recognizable conditions; thereby the CV-charging-depended timescale sets are efficient, reliable, quantifiable means at a range of C-rate variability (see Fig. S13). The formation of long, stable static-flat plateau of CV-charging timescale (i.e. ~10-12 minutes) at C-rate > 5C is recognizable with a contribution of the surface-elevated temperature at 35 ^oC as a maximal value.

The fast CV-charging timescale ≥ 5 minutes can be optimized at C-rate range of 1C-4C, respectively. Under an ever increasing demand on reliable, fast time-scale charge capacity, the super-architectonic GPS-MSTO@C (N-electrode anode) // GPS-SSF@C (P-electrode cathode) pouch models and modules are powerful Li-ion diffusion regimes, and improving hovering electron density for high-speed discharging and charging rates (see Figure S13).

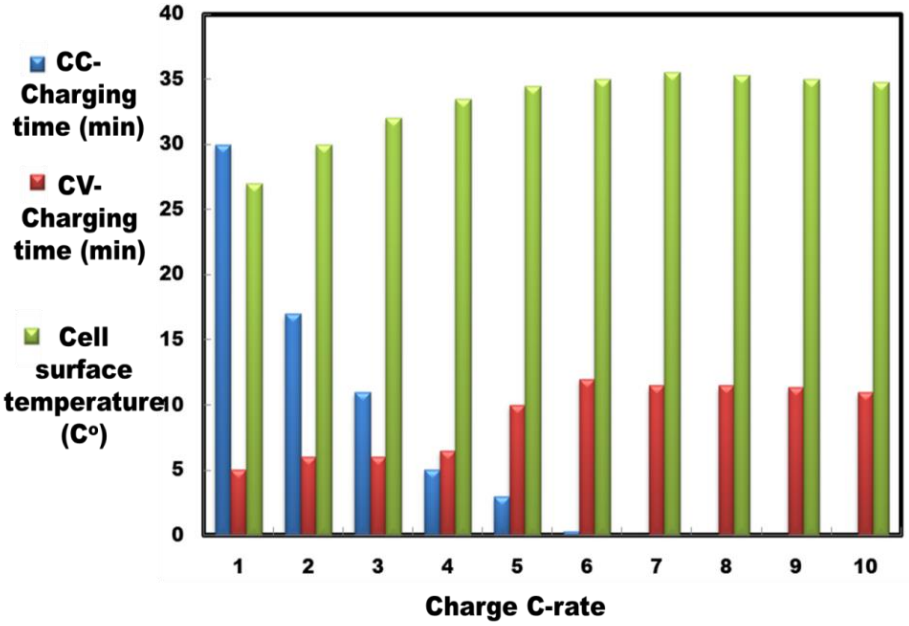

Fig. S13. Schematic diagram of charging time of GPS-modulated-LIB pouch models until 100% of (SOC) state-of-charge using normal CC-CV method. CC stages are in the blue color while CV stages are in the red color. Green color-bar shows the maximum outer surface temperatures elevation of the cell.

5. There are some spell error or typos throughout the manuscript, for example

(1) there should be space between number and unit;

(2) some the temperature unit in "Fabrication of LMPO@C cathodes and MSTO@C anode architectonic mesosponginess";

(3) "power" should be "powder" in "The power MSTO@C (anode) and SSF@C, CSN@C, and NR@C (cathodes) built-up electrode sets in the half-cell anode or cathode";

(4) please double-check other parts

We appreciate the reviewer comment. Per of this comment the whole manuscript and supporting information sections were revised thoroughly and modified to avoid all of these typo.

Reviewer #2:

We really would like to acknowledge the reviewer comments and efforts.

This manuscript reported that the design porous structure materials can be used as electrode materials for Lithium ion battery. It is very interesting topic. But I did not think it is good study.

Q1- **First** of all, the porous materials is not good for electrode as the coulomb efficiency must be very low. In the manuscript it is not any things about CE.

A1- *We appreciate and thank the reviewer for his comment. Per of this comment more information and discussion related to the material merits have been added, also we have shadow a light on the CE for GPS-full scale LIB; Please see this additive to the main text, and supporting information as following:*

(a) New parts have been added to results and discussion part including:

- *Control synthesis of complex super-architectonics (GPS) cathode-/anode-geometrics (**Please see pages 12- 14**)*
- *Material* super-architectonics merits *(**Please see pages 16, 17**)*
- *Modification in "GPS cathode geometrics for half-cell GPS-modulated LIB models" section (**Please see pages 19- 23**)*
- *GPS cathode- and anode-electrode-geometrics-integrated full-scale LIBs (**Please see pages 27-32**)*

(b) New sections have been added to supporting information part including:

- *S S11. Super architectonic specific energy density of GPS-modulated full-scale LIB-model (**Please see pages S 21-S23**)*
- *S12. Optimization of full cell based (N/P)Cap balancing capacity ratio (**Please see page S24**)*
- *S13. The mass loading, areal capacity density and N/P capacity-ratio of GPS-MSTO@C//LMPO@C anode//cathode full-scale pouch LIB-model (**Please see page S25**)*
- *S15. A comparison between the GPS-SSF@C half-scale LIB and the other reported LiMnPO4 cathodes (**Please see page S 27**)*
- *S16. A comparison between the GPS-MSTO@C half-scale LIB and the other reported TiO_2 anodes(**Please see page S 28**)*
- *S17. A comparison between the GPS-SSF@C//MSTO@C full-cell LIB electrode system and the other reported $LiMnPO_4$//TiO_2 full cells (**Please see page S 29**)*

A combination of the finite GPS perspective and topographic space volumes, in general, offers GPS electrodes with fully-access-surfaces, free-space dynamic environments, and multi-scale building-blocks egress/ingress pathways including;

(i) multi-diffusive open-pore hole systems, connective meso-macroscopic windows along the entire and randomly dispersed NRs, CNS sheets and layers, and SSF-tower-star complex,

(ii) GPS building architects "block-by-block" with a large density of exposed active facets surface (containing numerous sites of connective multi-diffusible dimensions of the exposed bubbly meso-macro-free spaces open-pore system), and

(iii) multi-vast-mouth vacancies in highly-dense mesopores and mesogrooves, inter-trapped free occupation mesocage cavities, ridge-gate windows, cave nests, and intra-formational smooth shell/belt-walled/rounded fence-rims along the GPS surfaces.

These vast free surface-volume spaces can accommodate and enhance the multicentral dimensionality diffusion of Li^+-ions through their discharge (insertion, lithiation)/charge(delithiation, extraction) processes and their transfer along the electrolyte/electrode interfaces (Scheme 2).

Regarding to CE ***(Please see pages 30, and 31)*** *as follows:*

Super-architectonic GPS Coulombic efficacy (CE) of full-scale SSF@C GPS-cathode // MSTO@C GPS-anode models describes the charge efficiency, by which Li^+ ions/electrons are transferred into powerful GPS multiple orientations and super-surface topographies of our distinguishable super-architectonic batteries. CE is the effective ratio between the total values of extracted and inserted charging from the distinct super-architectonic GPS-battery over one-full-cycle. For developing a scalar optimization perspective of GPS-modulated LIB-EVs, we investigate a fast-charging pattern of architectonic bundled-layers of GPS-MSTO@C (N-electrode anode) // GPS-SSF@C (P-electrode cathode) pouch models by applying constant current and voltage (named as CC-CV) protocol. A set of fast-charging experiments is recorded for GPS-modulated-LIB pouch models at different C-rate values, ranging from 1C to 10C, and temperature between 25°C to 35°C (see supporting information S19 & Figure S13). The CC-charging timescale decays with an increase of the charging rate in the applying range from 1C to 5C. The CC-charging timescale dependent sets at C-rate > 5C are not recognizable conditions. Therefore, the CV-charging timescale dependent sets are efficient, reliable, and quantifiable at the range of C-rate variabilities (see Fig. S13). The formation of long, stable static-flat plateau of CV-charging timescale (i.e. approximately 10 to 12 minutes) at C-rate > 5C is recognizable with a contribution of the surface-elevated temperature at 35°C as a maximal value. The fast CV-charging timescale ≥ 5 minutes can be optimized at C-rate range ~~of~~ from 1C to 4C, respectively. Under an ever-increasing demand on reliable and fast time-scale charge capacity, the super-architectonic GPS-MSTO@C (N-electrode anode) // GPS-SSF@C (P-electrode cathode) pouch models and modules are powerful in Li^+ ion diffusion regimes, and improving hovering electron density for high-speed discharging and charging rates.

The multi-criteria optimization of outstanding cycle performance, long-term stability, and Coulombic efficacy of full-scale super-architectonic GPS-MSTO@C (N-electrode anode) // GPS-SSF@C (P-electrode cathode) models and modules is studied at C-rate of 1C within 2000 cycles between 1.5V and 3.8 V vs. Li/Li^+ (Fig. 7d). Note, the magnification of the first 200 cycles of the charging/discharging performance is recorded in Figure 7e. The super-architectonic GPS-modulated LIB model retains 77.5% specific discharging capacity from its original value of 156.3 $mAhg^{-1}$ after 2000 cycles, and Coulombic efficacy of approximately 99.6% at C-rate of 1C, and at 25°C. For a wide range of charging/discharging cycles (i.e., >2000 cycles), the super-architectonic full-scale GPS-modulated LIB model is attained approximately 100% of its Coulombic efficacy. In general, the complex super-architectonic full-scale GPS-modulated LIB models demonstrate an outstanding structural design stability, high specific charging/discharging capacity, high rate capability, high-speed discharging and charging rates and long cycle life (see Scheme 3 and Figure 7).

Q2- Second the tap density of porous structure will be low. It is not any discussion about it.

A2- *We appreciate and thank the reviewer for his comment. Per of this comment the tap density is added; Please see this additive to the supporting information (S.18,* ***Please see page S30****) as follows:*

S 18. Tap density of the super-architectonic GPS-$LiMnPO_4$@C cathode geometrics

Due to the increasing demand and the urgent need of the LIBs in the field of consumer electronics and EVs, an important characteristic is the tap density being exploited. The tap density was mainly influenced by the material morphology, particle size and the distribution of powder particles. Design of spherical particles was used to increase the tap-density. Developing new LMPO structures with both high rate performance and high tap density is challenging and appealing for the preparation of cathode materials [Ref-S24, Ref-S25].

To calculate the tap density of GPS-LMPO@C modulated LIBs, we used ZS-102 tap density meter (Liaoning Institute of Research Tools Co., Ltd.) to measure the tap density of the super-architectonics built-in LIB models. In such super-architectonic LIB models or modules, the optimal carbon content should not be more than 5%. The carbon content of SSF@C composites is found in the optimal range of about 4% (lower than 5%) [Ref-S26].
A powerful tool to develop the super architectonic engineering design of GPS-MSTO@C anodic and GPS-LMPO@C of geometric-SSF@C, -CSN@C and -NR@C cathode electrodes can be achieved by a rational mass-loading control. The high-density GPS SSF@C super-architectonics modulated LIBs shows excellent high rate performance, a high tap density (~1.51 g cm^{-3}) compared to 1.24 and 1.02 g cm^{-3} of GPS-CSN@C, and GPS-NR@C cathode geometrics, respectively. The finding indicates the effect of GPS complex super-architectonic SSF@C in its excellent electrochemical performance, particularly during the Li^{+}-insertion (cathodic, reduction, lithiation) /extraction (anodic, oxidation, delithiation) processes. Together, the GPS-SSF@C super-architectonics can be a potential candidate for high-performance LIBs.

Q3- Third it is not good writing. In the main text, the advantages of the structure was listed, but there is not experimental supported, such the Li ion transfer number and the exchange current density.
A3- We appreciate this valuable comment. Per of this comment, the specific energy density, N-, and P-electrode cell capacity balancing, experimental and theoretical calculations of specific energy density, Optimization of full cell based $(N/P)_{Cap}$ balancing capacity ratio, and estimation of volumetric energy density have been highlighted and added; Please see this additive to the supporting information (S.11- S 16) as follows:

- *S11. Super architectonic specific energy density of GPS-modulated full-scale LIB-model* ***(Please see pages S 21-S23)***
  - Theoretical calculation of GPS specific energy density: ***(Please see page S21)***
  - S11- A- (i) The contribution of each component of LMPO@C and MSTO@C super-architectonics built-in full cell specific capacity: ***(Please see page S21)***
  - S11- A- (ii) N-, and P-electrode cell capacity balancing: ***(Please see page S22)***
- S11- B - Practical method-based experimental sets of super-architectonics built-in LIBs ***(Please see page S22)***
- S11-C- Key difference between experimental and theoretical calculations of specific energy density of full-scale GPS-LIBs ***(Please see page S23)***
- S12. Optimization of full cell based $(N/P)_{Cap}$ balancing capacity ratio ***(Please see page S24)***
- S13. The mass loading, areal capacity density and N/P capacity-ratio of GPS-TO@C//LMPO@C anode//cathode full-scale pouch LIB-model ***(Please see page S25)***
- S14. GPS volumetric energy density of super-architectonics built-in LIB-designs ***(Please see page S26)***

Q4- Fourth, the quality of image is too poor.
A4- We thank the reviewer for his comment. All figures have been provided with high quality.

Q5- Fifth the capacitance of porous materials is not compared with the normal or commercialization or theoretical capacity.

A5- We would like to thank reviewer for this comment. Per of this comment please see this additive in supporting information as following:

S13(A,B and C) and comparisons S17-S19,

- S11. Calculating processes of specific energy density of GPS-(MSTO@C// LMPO@C) full-scale LIB-model ***(Please see page S20- S22)****; which* includ The contribution of each component of LMPO@C and MSTO@C architectural-design building-blocks-in full cell specific capacity: ***(Please see page S20)***, (ii) N-, and P-electrode cell capacity balancing ***(Please see page S21)***, B - Practical method-based experimental sets of architectural-design building-blocks-in LIBs ***(Please see page 22)****, and* C- Key difference between experimental and theoretical calculations of specific energy density of full-scale LIBs ***(Please see page 22)***
- *S11. Super architectonic specific energy density of GPS-modulated full-scale LIB-model* ***(Please see pages S 21-S23)*** *Including:*
  - Theoretical calculation of GPS specific energy density: ***(Please see page S21)***
  - S11- A- (i) The contribution of each component of LMPO@C and MSTO@C super-architectonics built-in full cell specific capacity: ***(Please see page S21)***
  - S11- A- (ii) N-, and P-electrode cell capacity balancing: ***(Please see page S22)***
  - S11- B - Practical method-based experimental sets of super-architectonics built-in LIBs ***(Please see page S22)***
  - S11-C- Key difference between experimental and theoretical calculations of specific energy density of full-scale GPS-LIBs ***(Please see page S23)***
- *S15. A comparison between the GPS-SSF@C half-scale LIB and the other reported LiMnPO4 cathodes* ***(Please see page S 27)***
- *S16. A comparison between the GPS-MSTO@C half-scale LIB and the other reported TiO_2 anodes****(Please see page S 28)***
- *S17. A comparison between the GPS-SSF@C//MSTO@C full-cell LIB electrode system and the other reported $LiMnPO_4$//TiO_2 full cells* ***(Please see page S 29)***

S11. Super architectonic specific energy density of GPS-modulated full-scale LIB-model

The calculation and quantification methods for specific energy density of GPS-(MSTO@C N-anode// GPS-LMPO@C P-cathode full-scale LIBs are carried out based on the expected theoretical model and real experiment sets of the super-architectonic contents of the LMPO@C and MSTO@C P-cathode and N-anode electrodes-modulated into full-scale LIBs. Here, we provide intensive studies based on the theoretical and practical or experimental models as follows:

A- Theoretical calculation of GPS specific energy density:

In the designed integrated super-architectonic built into the GPS-full-scale LIB, the nominal open circuit voltage (V_{OC}) along P-cathode and N-anode electrodes-modulated CR2032 coin cells can be detected according to the equations:

$$V_{OC} = V_{+} - V_{-}$$

$$V_{OC} = 4.1\ V - 1.76\ V = 2.34\ V,$$

Where V_{+} represents the potential of half-cell of GPS-LMPO@C P-electrode that equalized to 4.1 V, and V_{-} is the potential of GPS-MSTO@C N-electrode that equalized to 1.76 V.

Faraday's law is used to calculate the theoretical specific cell capacity of a cell in $mAhg^{-1}$.

$$Q_{theoretical} = (nF) / (3600*M_w)$$

Where, F is the Faraday constant, n is the number of charge carrier, and M_w is the molecular weight of the architect materials electrode surfaces. The $Q_{theoretical}$ for GPS-LMPO cathode-base electrode is found to be 171 mAh g^{-1}. Where, M_w of GPS-LMPO is 156.85 g mol^{-1}, n=1 and Li^+=1. F=96 485.3329 sA mol^{-1}. In addition, $Q_{theoretical}$ for common-used anodic electrode is as follows: nano-sized TiO_2= 335 mAh/g [Ref-S1-Ref-S3].

S11- A- (i) The contribution of each component of LMPO@C and MSTO@C super-architectonics built-in full cell specific capacity:

According to TG and EDS analyses, the relative composition contents of in cathode- and anode-based GPS super-architectonics are determined. The obtained results indicated the carbon content to be ~ 4.3 wt % in the LMPO@C compositions.

- Therefore, the theoretical specific capacity of LMPO@C P-electrode can be calculated as follows: ~ (335 mAh/g * 0.043 + 171 mAh/g * 0.9996) ~ 185.33 mAh/g.

S11- A- (ii) N-, and P-electrode cell capacity balancing

In fact, a significant effect of the N/P ratio on the electrochemical response is an important factor in full cell efficiency. The lithium plating during charging is firmly attached to N/P ratio. The lithium coating causes irreversibility and is assembled during cycling, ultimately reducing the loss of capacity, mechanical swelling and possibly a short inner circuit. To avoid the danger of metallic lithium plating, this is considered as retrospective aging process and safety, one should control the mass balancing capacity ratio of P- or N-electrode materials. The cell capacity is controlled by the key value of specific capacity of each of the P- or N-electrode materials presented in the LIB full cell [Ref-S4 -Ref. S6]. In this study, in order to reconcile these two contrast options, the LIB-Model is designed to extend 3D super-scalable full-scale GPS-LMPO@C//MSTO@C cathode//anode stacked layers pouch LIB-model under optimized mass loading and $((N:P)_{Cap}$ capacity ratio ≈ 1.02 – 1.1 :1.

- Assuming an ideal N / P ratio for positive and negative electrode materials in a manner commensurate with its conceptual strength, the ideal capacity ratio for the full scale model (GPS-LMPO@C//MSTO@C) is as follows: 171 Ah kg^{-1}/335 Ah kg^{-1} = 0.51
- Based on the calculation, for an ideal battery with 171 Ah of capacity, 1 kg of $LiMnPO_4$@C and 0.51 kg MSTO@C are required for design.
- The combined mass fraction of both P- and N-electrodes in the practical pouch LIB cell key-component constitutes (i.e., conductive electrolyte, polymeric membrane separator, current electrodes and package cortices, **see Figures S1**, is 34%, leading to that the full scale GPS-LIB with a specific capacity of ((171 Ah)/(1 kg+0.51 kg))/1.34 is about 84.5 Ah .kg^{-1}.

The theoretical mode of calculated specific energy of GPS-LMPO@C//MSTO@C battery can be quantified as equal to (2.34 V *84.5 Ah kg^{-1})= 197.7 Wh kg^{-1}.

S11- B - Practical method-based experimental sets of super-architectonics built-in LIBs

In galvanostatic cycling test (i.e., only at constant current), the graphically specific energy of super-architectonic built into the GPS-full-scale LIB can be detected from the charge–discharge voltage-capacity profile at 1C as follows:

- The specific energy for the GPS-LMPO@ C cathode (Wh/kg) is = the average working voltage of the super-architectonics built-in LIBs in (V) x maximum discharge capacity delivered by cell (Ahkg^{-1}).

- The specific capacity delivered by cell ($Ahkg^{-1}$) at 1C = 156.3 $Ahkg^{-1}$.
- The specific energy for the GPS-cathode (Wh/kg) = 2.6 V x 156.3 $Ahkg^{-1}$ =406.4 Wh/kg.
- Thus, the specific energy density of full-cell super-architectonic built into the GPS-full-scale LIB ($Whkg^{-1}$) = the estimated mass fraction of a cathode active material in a LIB cell (in pouch-type, mass fraction is 44% (see S1)) x Specific Energy for the cathode ($Whkg^{-1}$).

- **Therefore, practical value of the specific energy density of the GPS-LMPO@C//MSTO@C full-scale LIB is 178.8 $Whkg^{-1}$.**

S11-C- Key difference between experimental and theoretical calculations of specific energy density of full-scale GPS-LIBs

For both the intensive determination of specific energy density for the super-architectonic built into the GPS-full-scale LIB, the practical and theoretical values are of ***178.8 $Whkg^{-1}$ (practically) and 197.7 $Whkg^{-1}$ (theoretically)***, respectively. The low value of specific energy density in a practical determination may attributed to

(iii) the Li^+-ions can't be completely removed from the N-electrode and P-electrode surface topographies, and

(iv) non-usable cutoff voltage profiles to clean-up N-electrode and P-electrode surface topographies to remove the rest Li^+ ion on the interlay complex super-architectonics, constraining the perfect charge-discharge rate.

The proposed GPS-MSTO@C//LMPO@C full-scale battery system integrates the latest advances in Li-battery technology to create a battery that delivers outstanding electrochemical performance.

S15. A comparison between the GPS-SSF@C half-scale LIB and the other reported $LiMnPO_4$ cathodes

To show evidence of the effectiveness of the super-architectonic GPS-LMPO@C and GPS-MSTO@C anode geometrics, building-blocks-in a wide-range of egress/ingress egress/ingress hierarchy, and super topographic-surface heterogeneity, roughness and anisotropy on the GPS-designated LIBs, we offer intensive studies of the key parameters in terms of rate capability, Coulombic efficiency, reversible capacity and long-term cycle stability of our GPS LIBs and other reported LIB designs, as one can see in Table S1-S3.

Table S1 A comparison between the GPS-LMPO (with SSF@C geometrics) half-scale LIB and normal and conventional LMPO cathode-LIBs

Cathode material	Nominal Voltage (V)	Cycles	Specific Capacity mA h g^{-1}	Coulombic efficiency	Ref
$LiMnPO_4$@C	4.1	retained ~100% of its reversible capacity after 100 cycles	155 At 0.5C	Not mentioned	**21**
$LiMnPO_4$@C	4.1	capacity retained 120 $mAhg^{-1}$ after 50 cycles	153.4 at 0.1C	Not mentioned	**37**
$LiMnPO_4$@C	4.1	capacity retained 89.1 $mAhg^{-1}$ after 500 cycles	147.9 at 1C	Not mentioned	**Ref-10**
$LiMnPO_4$	4.1	capacity retained 125 $mAhg^{-1}$ after 30 cycles	133 at 0.1 C	Not mentioned	**17**
$LiMnPO_4$@C (GPS-SSF@C)	4.1	Retains ~100% after 100 cycles	133 at 1C	~100%	**Current Work**

S16. A comparison between the GPS-MSTO@C half-scale LIB and the other reported TiO_2 anodes

Table S2 A comparison between the GPS-MSTO@C half-scale LIB and the other reported TiO_2 anodes.

Anode material	Nominal Voltage (V)	Cycles	Specific Capacity mA h g^{-1}	Coulombic efficiency	Ref
Rutile TiO_2	1.7	retained 50% of its reversible capacity after 100 cycles	250 At 0.1C	~ 100% after 100 cycles	**Ref [S11]**
Rutile TiO_2	1.5	retained 77% of its reversible capacity after 40 cycles	223 at 0.1C	Not mentioned after 100 cycles	**Ref [S12]**
Anatase TiO_2	1.73	76% of its initial capacity after 30 cycles at 0.2C	~ 300	Not mentioned	**Ref [S13]**
P25, a commercial titania powder from Degussa	1.7	61% of its initial capacity after 30 cycles at 0.2C	95	Not mentioned	**Ref [S13, S14]**
TiO_2	1.74	70% of its initial capacity after 100 cycles at 0.2C	270	Not mentioned	**Ref [S15]**
TiO_2	0.8	55% of its initial capacity after 30 cycles	310	~100%	**Ref [S16]**
TiO_2@C (GPS-MSTO@C)	1.7	87% of its initial capacity after 100 cycles at 1C	231	Not mentioned	**Current Work**

S17. A comparison between the GPS-SSF@C//MSTO@C full-cell LIB electrode system and the other reported $LiMnPO_4$//TiO_2 full cells

Table S3 A comparison between the GPS-SSF@C//MSTO@C full-cell LIB electrode system and the other reported $LiFePO_4$//TiO_2 and $LiMnPO_4$//TiO_2 full cells.

Cathode material	Anode material	Nominal Voltage (V)	Cycles	Specific Capacity mA h g^{-1}	Coulombic efficiency	Ref
$LiFePO_4$	Anatase TiO_2 hollow nanofibers	1.4	retained 88% of its reversible capacity after 300 cycles	103	> 99 %	**Ref [S17]**
$LiFePO_4$	Rutile TiO_2	1.8	retained 50% of its reversible capacity after 40 cycles	150	Not mentioned	**Ref [S18]**
$LiFePO_4$	Anatase TiO_2	1.6	81% of its initial capacity after 300 cycles at 20C	160	Not mentioned	**Ref [S19]**
$LiFePO_4$	anatase/graphene	1.6	700	127	~ 100%	**Ref [S20]**
LiFePO4	spinel $Li_4Ti_5O_{12}$/C	1.8	Retain 98.1% after 400 cycles	167	~100%	**Ref [S21]**
$LiFePO_4$	spinel $Li_4Ti_5O_{12}$	1.65	Retain 98.9% after 100 cycles	150	~100%	**Ref [S22]**
$LiMnPO_4$	$Li_4Ti_5O_{12}$	2.5	Retain ~100% after 300 cycles at C/2	105	~100%	**Ref [S23]**
$LiMnPO_4$@C (GPS-SSF@C)	TiO_2@C (GPS-MSTO@C)	2.6	Retains 77.5% after 2000 cycles at 1C	156.3	~100%	**Current Work**

Reviewer #3:

We really would like to acknowledge the reviewer comments and efforts. Per of this respectful vision, we thoroughly amended our manuscript taking all points raised in our consideration

This work realizes the coupling of a series of super hierarchy and interlay-complex superstructures of anode and cathode (GPS), which were fabricated with irregular surface ripples, bumps, undulations, and anticlines and integrated into half- and full-cell LIB models to allow non-prescriptive cycle usages, loading, diffusion, and interaction and to achieve excellent rate capabilities. After integrating GPS cathode- and anode-electrode geometrics into precisely defined LIB pattern models, the LIBs showed an outstanding long-term cycling performance for 2000 cycles at 1C. In my opinion, this work displays an effective method for the construction of highly efficient electrode materials but overall I suggest some questions should be addressed in the manuscript.

Q1. The English needs a lot of edition throughout the paper. The authors should pay attention to the use of the article, conjunction, and comma. There are some syntax errors in sentences or phrases; several sentences are contextually incorrect. Some examples are below:
"These GPS configurations preserve the multi-scale and interior space complexities as well as the vortex flow dynamics that are connectively arranged in lateral/longitudinal exposure modulates …"
"These intrinsic features may lead to create ageless reachable LIBs …"
"The orientation of SSF@C-electrode superstructure along vertical, lateral and longitudinal axes, which had upper-top-capped pyramidal prisms makes the charge/discharge rate more facile."
"Accordingly, we studied the temperature dependence functionality of these cathodes versus their electrical conductivity …"

A1- We appreciate the reviewer comment. Per of this comment the whole manuscript carefully revised and covered all of these comments, in addition, the language of the manuscript and supporting is revised by English Company.

Q2. Some phrases are used in a non-standard manner, for example, multi-gate-in-transport, land energy density, power electron density, spatial rate performance capabilities, electronic surfaces, capability performance rates, and C-shell dresser.
A2- Thanks for this comment. Per of this comment the manuscript was revised and improved, please see modification in the revised form with blue font.
Q3. The format of chemical formula should be detailedly checked throughout the manuscript.
A3- Thanks for this observation. Per of this comment the chemical formula was revised and modified.

Q4. What's the tap density of GPS materials? Then, a table should be added to compare with other reported values in literatures.
A3- We appreciate the reviewer comment. Per of this comment, the following modification has been done as follows:

- *S15. A comparison between the GPS-SSF@C half-scale LIB and the other reported LiMnPO4 cathodes (**Please see page S 27**)*

S15. A comparison between the GPS-SSF@C half-scale LIB and the other reported $LiMnPO_4$ cathodes

To show evidence of the effectiveness of the super-architectonic GPS-LMPO@C and GPS-MSTO@C anode geometrics, building-blocks-in a wide-range of egress/ingress egress/ingress hierarchy, and super topographic-surface heterogeneity, roughness and anisotropy on the GPS-designated LIBs, we offer intensive studies of the key parameters in terms of rate capability, Coulombic efficiency, reversible capacity and long-term cycle stability of our GPS LIBs and other reported LIB designs, as one can see in Table S1-S3.

Table S1 A comparison between the GPS-LMPO (with SSF@C geometrics) half-scale LIB and normal and conventional LMPO cathode-LIBs

Cathode material	**Nominal Voltage (V)**	**Cycles**	**Specific Capacity mA h g^{-1}**	**Coulombic efficiency**	**Ref**
$LiMnPO_4$@C	4.1	retained ~100% of its reversible capacity after 100 cycles	155 At 0.5C	Not mentioned	**21**
$LiMnPO_4$@C	4.1	capacity retained 120 $mAhg^{-1}$ after 50 cycles	153.4 at 0.1C	Not mentioned	**37**
$LiMnPO_4$@C	4.1	capacity retained 89.1 $mAhg^{-1}$ after 500 cycles	147.9 at 1C	Not mentioned	**Ref-10**
$LiMnPO_4$	4.1	capacity retained 125 $mAhg^{-1}$ after 30 cycles	133 at 0.1 C	Not mentioned	**17**
$LiMnPO_4$@C (GPS-SSF@C)	4.1	Retains ~100% after 100 cycles	133 at 1C	~100%	**Current Work**

S16. A comparison between the GPS-MSTO@C half-scale LIB and the other reported TiO_2 anodes

Table S2 A comparison between the GPS-MSTO@C half-scale LIB and the other reported TiO_2 anodes.

Anode material	Nominal Voltage (V)	Cycles	Specific Capacity mA h g^{-1}	Coulombic efficiency	Ref
Rutile TiO_2	1.7	retained 50% of its reversible capacity after 100 cycles	250 At 0.1C	~ 100% after 100 cycles	**Ref [S11]**
Rutile TiO_2	1.5	retained 77% of its reversible capacity after 40 cycles	223 at 0.1C	Not mentioned after 100 cycles	**Ref [S12]**
Anatase TiO_2	1.73	76% of its initial capacity after 30 cycles at 0.2C	~ 300	Not mentioned	**Ref [S13]**
P25, a commercial titania powder from Degussa	1.7	61% of its initial capacity after 30 cycles at 0.2C	95	Not mentioned	**Ref [S13, S14]**
TiO_2	1.74	70% of its initial capacity after 100 cycles at 0.2C	270	Not mentioned	**Ref [S15]**
TiO_2	0.8	55% of its initial capacity after 30 cycles	310	~100%	**Ref [S16]**
TiO_2@C (GPS-MSTO@C)	1.7	87% of its initial capacity after 100 cycles at 1C	231	Not mentioned	**Current Work**

S17. A comparison between the GPS-SSF@C//MSTO@C full-cell LIB electrode system and the other reported $LiMnPO_4$//TiO_2 full cells

Table S3 A comparison between the GPS-SSF@C//MSTO@C full-cell LIB electrode system and the other reported $LiFePO_4$//TiO_2 and $LiMnPO_4$//TiO_2 full cells.

Cathode material	Anode material	Nominal Voltage (V)	Cycles	Specific Capacity mA h g^{-1}	Coulombic efficiency	Ref
$LiFePO_4$	Anatase TiO_2 hollow nanofibers	1.4	retained 88% of its reversible capacity after 300 cycles	103	> 99 %	**Ref [S17]**

$LiFePO_4$	Rutile TiO_2	1.8	retained 50% of its reversible capacity after 40 cycles	150	Not mentioned	**Ref [S18]**
$LiFePO_4$	Anatase TiO_2	1.6	81% of its initial capacity after 300 cycles at 20C	160	Not mentioned	**Ref [S19]**
$LiFePO_4$	anatase/graphene	1.6	700	127	~ 100%	**Ref [S20]**
LiFePO4	spinel $Li_4Ti_5O_{12}$/C	1.8	Retain 98.1% after 400 cycles	167	~100%	**Ref [S21]**
$LiFePO_4$	spinel $Li_4Ti_5O_{12}$	1.65	Retain 98.9% after 100 cycles	150	~100%	**Ref [S22]**
$LiMnPO_4$	$Li_4Ti_5O_{12}$	2.5	Retain ~100% after 300 cycles at C/2	105	~100%	**Ref [S23]**
$LiMnPO_4$@C (GPS-SSF@C)	TiO_2@C (GPS-MSTO@C)	2.6	Retains 77.5% after 2000 cycles at 1C	156.3	~100%	**Current Work**

S 18. Tap density of the super-architectonic GPS-$LiMnPO_4$@C cathode geometrics

Due to the increasing demand and the urgent need of the LIBs in the field of consumer electronics and EVs, an important characteristic is the tap density being exploited. The tap density was mainly influenced by the material morphology, particle size and the distribution of powder particles. Design of spherical particles was used to increase the tap-density. Developing new LMPO structures with both high rate performance and high tap density is challenging and appealing for the preparation of cathode materials [Ref-S24, Ref-S25].

To calculate the tap density of GPS-LMPO@C modulated LIBs, we used ZS-102 tap density meter (Liaoning Institute of Research Tools Co., Ltd.) to measure the tap density of the super-architectonics built-in LIB models. In such super-architectonic LIB models or modules, the optimal carbon content should not be more than 5%. The carbon content of SSF@C composites is found in the optimal range of about 4% (lower than 5%) [Ref-S26].

A powerful tool to develop the super architectonic engineering design of GPS-MSTO@C anodic and GPS-LMPO@C of geometric-SSF@C, -CSN@C and -NR@C cathode electrodes can be achieved by a rational mass-loading control. The high-density GPS SSF@C super-architectonics modulated LIBs shows excellent high rate performance, a high tap density (~1.51 g cm^{-3}) compared to 1.24 and 1.02 g cm^{-3} of GPS-CSN@C, and GPS-NR@C cathode geometrics, respectively. The finding indicates the effect of GPS complex super-architectonic SSF@C in its excellent electrochemical performance, particularly during the Li^+-insertion (cathodic, reduction, lithiation) /extraction (anodic, oxidation, delithiation) processes. Together, the GPS-SSF@C super-architectonics can be a potential candidate for high-performance LIBs.

Q5. More evidences should be provided to confirm the pyramid structure.

*A5- Thank you so much for this nice vision and constructive comment. Per of this comment further information and discussion related to the material control is added. New section has been added to Results and Discussion part "Control synthesis of complex super-architectonics (GPS) cathode-/anode-geometrics (**Please see pages 12- 14**)" as follows:*

Control synthesis of complex super-architectonics (GPS) cathode-/anode-geometrics

Control synthesis of large-scale giant porous complex super-architectonics (GPS) is mainly composition- and time-dependent protocol that enabled well-defined growth GSP reaction kinetics to build up block-by-block hierarchy. As a result, super-architectonics are fabricated with structural GPS-building-blocks-in a wide-range of (i) distinguishable geometrics in 3-dimesnional (3D) and multi-directional orientations (lateral, vertical, circular, zigzag, and longitudinal), (ii) egress/ingress models such as caves, channels and grooves, and (iii) giant topographic-surfaces including ripples, winglets, protuberances, irregular bumps, V-hooks, undulations, and anticlines. Accordingly, well-designed super-architectonics (GPS) LMPO@C-cathodes, including three variable geometrics solanum star-shaped flower (SSF@C), mesocave nanorods (NRs@C), and axially edged stack sheets (CSN@C) are successfully fabricated under our protocol synthesis. The anode-based GPS anatase MSTO@C architectonic geometrics and super surface topographies are fabricated with multi-layered shells dressed mesosphere core and vertically oriented along its central axes. The structurally-shaped architectonics of MSTO@C GPS-anode are attained the interior space complexities and vortex flow dynamics under our realistic synthesis conditions. The simple synthesis protocol provides a powerful tool to develop the architectonic engineering design of GPS-MSTO@C anodic and GPS-LMPO@C of geometric-SSF@C, -CSN@C and -NR@C cathode electrodes in a rational mass-loading control. These GPS electrode geometrics integrated into CR2032 coin cells are the key enabling fabrication of low-cost super-architectonics built-in LIB-models and modules with ever-decreasing timescale of discharge capacity and path-dependent battery with high-energy density.

In this regards, the complex super architectonic LMPO-GPS geometrics, namely, SSF, CSN, and NR, are then tailored by varying the manganese anions (i.e., chloride, sulfate, and nitrate, respectively) and by controlling the time-dependent particle-to-particle growth under the optimization conditions, such as pH solution, growth-assisted agent, and high-temperature treatment. For a thorough grasp of the $LiMnPO_4$ crystals building-growth approach with various 3D-morphological structures, a sensible explanation can be determined as follows: First, nucleation-directing agents such as ethylene glycol and H_3PO_4, to some extent, affect the particle-to-particle growth direction. Second, the potential decrease in the power strength of precursor manganese-anions (i.e., NO_3-, SO_4^{2-}, and Cl^-) plays an extreme role in the kinetic- and thermodynamic-control growth-path mechanism, leading to the structural optimization of GPS morphology, and the modulation of 3D GPS multidirectional geometrics. Third, the environment synthesis conditions provide large surface scales of ripples, irregular bumps, undulations, anticlines, and active top-zone Mn^{2+}/Mn^{3+} espoused surface for a facile lithiation/delithiation process. Consequently, the decrease in the reduction power of manganese-anions was in this order NO_3- > SO_4^{2-} > Cl^-, leading to pronounced changes in complex super-architectonic (GPS) geometrics in this sequence of NRs - CSN- SSF structures, respectively. The addition of manganese sources with (i) NO_3- , (ii) SO_4^{2-}, and (iii) Cl^- anion species with similarly well-controlled synthesis condition and composition guides fabricating of (i) 1D-model open-top mesopore NRs, passing through (ii) axially-edged plate sheets stacked circularly around central axis and concentrically formed a cylinder sphere-hole-like cage nest (CSN) structure, to (iii) 3D solanum star-shaped flowers with multi-branchlet nanorods spreading out from central core in to lateral and axial directions

(SSF) structure, respectively. The mechanistic formation of NRs, CSN nd SSF geometrics is evidenced from the microscopic patterns, including a top- and plane-view (FE-SEM) field emission scanning electron microscope and (HR-TEM) a high-resolution transmission electron microscopy (Figs. 1, 2, S2, and S3). Furthermore, facile electron/Li^+ ion mobility and highly conductive surfaces for MSTO-anode and SSF-, CSN- and NR-cathode composites are improved by well-ordered and sustainable modification by ~5nm C-shell dressers along entirely giant surface ripples, irregular bumps, undulations, and anticlines. These giant topographic surfaces affect high rate performance and tap density, and cyclic stability characteristics of half- or full-scale GPS-LIBs (see supporting information S1-S19). The integration of GPS interlay-complex architectonic anode/cathode geometrics into half-/full-scale LIBs may allow multi-gate-in-transport electron/ion mobility in building-blocks egress/ingress paths. These diverse pathways, including the upper, middle, and lower multi-zone crystal patterns, and for evaluating the frontal edge/apex/central/corner access sites are given their potentials in the design of GPS-LIB models and modules with superb specific capacities, high energy density, facile discharge–discharge rates, and extended long-term power stability. The GPS complex architectonic anode/cathode surface topographies that have irregular ripples, bumps, undulations and anticlines significantly affect electrochemical performance of both half- and full-cell LIB designs in terms of non-prescriptive cycle usages, heavily interior Li^+ ion loads, and spatial rate performance capabilities (Scheme 1).

Q6. Please pay more attention to the references. There are several ill-formed abbreviations of journal names.

A6- Thanks for this observation. Per of this important comment, references have carefully revised and modified.

Finally, we would like to thank the reviewers for their valuable comments that improved the manuscript thoroughly. We would like to emphasize that all comments have been considered and notified in our manuscript. Please see our response and the accordance change in the entire manuscript (blue color).

Large-Scale Giant Architectonic Electrodes Designated with Complex Geometrics and Super Topographic Surfaces for Fully Cycled Dynamic LIB Modules

H. Khalifa, [a] S.A. El-Safty,*[a] M.A. Shenashen,[a] A. Reda, [a] A. Elmarakbi [b]

[a]*National Institute for Materials Science (NIMS), Sengen 1-2-1, Tsukuba, Ibaraki 305-0047, Japan. E-mail: sherif.elsafty@nims.go.jp*

[b]*Department of Mechanical & Construction Engineering, Faculty of Engineering and Environment, Northumbria University, Newcastle upon Tyne, NE1 8ST, UK.*

Large-Scale Giant Architectonic Electrodes Designated with Complex Geometrics and Super Topographic Surfaces for Fully Cycled Dynamic LIB Modules

Abstract: Given exceptional specific discharge capacity, excellent energy density, high rate capability, fast charge capacity, and long-term cycling stability, large-scale giant porous complex super-architectonics (GPS) integrated into anode/cathode complex geometrics improve the full-model lithium ion batteries (LIBs). We examine the integration of a series of anode and cathode (GPS) super-architectonics into half- and full-cell LIB models to allow non-prescriptive charge/discharge cycles, and to achieve spatial rate performance capabilities. As a distinguishable GPS model, the super-architectonics included multi-directional orientation geometrics, building-blocks egress/ingress pathways, and giant loophole-on-surface topographies of ripples, irregular bumps, undulations, and anticlines offer a set of fully functional multi-axial/dimension GPS cathode- and anode-electrode geometrics and multi-gate-in-transports of electron/Li^+ ions in diverse pathways. Our precisely defined GPS-modulated LIB models generate high-power and volumetric-energy density, excellent long-term cycling durability without deterioration in its capacity under a high energy density, and a comparable high tap density. GPS-integrated LIB modules provide superior durability (i.e., maintaining high specific capacity ~77.5% within long-term life period of 2000 cycles) and average Coulombic efficacy of ~99.6% at 1 C. Powerful and robust super-architectonic GPS building-blocks-in full-scale LIB designs offer outstanding specific energy density of ≈179 Wh kg^{-1} for a future market of LIB-EVs with longest driving range. The key leap super-surface topographies of LIB-GPS modules are critical in creating ever-changing charge/discharge cycles, "fully cycled dynamics," affordable on-/off-site storage, and super-large door-in transport of Li^+-ion/electron, thereby highlighting its promising storage modules and rechargeable lithium batteries.

Keywords: Super architectonics, capacity storage; super-surface topographies, anode/cathode; complex geometrics, lithium-ion batteries (LIBs); fully cycled dynamics; electric vehicles (EVs).

Introduction

Structural design optimization of anode/cathode integrated lithium-ion batteries (LIBs) with nanoscale and super architectonics would improve their high power and energy density performances and safety domains. Among diverse types of rechargeable batteries in global LIB industry market, LIBs are promising candidate because of their higher gravimetric, volumetric energy, high operating voltage, and power density, and low self-discharge compared with other commercial batteries [1-3]. Nowadays, LIBs are technically efficient to create a dynamically integrated zero-emission vehicle (ZEV) such as electric vehicle (EV), and plug-in hybrid electric vehicle (PHEV) [1-7]. Under ever-increasing demands on economic, reliable and efficient structural design of LIBs, sustainable, environment-friendly, low-cost, and safe anode/cathode LIB systems must be developed. The idealized LIB model should have a high energy density, excellent charging and discharging rates, long cycle life, high plateau voltage, and high specific capacity to be in complete agreement and be compatible with necessities of the constantly developing industries of portable electronic devices (PEDs) and EVs. Various approaches have been proposed to overcome the shortcomings of LIB design procedures in terms of actual system performance in theory and practical implementation in potential applications. For instance, optimal LIB-mutated anode/cathode electrode designs were reported by using multi-component composites, electronic and conductive cuticles, and hierarchically-shaped structures that can offer multi-diffusive open sites for promising storage modules [8-14].

Many studies have been attempted to find best cathode material performances in terms of structural stability, high safety, and low cost that can replace hazardous $LiCoO_2$, $LiNiO_2$, or $LiMn_2O_4$ cathode

materials. Phosphor-olivine-structured composites, such as $LiXPO_4$ (X = Ni, Co, Mn, and Fe, with a theoretical capacity of ~170 $mAhg^{-1}$) were received much attention as excellent and newly emerging cathode candidates that can be used for the forthcoming generation of LIBs [15-18]. Following the work of Goodenough et al. (1997) on the electrochemical behavior of $LiXPO_4$ [19], $LiFePO_4$ (LFPO) and $LiMnPO_4$ (LMPO) materials were highlighted as excellent cathodes for practical implementation of rechargeable LIBs [20-22]. These LMPO-integrated LIB geometrics have shortcoming of their stable cyclability and rate capability, considering their poor electronic and ionic conductivities [23, 24]. Although LFPO materials have been widely commercialized, LMPO materials showed a good energy density because its 20% Mn^{2+}/Mn^{3+}elemental components have high energy density (4.1 V against Li/Li^+) compared with Fe^{2+}/Fe^{3+} redox potential (3.45V vs. Li/Li^+). Furthermore, LMPO materials were confirmed to be as safe and stable as $LiFePO_4$ [25]. Within structural optimization geometrics and surface parameters, the LMPO materials can be used easily as a very powerful built-in electrode in EVs. Exploring an alternative LMPO-cathode LIB design with nanoscale hierarchy, complex geometries, anisotropic compositions, surface interface functions, and morphological variabilities may introduce new possibilities for development of a heterogeneous LIB models. Superstructures of anode and cathode designated as half- and full-cell LIB models are expected to allow non-prescriptive cycle usages, to achieve spatial rate performance capabilities, and to produce high specific capacity without deterioration and high energy density for future market of LIB-EVs with longest driving range.

To modulate a low cost LIB-EV, common and abundant metal oxide geometrics were exhibited promising anode fabrics for LIBs [26]. TiO_2-anatase is an excellent anode material among most of these oxide fabrics. Due to inherent characteristics of its nature such as eco-friendliness, low cost, non-toxicity, pollution-free and low polarization, TiO_2-modulated anodic electrodes produced LIB models with excellent rate-based reversibility and capability, long-period cycling, and promising

behavior as an Li^+-insertion electro-active host [26-30]. The interfacial mobility of TiO_2 crystal lattice domains was offered phase transition dominates from I41/amd (space group)-tetragonal TiO_2 to Imma (space group)-orthorhombic lithium-rich $Li_{0.5}TiO_2$ geometrics. The movements along the electronic model system of TiO_2 anode were a key broadening the complex super-architectonics. The TiO_2 negative anode (i.e., N-electrode) enabled a bundle of LIB features based robust design stability and long-term reversibility [31, 32]. The influence of the structural phase transitions along the TiO_2 interfacial crystal lattice from poor-to-rich lithium structures (i.e., $Li_{0.01}TiO_2$ to $Li_{0.5}TiO_2$ composition geometrics) provided anode electrode cuticles for multiple lithiation/delithiation cycles [31, 32]. Therefore, controlling the fabrication of low-cost anode/cathode fabrics with intrinsic atomic-scale organization, structural configurations, nano-geometrical assemblies, and structurally shaped hierarchy is crucial in developing green energy and storage battery designs with a long life usage cycles [33-38].

For intensive progress in manufacturing output and deployment of LIBs, integrating the artificial nature of fabric anode or cathode materials into all module configurations is pivotal [37, 38]. For a future LIB design perspective, a rich diversity of gate-diffusion for Li+ ions with multiple numbers of discharging (insertion, lithiation)/charging (delithiation, extraction) processes remians a challenge [11]. If the hierarchical cathode/anode architectures with irregular surface interfaces, morphologies, and anticlines were fabricated into LIB models, their features in terms of non-prescriptive cycle usages, spatial rate performance capabilities, and land energy density would enhance the future LIB market.

In this study, we designated a set of fully functional multi-axial/dimension giant porous complex super-architectonics (GPS) cathode and anode electrode geometrics into precisely defined LIB pattern models. The scalable, highly precise building of full-cell GPS-integrated-LIBs is achieved by using

novel GPS electrode super-surface topographies. The key aspects of super-architectonics in terms of interlaid complexity, building-blocks egress/ingress pathways, and giant topographic-surfaces of ripples, anticlines, angularities and undulated ridges significantly affect the performance of GPS-LIB models and modules. Super-architectonic GPS-integrated N- and P-electrodes boost the potential Li^+-ion egress/ingress capacity with high rate velocity, on-/off-site storage modules, and super-large door to transport Li^+-ion/electron. A set proximity of Li^+ ion accessible loophole-on-surfaces is one of the most effective solutions to avoid electrode-surface polarization and to boost the fully-cycled dynamic charge/discharge process within both half- and full-scale super-architectonic GPS-LIB-CR2032 coin cells. Powerful and robust super-architectonic SSF@C GPS-cathode//MSTO@C GPS-anode full-scales generate high-power LIBs with long-term cycling performance for 2000 cycles at 1C between 1.5V and 3.8V vs. Li/Li^+ without deterioration in its high energy density as a result of a comparably high tap density. The full-scale GPS-integrated LIB model successfully retains 77.5% of its first discharge capacity of 156.3 $mAhg^{-1}$, high Coulombic efficiency of ~99.6% for 2000 cycles, outstanding specific energy density of ≈179 Wh kg^{-1} for potential LIB-EVs regimes. A setting of super-architectonics full-cell GPS-LIBs provides a new perspective for battery-force-driven module industrialization with high safety concerns.

Experimental

GPS–TiO_2 super architectonic complexity (MSTO, anode)

The fabrication of anodic complex super architectonics designated as TiO_2 multi-layered shells dressed in a fine uniform mesosphere core and vertically oriented along its central axes (MSTO) is controlled via simple composition and time-dependent approach. In a typical procedure, a homogenous solution of 10 mM titanium butoxide dissolved in a mixture of 20 ml ethanol, 10 ml hydrochloric acid (2M), and 20 ml acetonitrile is prepared. The pH of this mixture is controlled at 9.2

by dropwise addition of NH_4OH (0.5 ml, 28%) with continuous rate ~ 50 µl/min, and under stirring for 2 h. The alkaline mixtures (pH= 9.2) are kept in 100 ml autoclave, Teflon-lined stainless-steel, and then treated at 170 °C for a time period of 12 h. The produced solid yield is collected using centrifuge, and washed by a mixture of H_2O/C_2H_5OH solution. The as-made solid is dried overnight at 50 °C under vacuum conditions, and then calcined at 450 °C for 4 h to MSTO anodic complex super architectonic materials.

GPS-LMPO models of super architectonic cathodes

Control over the nucleation and growth directions, unique surface morphology and composition leads to formulation of large-scale, multi-functional complex super architectonic models of $LiMnPO_4$ (LMPO) GPS-geometrics. Three different complex super architectonic materials oriented at cathode patterns as designated as (i) solanum star-shaped flowers (SSF) that have multi-branchlet nanorods spreading out from central core to lateral and axial directions, (ii) axially-edged plate sheets stacked circularly around central axis, and (iii) concentrically formed cylinder sphere-hole-like cage nest (CSN) and open-top mesopore nanorods (NR) cathode materials.

In a typical synthesis protocol of complex SSF super architectonic (LMPO) geometrics, the elemental molar ratio of Li: Mn: P in the formulation and main composition of manganese chloride tetrahydrate ($MnCl_2{\cdot}4H_2O$), phosphoric acid (H_3PO_4), and lithium acetate ($CH_3COOLi{\cdot}2H_2O$) is equivalent to 3:1:1. A mixture of 20 ml-H_2O/2 ml-C_2H_5OH/ 3 ml-$HOCH_2CH_2OH$ (i.e., ethylene glycol) is used to form a homogenous $H_3PO_4/MnCl_2{\cdot}4H_2O$ solution by stirring-assisted protocol for 1 h. After that, a solution of H_3PO_4 is added dropwise at rate of 0.5 ml/min to $MnCl_2{\cdot}4H_2O$ under stirring for 1 h. A solution of $CH_3COOLi{\cdot}2H_2O$ is formed in 20 ml-H_2O/2 ml-C_2H_5OH/ 3 ml-$HOCH_2CH_2OH$ mixture, and then stirred for 1 h at 30 °C. The ($CH_3COOLi{\cdot}2H_2O$) solution was added dropwise to the $H_3PO_4/MnCl_2{\cdot}4H_2O$ mixture at additive rate of 0.5 ml/min. The composition domain with total molar

ratio of Li: Mn: P in the mixture is equivalent to 3:1:1. The yielded component is treated under stirring-assisted method for 6 h, and at a pH level of 7. The SSF-GPS mixtures are kept in 100 ml autoclaves, and then treated at 170 °C for time-period of 12 h. The produced solid SSF-GPS yield is collected using centrifuge at 4000 rpm, and washed by a mixture of H_2O/C_2H_5OH solution. The as-made solid is dried overnight at 60 °C under vacuum and then calcined at 600 °C for 6 h to form SSF-GPS cathode complex super architectonic materials. By using the same procedures including the pH level of 7, and the Li:Mn:P molar ratio of 3:1:1, different manganese sources such as manganese sulfate hydrate ($MnSO_4 \cdot xH_2O$) and manganese nitrate hydrate ($Mn(NO_3)_2 \cdot xH_2O$) , the CSN- and NR-GPS complex super architectonics can be successfully fabricated.

Fabrication of complex LMPO@C cathodes and MSTO@C anode super architectonics

To enhance the electronic conductivity and cyclic stability of the MSTO anode and SSF, CSN, and NR cathode composites, the GPS anode/cathode surface is covered by well-ordered dressing of nano-carbon (C) shell ~5 nm. The nano-C-shell coating along super architectonic SSF@C-, CSN@C-, and NR@C-cathodes and MSTO@C-anode surfaces is formed under 15-min ultra-sonicated assisted method in the presence of heterogeneous C_2H_5OH/glucose (**$C_6H_{12}O_6 \cdot H_2O$** 5 wt%)/ SSF-, CSN-, NR-, and MSTO-powder mixture. The heterogeneous mixture is attained in-100 ml autoclaves and mixed under stirring for 30 min in a microwave oven at 80 °C. The resulting black-powder precipitate is collected by using centrifuge at 4000 rpm, and washed by a mixture of H_2O/C_2H_5OH solution, and dried overnight at 50 °C in an electric oven under vacuum conditions. The as-made solid is dried overnight at 50 °C under vacuum and then calcined at 600 °C for 2 h (with rate of 5 °C/ min) to form super architectonic SSF@C-, CSN@C-, and NR@C-cathodes and MSTO@C-anode fabrics.

Configuration of super-architectonics-integrated GPS-LIB CR2032 coin-cell models and pouch-type modules

The half- and full-cell configurations of the super-architectonics GPS-LIBs are tailored by using the GPS cathode/anode electrodes. Well-designed CR2032 coin cells with GPS hybrid super-architectonic models are formed by using LMPO@C-cathode-based solanum star-shaped flower (SSF@C), mesocave nanorods (NRs@C), and axially edged stack sheets (CSN@C). The GPS-CR2032 anode-based MSTO@C architectonic geometrics with super surface topographies are also configured as N-electrode. We fabricated the working electrodes of GPS-modified 8 µm-Cu-foils (N-anode) and GPS-modified 12 µm-Al-foils (P-cathode), respectively, and other reference/counter (lithium foil) electrodes to form CR2032 coin cells of complex GPS super-architectonic in a glovebox under argon gas, Figure S1. Such GPS-built-in CR2030 LIBs are promising to design GPS-LIB-powered engineering modules and models with betterment safety factors, and electrochemical performances (see supporting information S1-S19).

Under our synthesis conditions of electrodes, the densely packed SSF@C-Al-foil P-electrode shows excellent GPS-LIB performance and a high tap density (~1.51 g cm^{-3}) compared to 1.24 and 1.02 g cm^{-3} for CSN@C-Al-foil, and NR@C-Al-foil electrodes, respectively (see supporting information S18). Therfore, the GPS SSF@C-cathode is used for the electrochemical measurement of powerful full-scale LIB CR2032 coin-cell models and cylinder- or pouch-type modules. The full-scale GPS-LIBs are based on integration of MSTO@C (anode or negative electrode) //SSF@C (cathode or positive electrode) super architectonics in one coin-cell (see Figure S1).

The module configurations of the GPS super architectonic LIB initiatives are designed in bundled layers of pouch LIB-types. The CR2032 coin-cells are packed up in this pouch module under optimization conditions. A control of the mass-loading of N-anode and P-cathode electrodes and their ratio of capacity (i.e., balancing capacity of $(N/P)_{Cap}$ ratio) is demanded for outstanding trade–off

performance variability. A set of deterministic LIB cell performances is carried out under variable changes in the $(N/P)_{Cap}$ ratio to optimize the ideal GPS-LIB trade–off module reliability. Along with this practical set, the stacked GPS-CR2032 coin cells in pouch modules show a minimizing level of the EV-LIB design safety risks with maintaining their high specific energy density. The multi-criteria optimizations of GPS-LIB module design indicate that the quantifiable $(N:P)_{Cap}$ capacity ratio of 1.05:1 is reliable and efficient loading values for realistic configuration of GPS-LIB pouch-modules with outstanding energy power and large safety factors.

Architectonic anode/cathode GPS-LIB CR2032 coin-cell models

The formulated components of GPS-LIB CR2032 coin-cell models are mainly consisted of (i) 16 mm-circuitous-molded Li-foil used as reference or counter electrodes, (ii) a 20 mm-circular microscopic polymer membrane spacer/separator, (iii) a conductive electrolyte of 1 M $LiPF_6$ in a (1:1 v/v) mixture content of ethylene carbonate ($C_3H_4O_3$)/diethyl carbonate ($(C_2H_5O)_2CO$), and (iv) negative (N) and positive (P) working electrodes of GPS-modified 8 µm-Cu-foil (N-anode) and GPS-modified 12 µm-Al-foil (P-cathode), respectively. To enhance the coin-cell design stability, all components of GPS-LIB CR2032 coin-cell models are statically isolated for 24 hours prior to measurements. The static equilibration and infusion between the electrolyte of 1 M $LiPF_6$ and GPS-modified anode/cathode solid electrodes enhance the GPS-LIB model validation and design improvement. The key aspects of using microporous membrane separator and highly conductive electrolyte in cell components are the reliability-based optimization design of super-architectonics built-in GPS-LIBs. Super-architectonic GPS-modulated LIBs will significantly offer potential Li^+-ion egress/ingress capacity and high rate velocity, on-/off-site storage modules, and super-large door-in transport of Li^+-ion/electron, which reduce the wastage of GPS-LIBs reversible capacity.

The certainty of model safety issues with ever attaining high energy power is rather a key factor in verification of GPS-LIBs. In real GPS-LIB engineering, the mechanical compact of circuitous-molded 2032 coin-cell without deterioration of material properties is essential for LIB design uniformity, unit-to-unit conductivity, and performance variability. In this regard, a coin-cell crimper of CR20XX series is used to compress the cell model under specific conditions of a clean glove box with Ar gas, giving rise of solid electrode surface/ liquid electrolyte interfaces (SEI) (see supporting information S1-S18).

The negative (N) and positive (P) working electrodes of GPS-modified 8 µm-Cu-foil (N-anode) and GPS-modified 12 µm-Al-foil (P-cathode) are successfully fabricated by mixing specific powder amounts of architectonic GPS-materials of MSTO@C-based anode and SSF@C-, CSN@C- and NR@C-based cathode with a mixture of carbon black/ polyvinylidene fluoride (PVDF)-based binder/ N-methyl-2-pyrrolidone (NMP)-solution. The well-dispersed fine-particle slurries are obtained after stirring the mixture for 1 h. The mass ratio of the mixture components is 80: 15: 5 for GPS-electrodes, carbon-black, and PVDF, respectively. The structural GPS-building-blocks-in P- and N-electrodes are fabricated through simple casting protocol. First, the fine-particle slurries of SSF@C-, CSN@C- and NR@C-based mixtures are casted onto 12 µm-thick- and 16 mm-diameter- Al-foils for fabrication of a positive working electrode (P)-cathode. Second, the resultant MSTO@C slurries are also infused onto 8 µm-thick- and 16 mm-diameter- Cu-foils for fabrication of a negative working electrode (N)-anode. Third, both GPS (P)-cathode and (N)-anode electrodes are dried at 80 ^{o}C for 12 h. Fourth, the dried P- and N-electrodes are then compressed between twin rollers in glove-box and under argon gas. The key clues of mechanically well-defined compression of electrodes are as follows; (i) achievement of engineering robust packing and dense inclusion of GPS-foil surfaces, (ii) avoiding formation of spaces or voids at the interfacial binding surfaces, (iii) enhancement of the

electrode conductivity and uniform movement and mobility of electron/Li^+ ions, and (iv) boosting the confined diffusivity optimization along the deposited GPS film-layers.

Architectonics-integrated into bundled layer-by-layer pouch and 18650-cylindrical GPS-LIB-types

The configurations of architectonic GPS-LIB CR2032 coin-cell models into large-scale modules can be formulated by using both collar-fashion designs of (i) 18650-cylinders and (ii) bundled-layers of pouches. Note that we modulated a bundle of architectonic GPS-LIB CR2032 coin-cell into robust 18650-cylinder design to measure the volumetric energy density of the MSTO@C (anode) and SSF@C (cathode) LIBs. However, for a practical perspective, we used well-designated pouch types for most of the experimental measurements LIB models or modules.

The idealized module designs can be achieved under the control of several key experimental components. The first key is optimization of the balancing capacity ratio of $(N/P)_{Cap}$ to fabricate GPS-LIBs with betterment safety factors and correlating with high specific energy power. The actual ratio of capacity is 1.05:1, as an ideal ratio for controlling the outstanding trade-off parameters. The second key component is the optimal performance under specific GPS-loading amount variations, corresponding to correlation of 7.14 and 13.3 $mg.cm^{-2}$ (i.e., mass/coverage area, mg/cm^2) for N-anode and P-cathode electrodes, respectively. Figure S2 shows evidence that the required active mass of the GPS-LMPO@C-cathode and GPS-MSTO@C-anode in sets of bundled-layers of pouch model components is 2.79 g and 1.43 g respectively. The third key component is robust building blocks of bundled layers onto electrodes. For instance, the GPS LIB pouch module is built with a bundle of stacked layers onto the electrode skin-surface backbones and oriented along cuticle sides as follows: 8-anode//7-cathode layers and along 14 sides of both 8µm-Cu-foils (N-electrode) and 12µm-Al-foils (P-electrode), respectively (see supporting Information and Scheme 1). The fourth key component is

uniformly-shaped set. In the stage of structural module design, the ordered set is fabricated through unit-to-unit packing of the multiple rolls of GPS-LIB CR2032 coin-cells into fashionable assembly collars while maintaining safety betterment parameters and high structural performance GPS-module design (Scheme 1A).

(Scheme 1)

Results and Discussion

Control synthesis of complex super-architectonics (GPS) cathode-/anode-geometrics

Control synthesis of large-scale giant porous complex super-architectonics (GPS) is mainly composition- and time-dependent protocol that enabled well-defined growth GSP reaction kinetics to build up block-by-block hierarchy. As a result, super-architectonics are fabricated with structural GPS-building-blocks-in a wide-range of (i) distinguishable geometrics in 3-dimesnional (3D) and multi-directional orientations (lateral, vertical, circular, zigzag, and longitudinal), (ii) egress/ingress models such as caves, channels and grooves, and (iii) giant topographic-surfaces including ripples, winglets, protuberances, irregular bumps, V-hooks, undulations, and anticlines. Accordingly, well-designed super-architectonics (GPS) LMPO@C-cathodes, including three variable geometrics solanum star-shaped flower (SSF@C), mesocave nanorods (NRs@C), and axially edged stack sheets (CSN@C) are successfully fabricated under our protocol synthesis. The anode-based GPS anatase MSTO@C architectonic geometrics and super surface topographies are fabricated with multi-layered shells dressed mesosphere core and vertically oriented along its central axes. The structurally-shaped architectonics of MSTO@C GPS-anode are attained the interior space complexities and vortex flow dynamics under our realistic synthesis conditions. The simple synthesis protocol provides a powerful tool to develop the architectonic engineering design of GPS-MSTO@C anodic and GPS-LMPO@C of geometric-SSF@C, -CSN@C and -NR@C cathode electrodes in a rational mass-loading control. These GPS electrode geometrics integrated into CR2032 coin cells are the key enabling fabrication

of low-cost super-architectonics built-in LIB-models and modules with ever-decreasing timescale of discharge capacity and path-dependent battery with high-energy density.

In this regards, the complex super architectonic LMPO-GPS geometrics, namely, SSF, CSN, and NR, are then tailored by varying the manganese anions (i.e., chloride, sulfate, and nitrate, respectively) and by controlling the time-dependent particle-to-particle growth under the optimization conditions, such as pH solution, growth-assisted agent, and high-temperature treatment. For a thorough grasp of the $LiMnPO_4$ crystals building-growth approach with various 3D-morphological structures, a sensible explanation can be determined as follows: First, nucleation-directing agents such as ethylene glycol and H_3PO_4, to some extent, affect the particle-to-particle growth direction. Second, the potential decrease in the power strength of precursor manganese-anions (i.e., NO_3-, SO_4^{2-}, and Cl^-) plays an extreme role in the kinetic- and thermodynamic-control growth-path mechanism, leading to the structural optimization of GPS morphology, and the modulation of 3D GPS multidirectional geometrics. Third, the environment synthesis conditions provide large surface scales of ripples, irregular bumps, undulations, anticlines, and active top-zone Mn^{2+}/Mn^{3+} espoused surface for a facile lithiation/delithiation process. Consequently, the decrease in the reduction power of manganese-anions was in this order NO_3- > SO_4^{2-} > Cl^-, leading to pronounced changes in complex super-architectonic (GPS) geometrics in this sequence of NRs - CSN- SSF structures, respectively. The addition of manganese sources with (i) NO_3- , (ii) SO_4^{2-}, and (iii) Cl^- anion species with similarly well-controlled synthesis condition and composition guides fabricating of (i) 1D-model open-top mesopore NRs, passing through (ii) axially-edged plate sheets stacked circularly around central axis and concentrically formed a cylinder sphere-hole-like cage nest (CSN) structure, to (iii) 3D solanum star-shaped flowers with multi-branchlet nanorods spreading out from central core in to lateral and axial directions (SSF) structure, respectively. The mechanistic formation of NRs, CSN nd SSF geometrics is evidenced from the microscopic patterns, including a top- and plane-view (FE-SEM)

field emission scanning electron microscope and (HR-TEM) a high-resolution transmission electron microscopy (Figs. 1, 2, S2, and S3).

Furthermore, facile electron/Li^+ ion mobility and highly conductive surfaces for MSTO-anode and SSF-, CSN- and NR-cathode composites are improved by well-ordered and sustainable modification by ~5nm C-shell dressers along entirely giant surface ripples, irregular bumps, undulations, and anticlines. These giant topographic surfaces affect high rate performance and tap density, and cyclic stability characteristics of half- or full-scale GPS-LIBs (see supporting information S1-S19). The integration of GPS interlay-complex architectonic anode/cathode geometrics into half-/full-scale LIBs may allow multi-gate-in-transport electron/ion mobility in building-blocks egress/ingress paths. These diverse pathways, including the upper, middle, and lower multi-zone crystal patterns, and for evaluating the frontal edge/apex/central/corner access sites are given their potentials in the design of GPS-LIB models and modules with superb specific capacities, high energy density, facile discharge–discharge rates, and extended long-term power stability. The GPS complex architectonic anode/cathode surface topographies that have irregular ripples, bumps, undulations and anticlines significantly affect electrochemical performance of both half- and full-cell LIB designs in terms of non-prescriptive cycle usages, heavily interior Li^+ ion loads, and spatial rate performance capabilities (Scheme 1).

Characteristics of complex super-architectonics (GPS) cathode-/anode-geometrics

The GPS complexities are built based on distinguishable orientation geometrics, building-blocks-in a wide-range of egress/ingress hierarchy, and super topographic-surface heterogeneity, roughness and anisotropy. The GPS-designated P- and N-electrodes of LMPO@C-cathodes, including SSF@C, CSN@C, and NR@C, as well as the MSTO@C anode architectonic geometrics and super surface topographies were investigated by using extensive variety of microscopic tools (Figs. 1, 2, S2, and S3) [36- 42]. The FE-SEM and HR-TEM microscopic patterns recorded along the top and side view

projects show an evidence of the control engineering of large-scale GPS, the unique and novel interlay-complex architectonic geometrics, multi-scale building-blocks egress/ingress pathways, and effective super surface topographies in terms of its heterogeneity, roughness and anisotropy.

Fig. 1

Fig. 2

The designated FE-SEM and HR-TEM profiles and energy-dispersive x-ray spectroscopy results for SSF@C-, CSN@C- and NR@C-cathode, and MSTO@C-anode reveal the unique effectiveness of GPS interlay-complex super-architectonics with novel geometrics and super topographic-surfaces on the feature of building-blocks-in LIB assembly. The intensive microscopic patterns reveal successful engineering of GPS P-cathode/N-anode electrodes with interlay-complex architectonic geometrics, arranged with multiple orientations (i.e., helical, latitudinal, and longitudinal directions), and modified with super surface topographies including irregular ripples, bumps, undulations and anticlines, ridges, and meso/macro-voids, respectively. As shown in Figure 1 &2, massively accessible building-blocks egress/ingress pockets are developed along GPS geometric, surface and structure component. For an engineering perspective, the GPS-anode/-cathode electrode cuticles offer open-gate-in-transports for the massive electrons/Li^+-ions movement. These massive transport gates enable potential Li^+-ion egress/ingress capacity with high rate velocity, leading to create GPS-LIBs with non-resisting spread electrons/Li^+-ion loads, and vast potential load/occupant/truck surface topographies during lithiation/delithiation processes. The rational super-architectonic designs of GPS P-cathode/N-anode electrodes into half- or full-scale CR2032 coin-cells allow GPS-LIB functions with a high tap density, short electron transport distance, and enhanced multi-diffusible ions kinetics, all of which may lead to ageless reachable battery with high loaded capacity, rate capability, cycle stability, and energy density (Figs. 1, 2, S11-S19).

Scheme 2 shows complex super-architectonics with a bundle of multi-axial systems along three–directional orientations that dominated along overlying all possible sides and faces and along the frontal edge/apex/central/corner sites. The systematic models show a real evidence of the formation of vast topographic-surface heterogeneity, roughness and anisotropy of GPS LMPO@C-cathodes, and GPS MSTO@C anode architectonics along all axes and facets (Scheme 2-middle). A combination of the finite GPS perspective and topographic space volumes, in general, offers GPS electrodes with fully-access-surfaces, free-space dynamic environments, and multi-scale building-blocks egress/ingress pathways including;

(i) multi-diffusive open-pore hole systems, connective meso-macroscopic windows along the entire and randomly dispersed NRs, CNS sheets and layers, and SSF-tower-star complex,

(ii) GPS building architects "block-by-block" with a large density of exposed active facets surface (containing numerous sites of connective multi-diffusible dimensions of the exposed bubbly meso-macro-free spaces open-pore system), and

(iii) multi-vast-mouth vacancies in highly-dense mesopores and mesogrooves, inter-trapped free occupation mesocage cavities, ridge-gate windows, cave nests, and intra-formational smooth shell/belt-walled/rounded fence-rims along the GPS surfaces.

These vast free surface-volume spaces can accommodate and enhance the multicentral dimensionality diffusion of Li^+-ions through their discharge (insertion, lithiation)/charge(delithiation, extraction) processes and their transfer along the electrolyte/electrode interfaces (Scheme 2).

(Scheme 2)

The scalability in atomic-arranged GPS-LMPO@C of SSF@C, CSN@C, and NR@C super-architectonics is further characterized via HR-TEM as shown in Figs. 1(i–k), S1(g–i), and S2(d–f), respectively. The orthorhombic olivine-super-architectonics are evident from the each selected area electron diffraction records, Figs. 1(k), S1(i), and S2(f). The top edge-view HR-TEM images of GPS

SSF@C, CSN@C, and NR@C reveal the crystal structures of the super-architectonics with interatomic spacing values of 0.458,1.05, 0.46,1.03, and 0.39,0.98 nm, respectively, corresponding to the clear GPS-{001} and GPS-{100} crystal planes of pure orthorhombic (space group: Pnma) structure, as an evidence XRD patterns of Pnma LMPO geometrics (JCPDS card no. 83-2092), see Figure 3 and S8 [36- 38]. The plane orientation of super-architectonics is mainly exposed along GPS-[010] AC-plane, enabling an optimization direction along P-electrode surfaces for rapid Li-ion diffusion, and high rate capability among other crystal-plane directions [37-40]. Figure 2(f) shows GPS MSTO@C lattice pattern with d-inter-spacing value ~0.352 nm of thermodynamically-sable super-architectonic tetragonal anatase-(101) plane surface, as an evidence based on XRD pattern of $I4_1/amd$ space group for the pure anatase GP-MSTO crystal (JCPDS 21-1272), see Figure S10.

For ideal electrode models, the decoration of GPS with highly conductive ~5nm-carbon layers is a key for the followings:

(i) Stabilization of the well-structured robustness of LMPO P-cathode and MSTO N-anode from dissolution or atomic dislocation during multiple (insertion, lithiation)/(delithiation, extraction) processes.

(ii) Enhancement of the GPS-LMPO P-cathode and GPS-MSTO N-anode topographic-surface characteristics in terms of heterogeneity, roughness and anisotropy gradients, leading to optimal performance of GPS-LIB designs

The carbon-dressed super-architectonics of the cathode/anode can influence LIBs by strengthening their power density, creating powerful Li-ion diffusion regimes, and improving hovering electron density for high-speed discharge rates.

For deterministic optimization of GPS complex super-architectonics, Fourier transform infrared spectroscopy, Raman spectra, thermal analyses, N_2 isotherms, X-ray photoelectron spectroscopy, and x-ray diffraction characterizations are also performed to examine the structurally stable orthorhombic

olivine-super-architectonic GPS-[010]-LMPO@C cathodes and GPS-[101]-anatase MSTO@C geometrics, building blocks egress/ingress along meso-, and macro-sponginess vacancies, surface heterogeneous composites, and anisotropic atomic-scale arrangement (Figures S4-S9).

Fig. 3

The scalable, robust design of half-/full-cell GPS-integrated LIB super-architectonics is achieved by using the anode N-electrode and cathode P-electrode surface topographies designed in CR2032 coin cells. Our goal is to create highly variable GPS-modulated LIB designs that could mimic the anode/cathode GPS orientations, configurations, and functionally open-ended-interfaces/ridges. The rich spatial distribution complexity along the P- and N-electrode surfaces may lead to the ever-changing charge/discharge participatory usage cycles and "fully cycled dynamics" of LIBs.

GPS cathode geometrics for half-cell GPS-LIB models

The GPS-modulated LIB designed with different surface GPS geometrics allowed us to study the electrochemical performances of half-cell cathode LIBs. We designed half-cell LIBs based on GPS-modulated LIB fabrics, such as GPS-SSF@C, -CSN@C, and -NR@C (see Figure S1). The measurements are presented in Figs. 4 to 6. The object of built-in GPS cathode-LIB is to study a key of multi-scale super-architectonic accessibilities, fully-access-surfaces, and free-space dynamic environments along the P- electrode cuticles in the super-GPS LIB-EV model with superior lithiation/delithiation cycling stability and continuous Li^+ ion insertion/extraction processes.

Cyclic voltammetry (CV) is recorded to study the excellent electrochemical super-architectonic performances of GPS-SSF@C, -CSN@C, and -NF@C CR2032 coin cells as half-scale LIBs. In general, the electrochemical optimization shows evidence of the effectiveness of the super-architectonic GPS-LMPO@C building blocks egress/ingress pathways along (i) surface vacancies of vortices, curvature angularities, nests, hole-like caves, and undulated ridges, (ii) multi-directional and

dimensional entrances of channels, vascular pipes, sheet layers, and (iii) crystal geometric edges, vertices, steps, and terraces. These giant topographic surfaces create special diffusion systems for high mobility of electron/Li^+ ions and offer excellent capacity storage, durability, and capability of LIBs [43- 46].

Fig. 4

To modulate the spatial cathodic electrode with potential optimal performance of half-cell GPS-LIB designs, we study the cyclic voltammogram (CV) for GPS SSF@C, CSN@C, and NR@C cathodes over the voltage window 3.0V to 4.5V vs. Li/Li^+ optimization at a sweep rate of 0.1 mV/s. Figure 4a represents the effect of GPS complex super-architectonics in the enhancement of electrochemical performance. The result shows evidence that the oxidation/reduction peaks for GPS SSF@C, CSN@C, and NR@C is specifically observed at 4.15/3.94 V, 4.19/3.90 V, and 4.23/3.83 V, respectively. The CV experiments of SSF@C for the first cycle are recorded at 0.1, 0.2, 0.5, 1, and 5 mVs^{-1} from 3.0V to 4.5V (Fig. 4(b)). The values of representative voltages of oxidation and reduction peaks are increased and decreased with the scan-rate increase. However, the representative current profiles of both oxidation and reduction peaks are increased along with scan-rate.

Figure 4(c) illustrates the charge-discharge voltage profiles of first cycle SSF@C cathode half-cell at different cycles (1st, 2nd, 50th, 100th, and 500th cycles) with a sweep rate of 0.1 mVs^{-1} from 3.0V to 4.5V. The result shows that the highly symmetric and spiculated peak profiles for Mn^{2+}/Mn^{3+} can be easily observed at 3.94/4.15V for GPS-SSF@C cathode within the cycles. This finding indicates the effect of GPS complex super-architectonic SSF@C in its excellent electrochemical performance, particularly during the Li^+-insertion (cathodic, reduction, lithiation) /extraction (anodic, oxidation, delithiation) processes [47, 48]. The GPS CV-curves associated with the charge/discharge processes are attributed to the optimal performance of SSF@C with the cycles and its excellent reversibility for the 500 tested cycles.

To investigate the geometric effect of GPS super-architectonics on the discharge capacity of cathode-half-cell LIBs, we study the behavior of specific discharge capacity ($mAhg^{-1}$) of the diverse GPS-SSF@C, -CSN@C, and -NR@C P-electrodes in half-cell LIBs at 0.1C to 20C (Figure 4(d)). The 1st discharging specific capacity of GPS-LIB models increases in this sequence; SSF@C- > CSN@C- > NR@C GPS-based cathode geometrics at overall scan rates (i.e., 0.1C to 20C). The charge–discharge cycle performance profiles of SSF@C, CSN@C, and NR@C GPS super-architectonics are shown in Figure 5. The first charge/discharge cycles of GPS super-architectonic cathodes are recorded with a range of voltages from 3.0 to 4.5 V vs. Li/Li^+ at 0.1 C. The GPS super-architectonic half- cells are charged and attained at 4.5 V for 1 h prior to discharging them until 3.0V at 0.1 C. Among all GPS super-architectonic cathodes, the SSF@C GPS cathode shows an excellent discharging capacity of 159.4 mAh g^{-1} at the first cycle compared to other GPS CSN@C and NR@C super-architectonics (132.4, and 99.7 mAh g^{-1}, respectively) at 0.1C. The high value of discharge capacity of SSF@C GPS cathode indicates its short electron transport distance, and intensive, multi-diffusible Li^+-ion loads in lithiation/delithiation cycling processes.

Fig. 5

The GPS interlaid-complex architectonics with novel geometrics and super surface topographies affect the building-blocks-in LIB charge/discharge cycles (see Fig. 5(b)). The first charge/discharge cycle curves of SSF@C GPS cathode are recorded at the range of 0.1 C- 20 C, by applying a voltage range from 3.0 to 4.5 V vs. Li/Li^+. The finding indicates that building-blocks-in LIB with SSF@C GPS cathode has good tap density, short electron transport distance, and improved multi-scale egress/ingress pathways. These vast GPS super architectonic features may lead to create ageless and rechargeable LIBs with excellent-loaded discharge capacities over a wide range of current C-rates. Figure 5(c) shows the charge/discharge curves for SSF@C at a number of cycles (1st, 10th, 50th, 100th, and 500th cycles). The outstanding long-term cycling performance of this SSF@C GPS cathode can

be ascribed as the stability of its interlaid-complex super-architectonic structures over a long-term cycling within massive lithiation/delithiation processes. The retaining superiority of SSF@C GPS cathode in its cycling stability is clearly noticeable in Fig. 5(d). Specifically, SSF@C GPS super-architectonic attains 97.3% of its first cycle capacity value after 100 cycles at 1C. In turn, CSN@C and NR@C GPS super-architectonics retain only 84.8% and 31.1% of their first cycle capacity values, respectively. A slight decrease in the GPS SSF@C capacity after 100 cycles at 1C compared with other CSN@C and NR@C GPS interlaid-complex super-architectonics can be attributed to its orientations, configurations, functionally open-ended-surface vacancies, undulated ridges, and rich spatial distribution complexity along the whole electrode geometrics. The GPS SSF@C interlaid-complex super-architectonic is structurally stable enough to withstand formidable life-use cycles, and can offer high electrochemical reversibility during massive lithiation/delithiation processes.

Fig. 6

The super-architectonic capability performance rates of SSF@C, CSN@C, and NR@C GPS cathodes are crucial in meeting the advanced requirements of HEVs and EVs. To evaluate their rate capability, the cycling performance of these GPS SSF@C, CSN@C, and NR@C cathodes is tested at the C-rate range of 0.1 C - 5 C, then followed by back to C-rate of 0.1 C and 10 C, and finally back to 1 C, and 20C, with continuous operation of 10 cycles at each recorded C-rate (Figure 6). The GPS-cathode specific capacity of all SSF@C, CSN@C, and NR@C geometrics decreases with an increasing current rate. The super-architectonic SSF@C cathode shows good rate capability, and long-term cycle stability at all recorded C-rate and cycles. At specific C-rate of 20C, GPS super-architectonic SSF@C cathode observes (i) excellent discharge reversible capacity of approximately 58 mAh g^{-1} and 55.5 mAh g^{-1}, and (ii) retention of 96.8% and 92.7% from its first cycling capacity after 100 and 1000 cycles, respectively. Meanwhile, the discharge capacity of super-architectonic CSN@C GPS cathode is significantly reduced to 7.5 $mAhg^{-1}$ after 100 cycles at 20C during a repeated Li^{+} ion

insertion/extraction. This CSN@C GPS cathode also retains 0% of its first cycle capacity after 1000 cycles. Similarly, the NR@C GPS cathode retains 0% of its first cycle capacity at 20C. Taken together, these findings highlight the uniqueness of super-architectonic SSF@C GPS-cathode configurations characterized in GPS-LIB design direction. As a primary model of super-architectonic SSF@C GPS cathode, a set of multi-axial systems along three–directional dominates overlying along sides and faces in dense upward layers affect the rate performance capabilities (see Scheme 2). The orientation of super-architectonic SSF@C cathode along their GPS-vertical, -lateral and -longitudinal axes, which have upper-top-capped pyramidal prisms, makes the charge/discharge rate more facile (Scheme 2). A comparison in terms of rate capability, Coulombic efficiency, reversible capacity and long-term cycle stability is reported for GPS-LMPO (with SSF@C geometrics) half-scale LIB and other LMPO cathode-LIBs fabricated by normal and conventional conditions, (see supporting information S15). Table S1 shows evidence of the effectiveness of vast GPS super architectonic complexity, building blocks egress/ingress hierarchy, topographic-surface heterogeneity, and roughness and anisotropy of GPS LMPO@C-cathodes in the integration of half- scale LIBs.

The effect of GPS interlaid-complex architectonics with novel geometrics and super surface topographies on the non-resisting spread electrons/Li^+-ion loads and potential Li^+-ion egress/ingress capacity with high rate velocity is evident in our building-blocks-in cathode GPS-LIB assembly. To explore non-resisting Li+ ion with full occupant diffusions of P-electrodes, we examined the EIS experiment (i.e., electrochemical impedance spectroscopy) of GPS-SSF@C, -CSN@C, and -NR@C surfaces cathodes. The EIS results for SSF@C, CSN@C, and NR@C are presented as Nyquist plots in Fig. 6(b). The low- and high- frequency graphs indicate the existence of a slanted line and semicircle feature, respectively. The equivalent circuit describes the EIS findings, as shown as an inset in Fig. 6(b). The GPS equivalent circuit components are defined as previous studies [49-51]. The GPS-semicircular-arc at the highest frequency region is a function to the R_{ct} (charge transfer

resistance) value. The R_{ct} is equivalent to the diameter value of the semicircle curve taken along Z-axis. The diameter of GPS-SSF@C semicircle is smaller than that of other GPS-CSN@C and -NR@C super-architectonics. The lowness in R_{ct} value of GPS-SSF@C indicates its excellent Li^+-ion egress/ingress capacity with high rate velocity, on-off-site storage modules, and super-large door-in transport of Li^+-ion/electron during discharging (insertion, lithiation) and charging (delithiation, extraction) processes. Our finding gives enidence that the synergy of 5 nm-carbon layer-coated P-electrodes not only stablizes the GPS geometrics and super surface topographies of P-electrodes but also boots fully-cycled dynamic lithiation/delithiation processes. The GPS-LMPO-dressed carbon composites are naturally playing a key role for minimizing electrode resistance and achieving excellent electronic contact, electrical conductivity, and facile transport to withstand the formidable high-temperature environments of GPS-integrated LIBs. Accordingly, a set of temperature-dependent experiments versus electrical conductivity is recorded along the GPS-cathode integrated half-cell LIBs, as shown in Fig. 6(c). Our finding shows that the GPS-cathode LIBs attain high conductivity at 298K; however, GPS-SSF@C cathode-LIBs show the excellent conductivity at high temperature of ~250K to 455K. Specifically, the finding indicates that the super-architectonic GPS SSF@C cathode has extra-interconnected open-gate-in-transports on its geometrics and giant surface topographies, which would facilitate electrolyte penetration, improve electronic conductivity, and reduce the constraints on the diffusion of Li^{+-}ions.

Given its high capacity, high rate capability, and long cycling performance of half-scale cathode LIB CR2032 coin-cells, GPS SSF@C P-cathode electrodes are strong candidate cathodes for high performance of ageless reachable battery. The super-architectonic complexity, building blocks egress/ingress hierarchy, topographic-surface heterogeneity, roughness and anisotropy, and GPS-orientation and -arrangement integrated in GPS-SSF@C LIBs provide a dynamic free-space-access

environment and desirable seamless transition vacancy channels and tunnels, thereby making SSF@C P-electrode as a particular of interest for engineering perspective of high-power LIBs.

Super-architectonic GPS-MSTO@C anode geometrics for half-cell GPS-LIB models

The key influences of tectonic-power-driven sets of built-in GPS-MSTO@C N-anode LIB CR2032 coin-cells are studied. The MSTO@C GPS-anode super-architectonic electrode with novel geometrics and surface topographies would lead to low-cost fabrication avenue and GPS ever-decreasing discharge timescale building-blocks-in LIB assembly, and maintaining high-energy density for long-driving range of EVs. Figures S11 & S12 show the electrochemical performance of MSTO@C anodic GPS half-cell LIBs. The homogenous distribution of coated nanocarbon layers onto its GPS-anode geometrics and surface topographies influences the anode half-cell GPS-LIB model functions. To explore the effectiveness of MSTO@C as potential open-gate-in-transports in the anode half-scale GPS-LIB model, we studied its electrochemical optimization and robust GPS-LIB design (Figure S1). The potential charging/discharging capacity curves of the first cycle are measured at C-rates (i.e., 0.2 C, 1 C, 5 C, 10 C, and 20 C), Figure S11 (a). The galvanostatic charging/discharging capacity profiles of the built-in GPS-MSTO@C N-anode LIB CR2032 coin-cells are configured from 1V to 3V vs. Li/Li^+.

With a close look to the discharging profile, three numerical steps are recognized as a result of the following features. (i) The formulation of a solid-solution film with small Li^+-ion loads that are covered the MSTO@C electrode surface topography is evident. This initial stage of load/occupant/truck surface topographies is recognized by a rapid potential decrease from the open circuit voltage (OCV–3 V) to ca.1.7 V vs. Li/Li^+. (ii) The formation of long, stable static-flat plateau at potential of 1.7 V is achieved. At this stage, the half occupant/truck of the Li-insertion (i.e., lithiation) process is lodged the interfcial MSTO crystal sites. (iii) The large GPS Li- occupant/truck

insertion stage is indicated the interfacial-scale of fully-accessed pocket storage, at which long, and drastic decays in potential are occurred from 1.7 V to the cut-off voltage 1.0 V vs. Li/Li^+. Likely, three defining features describe the charging capacity profile of (i) GPS potential-depended monotonic capacity increases (from 1 to 1.96 V), at which Li-extraction (delithiation) process from accommodated GPS MSTO geometrics and super surface topographies is achieved. (ii) Continually-extracted Li^+-ions during delithiation process along long, stable static-flat plateau are recognized at this stage. (iii) A formation of a solid-solution film curvature at voltage of 3.0 V of roughly full extraction is occurred, respectively.

To explore the effect of the systematic models of GPS-MSTO@C N-anode LIB CR2032 coin-cells, we study the first cycle of GPS discharge specific capacity at a range of 0.2 C to 20 C (Figure S11b). The finding indicates excellent discharge reversible capacity of GPS-MSTO@C N-anode LIB CR2032 coin-cells. Furthermore, the non-resisting, massive electrons/Li^+-ions movements along GPS-MSTO@C N-anode geometrics and super surface topographies are evident from Nyquist plots of the EIS profiles (Figure S11c).

To evaluate the rate capability performance of GPS-MSTO@C N-anode LIB CR2032 coin-cells from 1.0 to 3.0 V, we investigate the discharging capacity cycles at the C-rate range of 0.1 C –to 10 C, then back to C-rate of 0.1 C and 10 C, and then finally back to 1 C, and 20 C, with continuous operation of 10 cycles up to 100 cycles at each recorded C-rate (Figure S12). The GPS-anode specific capacity of MSTO@C geometrics decreases with increasing the current rate (i.e., initial value is 314.6 $mAhg^{-1}$ at the first cycle, 0.1 C). The GPS MSTO@C anodic capacity decreased remarkably during the repeatable and continuous Li^+ ion insertion/extraction process of 158.3 $mAhg^{-1}$ at 20 C, and after 100-charging/discharging cycles.

The multi-accessibly open-gate-in-transports along GPS super-architectonic geometrics, and loophole-on-surface topographies including irregular ripples, bumps, undulations and anticlines,

ridges, and meso/macro-voids, respectively, play key roles in the retention of GPS-MSTO@C N-anode LIB CR2032 coin-cells. The stability of the potential Li^+-ion egress/ingress capacity with high rate velocity is also evident after the multiple charge/discharge cycles. To show the scalable, robust design of our anode half-cell GPS-integrated LIB super-architectonics, we offer comprehensive studies between the GPS-MSTO@C N-anode LIB CR2032 coin-cells and other TiO_2 anode LIBs that fabricated by normal and conventional conditions, (see supporting information S16).

GPS cathode- and anode-electrode-geometrics-integrated full-scale LIBs

We designed fully functional multi-axial/dimension GPS cathode- and anode-electrode geometrics into the precisely defined full-cell LIB pattern model. In GPS-modulated LIB designs, we used MSTO@C GPS anode//SSF@C GPS cathode as the preferred N-electrode and P-electrode surface topographies, respectively (Fig. 7 and Scheme 3). The GPS complex architectonic SSF@C-cathode//MSTO@C-anode LIB surface topographies are specified into CR2032 coin-cell types (see supporting information S1). This GPS full-cell LIB design sheds light on the key influences of vast super architectonic complexity, geometrics, vacancies and surface topographies on the sets of bundled layer-by-layer pouch models and on large-scale LIB module configurations. These key factors of super-architectonic GPS-modulated LIB significantly affect the non-prescriptive cycle usages, heavily interior Li^+ ion loads, spatial rate performance capabilities, specific energy density and high Coulombic efficiency. To approve our engineering perspective of proposed GPS- SSF@C// GPS-MSTO@C full scale LIBs, we offer comprehensive comparison studies between the GPS-modulated-LIB and other designated $LiFePO_4$//TiO_2 and $LiMnPO_4$//TiO_2 LIB cells that previously reported, (see supporting information S17).

To calculate the super-architectonic GPS cell-energy density of full-scale LIB modules, the bundled layers of MSTO@C GPS anode//SSF@C GPS cathode electrodes are specified in pouch-LIB-model

(see supporting information S14). The multiple bundled layers of incorporated amounts of GPS-MSTO@C (N-electrode anode) // GPS-SSF@C (P-electrode cathode) are 8-//7- layers, and along 14 surface topographic sides. These 8-anode//7-cathode surface topographic layers are substantially decorated with the 8 µm-Cu-foil and 12 µm-Al-foil platform electrodes, respectively. The GPS average working potential of GPS-MSTO@C (N-electrode anode) // GPS-SSF@C (P-electrode cathode) full-scale battery is 3.8 V, enabling highly practical specific energy-density of 178.8 $Whkg^{-1}$, in agreement to theoretical value of 197.7 $Whkg^{-1}$ for a full-scale GPS-LMPO@C//MSTO@C battery, (see more details studies of supporting information S11 A, B and C). The slight decrease of the practical energy density compared with its theoretical value of GPS-MSTO@C (N-electrode anode) // GPS-SSF@C (P-electrode cathode) full-scale LIB may be due to the difficulty to remove Li^+ ions completely during the fully-dynamic extraction. The full delithiation process of the occupant/truck Li^+ ion loads from the interfacial-scale of fully-accessed pocket storage requires cutoff voltage >3.0V.

Aiming to explore the safety and large timescale LIB-EV driving ranges with high power density, a model of full-scale GPS-MSTO@C (N-electrode anode) // GPS-SSF@C (P-electrode cathode) pouch LIBs is fabricated under optimization control of the mass-loading of N-anode and P-cathode electrodes and their ratio of capacity (i.e., balancing capacity of $(N/P)_{Cap}$ ratio). A set of full experiments is carried out for controlling a pouch model with optimal $(N/P)_{Cap}$ ratio, which leads to outstanding trade–off performance variability (see supporting information S12 - S14, and experimental section). Accordingly, the optimal accuracy of the mass-fraction of SSF@C GPS cathode components formulated in a pouch LIB model is about 44%, leading to specific energy density of the GPS-TO@C//LMPO@C full-scale LIB of 178.8 $Whkg^{-1}$.

For reliable structural design of large scale LIB modules, the volumetric energy density is ideal parameter of LIB engineering perspective (see supporting S14). The structural GPS-building-blocks-

in 18650-cylinder and bundled-layers of pouch models offer volumetric energy density of MSTO@C GPS-anode//LMPO@C GPS-cathode full-scale CR2032 LIB-module of 435.63 Wh/L and 247.68 Wh/L, respectively. Although, the GPS-modulated 18650-cylinders produce highly recognizable value, the bundled layer-by-layer pouch models represent the practical and optimal engineering designs for a wide range of electrochemical performances.

The mutual balancing capacity of $(N/P)_{Cap}$ ratio of super-architectonic GPS-MSTO@C (N-electrode anode) // GPS-SSF@C (P-electrode cathode) LIB-modules offers areal discharge capacity of 0.89 and 0.85 Ah/cm^2, respectively. The optimization of areal discharge capacity performance super-architectonic built-in pouch LIB models would be a more rational choice for the most effective solutions in terms of high specific energy density yet with large safety factors of the proposed super-architectonic GPS-built-in pouch LIB models. Such super-architectonic GPS-built-in LIBs are promising to enhance betterment of safety factor issues for GPS-LIB-powered engineering modules. The stability of the super-architectonic built-in SSF@C GPS-cathode // MSTO@C GPS-anode full-scale geometric and surface topographic LIB models is investigated by studying its discharge cycle performance as shown in Fig. 7(a). The architectonic GPS-modulated-LIB model retains 90.0 % of its first cycle discharge capacity after 100 cycles at 1 C. Figure 7(a) shows the typical first cycle of charging/discharging voltage patterns of full-scale GPS-modulated-LIB model cycles at C-rate range from 0.1 C to 20 C by applying a voltage range from 1.5V to 3.8V. The results reveal that the values of super-architectonic GPS-modulated LIB discharging capacities decrease with C-rate upsurge (i.e., from 0.1 to 20 C). The super-architectonic GPS-modulated LIB full-cell is maintained the discharge capacity of 108.3 $mAhg^{-1}$ at 20 C for its initial performance value.

The super-architectonic GPS-modulated LIB capability rates are investigated at the voltage range from 1.5 to 3.8 V and the C-rate range from 0.1 C – to 5 C, then back to C-rate of 0.1 C and 10 C, and finally back to 1 C and 20 C, with continuous operation of cycling variation up to 100 cycles at

each recorded C-rate (Figure 7c). The super-architectonic specific capacity of the full-cell SSF@C GPS-cathode//MSTO@C GPS-anode geometrics and surface topographies is decreased with an increase in the current rate. Feasible discharge capacity of a multiple cycles and C-rates indicates the superstructure effect on the overall scales of GPS-modulated-LIBs. The complex super-architectonics of SSF@C GPS-cathode // MSTO@C GPS-anode full-scale models or modules create ever-changing charge/discharge contributory usage of cycles, "fully cycled dynamics," affordable on-off-site storage modules, and super-large gate-in-transport of electron/Li^+-ion trails. Our finding indicates that the GPS P-cathode/N-anode electrodes integrated into full-scale CR2032 coin-cells are potential candidates to achieve the high power energy modules for LIB-EVs.

Fig. 7& Scheme 3

Super-architectonic GPS Coulombic efficacy (CE) of full-scale SSF@C GPS-cathode // MSTO@C GPS-anode models describes the charge efficiency, by which Li^+ ions/electrons are transferred into powerful GPS multiple orientations and super-surface topographies of our distinguishable super-architectonic batteries. CE is the effective ratio between the total values of extracted and inserted charging from the distinct super-architectonic GPS-battery over one-full-cycle. For developing a scalar optimization perspective of GPS-modulated LIB-EVs, we investigate a fast-charging pattern of architectonic bundled-layers of GPS-MSTO@C (N-electrode anode) // GPS-SSF@C (P-electrode cathode) pouch models by applying constant current and voltage (named as CC-CV) protocol. A set of fast-charging experiments is recorded for GPS-modulated-LIB pouch models at different C-rate values, ranging from 1C to 10C, and temperature between 25^{o}C to 35^{o}C (see supporting information S19 & Figure S13). The CC-charging timescale decays with an increase of the charging rate in the applying range from 1C to 5C. The CC-charging timescale dependent sets at C-rate > 5C are not recognizable conditions. Therefore, the CV-charging timescale dependent sets are efficient, reliable,

and quantifiable at the range of C-rate variabilities (see Fig. S13). The formation of long, stable static-flat plateau of CV-charging timescale (i.e. approximately 10 to 12 minutes) at C-rate > 5C is recognizable with a contribution of the surface-elevated temperature at 35°C as a maximal value. The fast CV-charging timescale ≥ 5 minutes can be optimized at C-rate range ~~of~~ from 1C to 4C, respectively. Under an ever-increasing demand on reliable and fast time-scale charge capacity, the super-architectonic GPS-MSTO@C (N-electrode anode) // GPS-SSF@C (P-electrode cathode) pouch models and modules are powerful in Li^+ ion diffusion regimes, and improving hovering electron density for high-speed discharging and charging rates.

The multi-criteria optimization of outstanding cycle performance, long-term stability, and Coulombic efficacy of full-scale super-architectonic GPS-MSTO@C (N-electrode anode) // GPS-SSF@C (P-electrode cathode) models and modules is studied at C-rate of 1C within 2000 cycles between 1.5V and 3.8 V vs. Li/Li^+ (Fig. 7d). Note, the magnification of the first 200 cycles of the charging/discharging performance is recorded in Figure 7e. The super-architectonic GPS-modulated LIB model retains 77.5% specific discharging capacity from its original value of 156.3 $mAhg^{-1}$ after 2000 cycles, and Coulombic efficacy of approximately 99.6% at C-rate of 1C, and at 25°C. For a wide range of charging/discharging cycles (i.e., >2000 cycles), the super-architectonic full-scale GPS-modulated LIB model is attained approximately 100% of its Coulombic efficacy. In general, the complex super-architectonic full-scale GPS-modulated LIB models demonstrate an outstanding structural design stability, high specific charging/discharging capacity, high rate capability, high-speed discharging and charging rates and long cycle life (see Scheme 3 and Figure 7).

Scheme 3A shows the simulated 3D projection of robust full-scale design optimization of GPS SSF@C GPS-cathode // MSTO@C GPS-anode full-scale architectonics after discharge capacity cycles. The systematic projection represents the powerful structural stability of super-architectonic GPS-building-blocks-in a wide-range of 3D distinguishable orientation geometrics, egress/ingress

vacancy models, and super topographic-surfaces after a number of charging/discharging cycles (i.e.≥ 2000) (Scheme 3B). The super-architectonic SSF@C GPS-cathode // MSTO@C GPS-anode platform electrodes provide built-in full-cell GPS-integrated LIBs with four key features.

First, multi-dimensional electron/Li^+-ion mobility is occurred as a result of including many GPS-building-blocks-in egress/ingress pathways along the upper, middle, and lower multi-zone crystal surface geometrics, as well as along the frontal edge/apex/central crystal sites. For instance, the SSF@C GPS-cathode with a top-upper square-based pyramid structure offers four-facet exposure surfaces that enable the diffusion of electrons/Li ions along the central site crystals, multi-edges, vertices, kinks, steps, and upper-top-zone surfaces (Scheme 3B).

Second, GPS-heavily interior loads, movements and diffusions of Li^+ ion along the axial directions and axis of coordinates (i.e. lateral, vertical, circular, zigzag, and longitudinal axes) ensured the mobility of electrons/Li^+ ions along the peripheral top electrode surfaces.

Third, the super-architectonic diffusion gates into the interlaid-complex vacancies, such as caves, holes, nests, windows, canals, ridges, cavities, and pipes may create GPS-modulated LIBs with superb specific capacities, high energy density, high-speed discharging/discharging rates, and extended long-term power stability.

Fourth, the loophole-on-surfaces with different topographies and curvatures including ripples, winglets, protuberances, irregular bumps, V-hooks, undulations, and anticlines are key roles in retaining LIBs, ensuring the continuous function and stability of electron/Li^+-ion transport pathways after 2000 cycles, and assuring the simultaneous diffusion of Li^+-ions during the lithiation/delithiation (discharging/charging) cycling processes for SSF@C GPS-cathode // MSTO@C GPS-anode full-scale architectonics.

The super-architectonic built-in SSF@C GPS-cathode // MSTO@C GPS-anode full-scale LIB model shows its excellent Li^+-ion egress/ingress capacity with high rate velocity, on-/off-site storage modules, and super-large door-in transport of Li^+-ion/electron during discharging (insertion, lithiation) and charging (delithiation, extraction) processes. Furthermore, the super-architectonic GPS proximity of Li^+ ion accessible loophole-on-surfaces and open-gate-in-transports is one of the most effective solutions to avoid geometric and surface topographic polarization and to boost the fully-cycled dynamics during discharge (insertion, lithiation) / charge (delithiation, extraction) processes. These GPS tectonic-power-driven SSF@C GPS-cathode // MSTO@C GPS-anode geometrics offer highly reversible capacity rate of LIBs, and structural stability to withstand under high-temperature environments.

Conclusions

We report on large-scale-GPS-integrated anode/cathode built-in half- and full-scale LIB modules. The GPS-LIB models demonstrated high-power and volumetric-energy density, high specific charging/discharging capacity, outstanding rate capability, high-speed discharging and charging rates and long cycle life. We designate GPS-LIB CR2032 coin-cells based on a series of vast GPS super architectonic complexities that are built with distinguishable orientation geometrics, building-blocks-in a wide-range of egress/ingress egress/ingress hierarchy, and topographic-surface heterogeneity, roughness and anisotropy. The alignment of GPS-specified P- and N-electrodes of LMPO@C-cathodes including SSF@C, CSN@C, and NR@C, as well as the MSTO@C anode architectonic geometrics and topographies is successfully controlled half- and full-cell LIB models and large-scale modules. Super-architectonics built-in GPS-LIBs offer high potential Li^+-ion egress/ingress capacity, high rate velocity, on-/off-site storage modules, and super-large door-in transport of Li^+-ion/electron, which can lead to reduce the wastage of reversible capacity of GPS-LIBs. The module configurations

of the GPS-modulated super-architectonic LIB initiatives are specified in bundled layer-by-layer pouch LIBs-type with outstanding energy power and large safety factors. For an engineering perspective, the super-architectonic GPS-modulated LIBs offer giant loophole-on-surfaces and open-gate-in-transports for the massive electrons/Li^+-ions movement, and potential Li^+-ion egress/ingress capacity. The GPS-LIB models show evidence of non-resisting spread electrons/Li^+-ion loads, and vast potential load/occupant/truck surface topographies during multiple number of lithiation/delithiation processes (i.e., > 2000 cycles). The GPS-LIB models or modules demonstrated a long-term stability and excellent discharge capacity retention of approximately 77.5% with a Coulombic efficiency of 99.6% for 2000 cycles at 1C. The key influences of tectonic-power-driven sets of GPS-modulated-LIB designs provide a high specific energy density of ≈179 Wh kg^{-1} for high timescale EV-driving range and power density. Our proposed powerful super-architectonic GPS-modulated LIB models could improve the low-cost design for new generation batteries.

References:

[1] J.-M. Tarascon, M. Armand, Issues and challenges facing rechargeable lithium batteries, Nature. 414 (2001) 359–367. doi:10.1038/35104644.

[2] C. Jiang, E. Hosono, H. Zhou, Nanomaterials for Nanostructured materials are currently of interest for lithium ion, Nanotoday. 1 (2006) 28. doi:http://dx.doi.org/10.1016/S1748-0132(06)70114-1.

[3] V. Aravindan, J. Sundaramurthy, P.S. Kumar, N. Shubha, W.C. Ling, S. Ramakrishna, S. Madhavi, A novel strategy to construct high performance lithium-ion cells using one dimensional electrospun nanofibers, electrodes and separators, Nanoscale. 5 (2013) 10636–10645. doi:10.1039/c3nr04486f.

[4] V. Aravindan, J. Gnanaraj, Y.-S. Lee, S. Madhavi, LiMnPO4 – A next generation cathode

material for lithium-ion batteries, J. Mater. Chem. A. 1 (2013) 3518. doi:10.1039/c2ta01393b.

[5] N.-S. Choi, Z. Chen, S.A. Freunberger, X. Ji, Y.-K. Sun, K. Amine, G. Yushin, L.F. Nazar, J. Cho, P.G. Bruce, Challenges Facing Lithium Batteries and Electrical Double-Layer Capacitors, Angew. Chemie Int. Ed. 51 (2012) 9994–10024. doi:10.1002/anie.201201429.

[6] O.K. Park, Y. Cho, S. Lee, H.C. Yoo, H.K. Song, J. Cho, Who will drive electric vehicles, olivine or spinel?, Energy Environ. Sci. 4 (2011) 1621–1633. doi:10.1039/c0ee00559b.

[7] J.H. Lee, C.S. Yoon, J.Y. Hwang, S.J. Kim, F. Maglia, P. Lamp, S.T. Myung, Y.K. Sun, High-energy-density lithium-ion battery using a carbon-nanotube-Si composite anode and a compositionally graded $Li[Ni_{0.85}Co_{0.05}Mn_{0.10}]O_2$cathode, Energy Environ. Sci. 9 (2016) 2152–2158. doi:10.1039/c6ee01134a.

[8] H. KhalifaS. A. El-Safty, A. Red, M. A. Shenashen, M. M. Selim, A. ElmarakbiH. A. Metawa. Theoretical and Experimental Sets of Choice Anode/Cathode Architectonics for High-Performance Full-Scale LIB Built-up Models, Nano-Micro Letters, 11(2019) 84. https://doi.org/10.1007/s40820-019-0315-8

[9] L. Guo, Y. Zhang, J. Wang, L. Ma, S. Ma, Y. Zhang, E. Wang, Y. Bi, D. Wang, W.C. McKee, Y. Xu, J. Chen, Q. Zhang, C. Nan, L. Gu, P.G. Bruce, Z. Peng, Unlocking the energy capabilities of micron-sized $LiFePO_4$, Nat. Commun. 6 (2015) 7898. doi:10.1038/ncomms8898.

[10] H. Liu, H. Yang, J. Li, A novel method for preparing LiFePO4nanorods as a cathode material for lithium-ion power batteries, Electrochim. Acta. 55 (2010) 1626–1629. doi:10.1016/j.electacta.2009.10.039.

[11] H. Khalifa, S. A. El-Safty, A. Reda, M. A. Shenashen, M. M. Selim, O. Y. Alothman, N. Ohashi , Meso/macroscopically multifunctional surface interfaces, ridges, and vortex-modified anode/cathode cuticles as force-driven modulation of high-energy density of LIB electric

vehicles, Sci. Rep. 9(2019) 14701. doi:10.1038/s41598-019-51345-z

[12] K. Zaghib, A. Mauger, F. Gendron, C.M. Julien, Surface effects on the physical and electrochemical properties of thin $LiFePO_4$ particles, Chem. Mater. 20 (2008) 462–469. doi:10.1021/cm7027993.

[13] H. Khalifa S.A. El-Safty A. Reda M. A. Shenashen A. Elmarakbi H. A. Metawa, Structurally folded curvature surface models of geodes/ agate rosettes (cathode/anode) as vehicle/truck storages for high energy density of LIBs, Batteries & Supercaps, (2019) https://doi.org/10.1002/batt.201900083

[14] J. Liu, J. Wang, X. Yan, X. Zhang, G. Yang, A.F. Jalbout, R. Wang, Long-term cyclability of LiFePO4/carbon composite cathode material for lithium-ion battery applications, Electrochim. Acta. 54 (2009) 5656–5659. doi:10.1016/j.electacta.2009.05.003.

[15] Y. Liu, J. Liu, J. Wang, M.N. Banis, B. Xiao, A. Lushington, W. Xiao, R. Li, T.K. Sham, G. Liang, X. Sun, Formation of size-dependent and conductive phase on lithium iron phosphate during carbon coating, Nat. Commun. 9 (2018) 1–8. doi:10.1038/s41467-018-03324-7.

[16] M. Zhang, N. Garcia-Araez, A.L. Hector, Understanding and development of olivine $LiCoPO_4$ cathode materials for lithium-ion batteries, J. Mater. Chem. A. 6 (2018) 14483–14517. doi:10.1039/c8ta04063j.

[17] D. Chen, W. Wei, R. Wang, X.F. Lang, Y. Tian, L. Guo, Facile synthesis of 3D hierarchical foldaway-lantern-like $LiMnPO_4$ by nanoplate self-assembly, and electrochemical performance for Li-ion batteries, Dalt. Trans. 41 (2012) 8822–8828. doi:10.1039/c2dt30630a.

[18] Z. Gong, Y. Yang, Recent advances in the research of polyanion-type cathode materials for Li-ion batteries, Energy Environ. Sci. 4 (2011) 3223–3242. doi:10.1039/c0ee00713g.

[19] A.K. Padhi, Phospho-olivines as Positive-Electrode Materials for Rechargeable Lithium Batteries, J. Electrochem. Soc. 144 (1997) 1188. doi:10.1149/1.1837571.

[20] N. Recham, J. Oró-Solé, K. Djellab, M.R. Palacín, C. Masquelier, J.M. Tarascon, Hydrothermal synthesis, silver decoration and electrochemistry of $LiMPO_4$(M = Fe, Mn, and Co) single crystals, Solid State Ionics. 220 (2012) 47–52. doi:10.1016/j.ssi.2012.05.031.

[21] J.N. Zhu, W.C. Li, F. Cheng, A.H. Lu, Synthesis of $LiMnPO_4$/C with superior performance as Li-ion battery cathodes by a two-stage microwave solvothermal process, J. Mater. Chem. A. 3 (2015) 13920–13925. doi:10.1039/c5ta02653a.

[22] M. Yonemura, A. Yamada, Y. Takei, N. Sonoyama, R. Kanno, Comparative Kinetic Study of Olivine Li_xMPO_4 (M=Fe, Mn), J. Electrochem. Soc. 151 (2004) A1352. doi:10.1149/1.1773731.

[23] C. Delacourt, L. Laffont, R. Bouchet, C. Wurm, J.-B. Leriche, M. Morcrette, J.-M. Tarascon, C. Masquelier, Toward Understanding of Electrical Limitations (Electronic, Ionic) in $LiMPO_4$ (M=Fe, Mn) Electrode Materials, J. Electrochem. Soc. 152 (2005) A913. doi:10.1149/1.1884787.

[24] D. Morgan, A. Van der Ven, G. Ceder, Li Conductivity in Li_xMPO_4 (M = Mn, Fe, Co, Ni) Olivine Materials, Electrochem. Solid-State Lett. 7 (2004) A30. doi:10.1149/1.1633511.

[25] J.-M. Tarascon, P. Poizot, S. Laruelle, S. Grugeon, L. Dupont, Nano-sized transition-metal oxides as negative-electrode materials for lithium-ion batteries, Nature. 407 (2000) 496–499. doi:10.1038/35035045.

[26] Y. Yang, Y. Bai, S. Zhao, Q. Chang, W. Zhang, Electrochemical performances of Si/TiO_2composite synthesized by hydrothermal method, J. Alloys Compd. 579 (2013) 7–11. doi:10.1016/j.jallcom.2013.05.023.

[27] D.-H. Lee, B.-H. Lee, A.K. Sinha, J.-H. Park, M.-S. Kim, J. Park, H. Shin, K.-S. Lee, Y.-E. Sung, T. Hyeon, Engineering Titanium Dioxide Nanostructures for Enhanced Lithium-Ion Storage, J. Am. Chem. Soc. 140 (2018) 16676–16684. doi:10.1021/jacs.8b09487.

[28] J. Xu, Y. Wang, Z. Li, W.F. Zhang, Preparation and electrochemical properties of carbon-doped TiO_2 nanotubes as an anode material for lithium-ion batteries, J. Power Sources. 175 (2008) 903–908. doi:10.1016/j.jpowsour.2007.10.014.

[29] J. Wang, Y. Bai, M. Wu, J. Yin, W.F. Zhang, Preparation and electrochemical properties of TiO_2 hollow spheres as an anode material for lithium-ion batteries, J. Power Sources. 191 (2009) 614–618. doi:10.1016/j.jpowsour.2009.02.056.

[30] G. Wang, Y. Qi, D. Zhang, J. Bao, L. Xu, Y. Zhao, J. Qiu, S. Yuan, H. Li, Rational Design of Porous TiO_2@N-Doped Carbon for High Rate Lithium Ion Batteries, Energy Technol. (2018) 1–29. doi:10.1002/ente.201800911.

[31] V. Aravindan, Y.S. Lee, R. Yazami, S. Madhavi, TiO_2 polymorphs in "rocking-chair" Li-ion batteries, Mater. Today. 18 (2015) 345–351. doi:10.1016/j.mattod.2015.02.015.

[32] G.F. Ortiz, I. Hanzu, T. Djenizian, P. Lavela, J.L. Tirado, P. Knauth, Alternative Li-ion battery electrode based on self-organized titania nanotubes, Chem. Mater. 21 (2009) 63–67. doi:10.1021/cm801670u.

[33] D. Hassen, M.A. Shenashen, A.R. El-Safty, A. Elmarakbi, S.A. El-Safty, Anisotropic N-Graphene-diffused Co_3O_4 nanocrystals with dense upper-zone top-on-plane exposure facets as effective ORR electrocatalysts, Sci. Rep. 8 (2018) 3740. doi:10.1038/s41598-018-21878-w.

[34] M.A. Shenashen, D. Hassen, S.A. El-Safty, H. Isago, A. Elmarakbi, H. Yamaguchi, Axially oriented tubercle vein and X-crossed sheet of N-Co_3O_4@C hierarchical mesoarchitectures as potential heterogeneous catalysts for methanol oxidation reaction, Chem. Eng. J. 313 (2017) 83–98. doi:10.1016/j.cej.2016.12.003.

[35] N. Akhtar, S. A. El-Safty, M. Khairy, W.A. El-Said, Fabrication of a highly selective nonenzymatic amperometric sensor for hydrogen peroxide based on nickel foam/cytochrome

c modified electrode, Sens. Actuators B Chem., 207 (2015) 158-166. https://doi.org/10.1016/j.snb.2014.10.038

[36] D. Hassen, M.A. Shenashen, S.A. El-Safty, M.M. Selim, H. Isago, A. Elmarakbi, A. El-Safty, H. Yamaguchi, Nitrogen-doped carbon-embedded TiO_2 nanofibers as promising oxygen reduction reaction electrocatalysts, J. Power Sources. 330 (2016) 292–303. doi:10.1016/j.jpowsour.2016.08.140.

[37] C. Sun, S. Rajasekhara, J.B. Goodenough, F. Zhou, Monodisperse porous $LiFePO_4$ microspheres for a high power Li-ion battery cathode, J. Am. Chem. Soc. 133 (2011) 2132–2135. doi:10.1021/ja1110464.

[38] F. Wang, X. Wang, Z. Chang, Y. Zhu, L. Fu, X. Liu, Y. Wu, Electrode materials with tailored facets for electrochemical energy storage, Nanoscale Horizons. 1 (2016) 272–289. doi:10.1039/c5nh00116a.

[39] B. Guo, H. Ruan, C. Zheng, H. Fei, M. Wei, Hierarchical $LiFePO_4$ with a controllable growth of the (010) facet for lithium-ion batteries, Sci. Rep. 3 (2013). doi:10.1038/srep02788.

[40] X.L. Wu, L.Y. Jiang, F.F. Cao, Y.G. Guo, L.J. Wan, $LiFePO_4$ nanoparticles embedded in a nanoporous carbon matrix: Superior cathode material for electrochemical energy-storage devices, Adv. Mater. 21 (2009) 2710–2714. doi:10.1002/adma.200802998.

[41] W. Warkocki, S.A. El-Safty, M.A. Shenashen, E. Elshehy, H. Yamaguchi, N. Akhtar, Photo-induced recovery, optical detection, and separation of noxious SeO_3^{2-} using a mesoporous nanotube hybrid membrane, J. Mater. Chem. A, 3 (2015) 17578-17589, DOI:10.1039/C5TA02827B.

[42] H. Gomaa, H. Khalifa, M. Selim, M. A. Shenashen, S. Kawada, A.S. Alamoudi, A. Azzam, A. Alhamid, Selective, photo-enhanced trapping/detrapping of arsenate anions using mesoporous blobfish head TiO_2 monoliths, ACS Sustainable Chemistry & Engineering, 5 (11) (2017)

10826–10839. DOI: 10.1021/acssuschemeng.7b02766.

[43] M. Khairy, S. A. El Safty, Mesoporous NiO nanoarchitectures for electrochemical energy storage: influence of size, porosity, and morphology, RSC Adv., 3 (2013) 23801-23809. DOI: 10.1039/C3RA44465A

[44] M. Khairy, S. A. El Safty, Promising supercapacitor electrodes based immobilization of proteins onto macroporous Ni foam materials, J. Energy Chem., 24 (1) (2015) 31-38. https://doi.org/10.1016/S2095-4956(15)60281-9

[45] M. Khairy, S. A. El Safty, Nanosized rambutan-like nickel oxides as electrochemical sensor and pseudocapacitor, Sens. Actuators B Chem., 193 (2014) 644-652 https://doi.org/10.1016/j.snb.2013.11.113

[46] D Hassen, S. A. El-Safty, K Tsuchiya, A Chatterjee, A Elmarakbi, M A Shenashen, M Sakai, Longitudinal Hierarchy Co_3O_4 Mesocrystals with High-dense Exposure Facets and Anisotropic Interfaces for Direct-Ethanol Fuel Cells, Sci. Rep., 6 (2016) 24330. doi: 10.1038/srep24330

[47] J. Zhang, J. Lu, D. Bian, Z. Yang, Q. Wu, W. Zhang, Solvothermal synthesis of hierarchical $LiFePO_4$ microplates with exposed (010) faces as cathode materials for lithium ion batteries, Ind. Eng. Chem. Res. 53 (2014) 12209–12215. doi:10.1021/ie501743b.

[48] Z. Jiang, Z.J. Jiang, Effects of carbon content on the electrochemical performance of $LiFePO_4$/C core/shell nanocomposites fabricated using $FePO_4$/polyaniline as an iron source, J. Alloys Compd. 537 (2012) 308–317. doi:10.1016/j.jallcom.2012.05.066.

[49] G. Qin, S. Xue, Q. Ma, C. Wang, The morphology controlled synthesis of 3D networking $LiFePO_4$ with multiwalled-carbon nanotubes for Li-ion batteries, CrystEngComm. 16 (2014) 260–269. doi:10.1039/c3ce41967c.

[50] M.Y. Emran, M.A. Shenashen, A.A. Abdelwahab, H. Khalifa, M. Mekawy, N. Akhtar, M.

Abdelmottaleb, S.A. El-Safty, Design of hierarchical electrocatalytic mediator for one step, selective screening of biomolecules in biological fluid samples, J. Appl. Electrochem. 48 (2018) 529–542. doi:10.1007/s10800-018-1175-5.

[51] W. Zhang, X. Zhou, X. Tao, H. Huang, Y. Gan, C. Wang, In situ construction of carbon nano-interconnects between the $LiFePO_4$ grains using ultra low-cost asphalt, Electrochim. Acta. 55 (2010) 2592–2596. doi:10.1016/j.electacta.2009.11.072.

Figure Captions:

Scheme 1 (A) 3D simulated projection of uniformly-shaped, super-architectonic GPS lithium ion batteries that built-in ordered set of bundled layers of pouch models. Large-scale GPS-LIBs module configurations can be fabricated through unit-to-unit packing of the multiple rolls of GPS-LIB CR2032 coin-cells into fashionable assembly collars with maintaining safety betterment parameters and high power density of rechargeable GPS-LIBs for electric vehicles (EVs). (B, C) The complex N- and P-electrode super-architectonics of of MSTO@C GPS-anode and LMPO@C GPS-cathodes, including SSF@C, CSN@C, and NR@C geometrics and surface topographies, respectively. The unique and novel architectonic geometrics are built with multi-scale building-blocks egress/ingress pathways, and effective super surface topographies in terms of its heterogeneity, roughness and anisotropy (B and C).

Scheme 2: (Top) A set of multi-axial systems along three–directional dimensions overlying along sides and faces in dense upward layers of GPS SSF@C super-architectonics. 3D objects of GPS SSF@C cathode recorded along with vertical, lateral and longitudinal axes, and upper-top-capped pyramidal prisms. **(Bottom)** The integral arrangement and orientation of axially-edge sheets CSN@C that organized and spreading to central axis. The GPS-CSN@C complex super-architectonics concentrically connected to the center feed points of main core axis. The GPS-orientation arrangement of hybrid SSF@C complex super-architectonics enabled in-out-plane of upper zone surface, a dynamic space environment and seamless transition of vacant channels and tunnels as promising candidates to optimize high-power GPS-LIBs.

Fig.1 FE-SEM, EDX-elemental mapping analysis, HR-TEM, and electron diffraction profiles of super-architectonics (GPS) LMPO@C-cathodes, including three variable geometrics solanum star-

shaped flower (SSF@C), mesocave nanorods (NRs@C), and axially edged stack sheets (CSN@C) that organized in multi-scale geometrics and super surface topographies. **(a-c)** Top- and (d & e) side-view FE-SEM patterns of SSF@C GPS cathode. (f) Energy-dispersive X-ray spectroscopy (EDX) and elemental mapping analysis (mass ratios) of SSF@C GPS-cathode of O (56.6%), Mn (21.8%), P (17.3%), C (4.3%), respectively. **(g)** Top- and **(h)** side-view FE-SEM patterns of CSN@C and NR@C GPS-cathodes; respectively. **(i)** Low magnification HR-TEM micrographs of SSF@C geometrics. **(j)** High magnification HR-TEM of lattice pattern at the edge with 4-6 nm clear thin layer C-coating on surface of SSF crystals. **(k)** Selected area electron diffraction (SAED) pattern image of SSF@C GPS-cathode with incident beam along the [010] crystallographic direction indicating the formation of orthorhombic olivine SSF@C crystals.

Fig. 2 (a, b and c) Top-view FE-SEM patterns of MSTO@C GPS anode surface topographies. **(d)** Energy-dispersive X-ray spectroscopy (EDX) and elemental mapping analysis of top-view surfaces of MSTO@C anode geometrics. The elemental mapping of MSTO@CGPS-anode designed with well-dispersed C-shell like layers along MSTO surface with percentage ratio of 64.4:34.2:2.4% corresponding to O: Ti: C elements, respectively. **(e)** HR-TEM micrographs for MSTO@C pattern at lattice-edge showing a clear 3~4 nm C-shell layers along the surfaces of MSTO super-architectonics. **(f-insert)** The ED o image of MSTO@C geometrics.

Fig. 3 (a) XRD patterns of LMPO@C-cathodes including SSF@C, CSN@C, and NR@C architectonic geometrics. **(b)** Olivine-like crystal structure at direction [010] for possible lithium pathways. (C) A model of GPS super-architectonic SSF@C, CSN@C and NR@C cathode orientation and super surface topographies.

Fig. 4 (a,b and c) Cyclic voltammogram (CV) of the electrochemical performance on the super-architectonic LMPO@C composites. **(a)** CV curves of LMPO@C-cathodes including SSF@C, CSN@C, and NR@C architectonic geometrics. **(b)** CV curves of SSF@C half-cell GPS-cathode at different sweep rate (0.1, 0.2, 0.5, 1.0 and 5.0 mVs^{-1}, and **(c)** CV curves of SSF@C half-cell cathode at different cycle numbers from 1^{st} cycle to 500 cycles at 0.1 mVs^{-1}. **(d)** First discharge capacity of half-cell SSF@C, CSN@C and NR@C GPS-cathodes at a current rate 0.1C- to-20C of half-cell LIBs. All electrochemical measurements for half-cell LMPO@C GPS-cathodes are operated within voltage range of 2.0–to 4.3 V, at 25ºC.

Fig. 5 (a-c) Effect of variable super-architectonic GPS-model cathode geometrics and super topographic-surfaces, C-rates ranged from 0.1C to 20C, and cycling behavior on the charging/discharging voltage patterns. **(a)** The charging/discharging voltage patterns of first cycle half-cell of SSF@C, CSN@C and NR@C GPS-cathode LIBs using CR2032-coin cell, at current rate 0.1C. **(b)** First cycle half-cell SSF@C GPS-cathode at different current rate from 0.1C to 20C. **(c)** Charge/discharge curves for SSF@C GPS-cathode as half-cell at a current rate 1.0C, at different cycle numbers up to 500 cycles. **(d)** Cycling performance stability of SSF@C, CSN@C and NR@C GPS-cathodes, at rate of 1C for 100 cycles. All super-architectonic GPS-modulated LIB measurements are operated at 25ºC.

Fig. 6 (a) Capability performance rates over a range from 2.0– to 4.3V among different complex super-architectonics with SSF@C, CSN@C and NR@C GPS-cathode geometrics and super topographic-surfaces at various current rates from 0.1C to 20C. **(b)** The electrochemical impedance spectroscopy (EIS) results of SSF@C, CSN@C and NR@C GPS-cathode geometrics and super topographic-surfaces. Inset of (b) is the equivalent circuit diagram agreement with the impedance

results of the EIS profiles. **(c)** Temperature-dependence graph of the electrical conductivity of complex super-architectonics for half-cell GPS-cathode geometrics and super topographic-surfaces. All samples exhibit good conductivity, particularly SSF@C GPS-cathode along tested temperature range (≃approximately 250 to 455K). All super-architectonic GPS-modulated LIB measurements are operated at 25^{o}C.

Fig. 7(a) Cycling performance of powerful complex super-architectonic full-scale SSF@C GPS-cathode // MSTO@C GPS-anode LIB-modulated LIB models for first 100 cycles. **(b)** Behavior of specific discharge capacity in $mAhg^{-1}$ versus current C-rates at 0.1C, 0.2C, 0.5C, 1C, 2C, 5C, 10C and 20C, in potential region from 1.5 to 3.8V vs. Li/Li^{+} for SSF@C//MSTO@C full-scale LIB-model. **(c)** Performance and behavior of the rate capability of SSF@C GPS-cathode // MSTO@C GPS-anode LIB-modulated LIB models over a range from 1.5 to 3.8V at various current rates from 0.1C to 20C. **(d)** Long term cycling performance (stability) and coulombic efficacy for SSF@C GPS-cathode // MSTO@C GPS-anode LIB-modulated LIB models, at rate of 1C up to 2000 cycles, in a voltage range from 1.5 to 3.8V at 25^{o}C. The magnification of first 200 cycles is exhibited in **Fig. 7(e)**.

Scheme 3 (A) Systematic representation of long-term lithiation/delithiation (discharge/charge) cycling process. 3D projection of stable, multi-scale super-architectonic (MSTO@C) GPS-anode and (CSN@C) GPS-cathode for high rate capability of Li^{+} ion power batteries after multiple cycles. **(B)** Feasible electron/ Li^{+} ion diffusion pathways along possible direction of multi-scale geometrics, as shown in 3D drawing projections of super-architectonic GPS-cathode/anode super topographic-surfaces. **(B-left)** A representative 3D design GPS-cathode geometries of solanum star-shaped flowers that have multi-branchlet nanorods spreading out from central core to lateral and axial directions SSF@C GPS-cathode, **(B-center)** axially-edged plate sheets stacked circularly around

central axis and concentrically formed a cylinder sphere-hole-like cage nest (CSN@C GPS-cathode, and **(B-right)** open-top mesopore nanorods of NRs-GPS cathode.

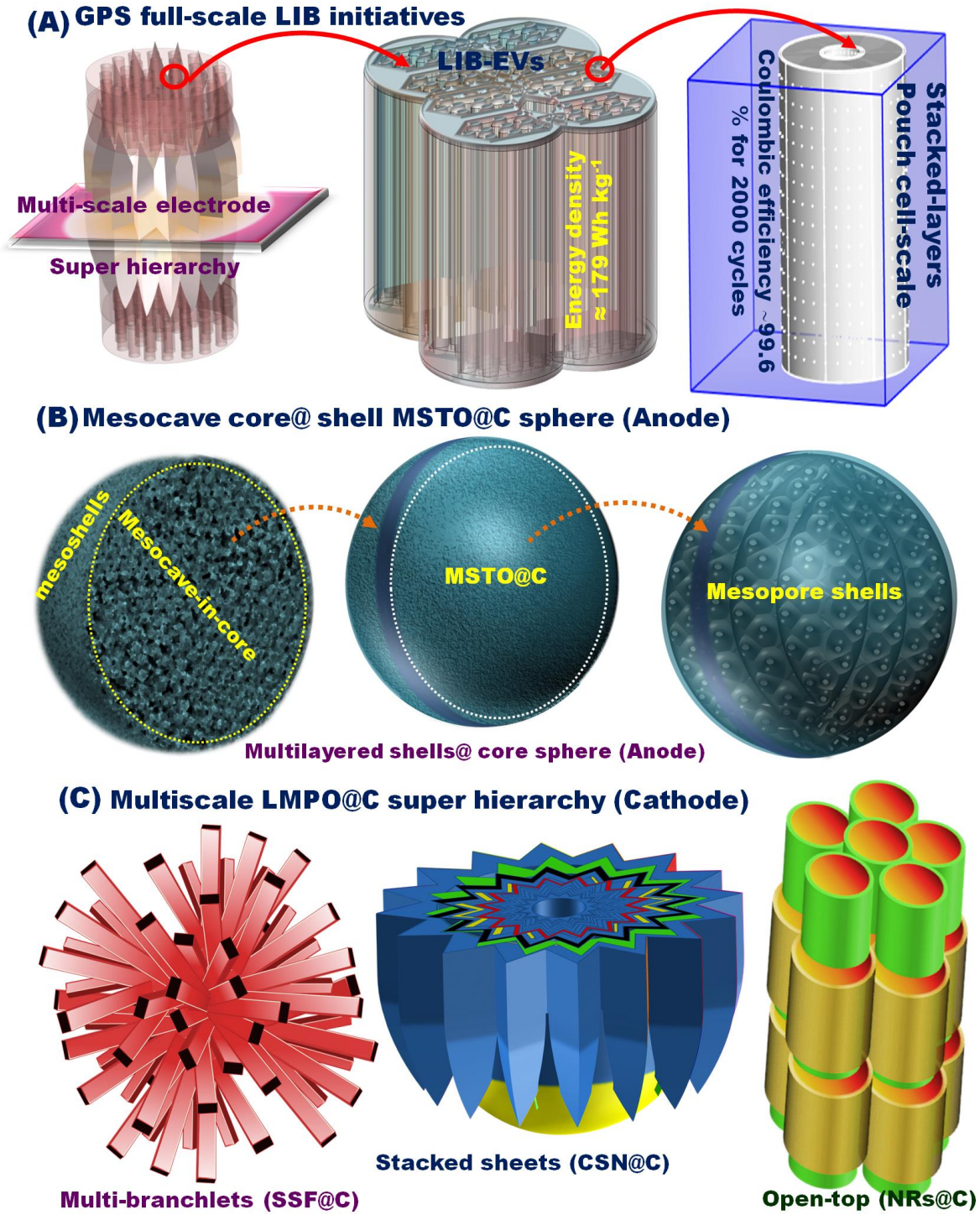
(A) GPS full-scale LIB initiatives
Multi-scale electrode
Super hierarchy
LIB-EVs
Energy density ≈ 179 Wh kg-1
Coulombic efficiency ~99.6 % for 2000 cycles
Stacked-layers Pouch cell-scale
(B) Mesocave core@ shell MSTO@C sphere (Anode)
mesoshells
Mesocave-in-core
MSTO@C
Mesopore shells
Multilayered shells@ core sphere (Anode)
(C) Multiscale LMPO@C super hierarchy (Cathode)
Multi-branchlets (SSF@C)
Stacked sheets (CSN@C)
Open-top (NRs@C)

Scheme 1

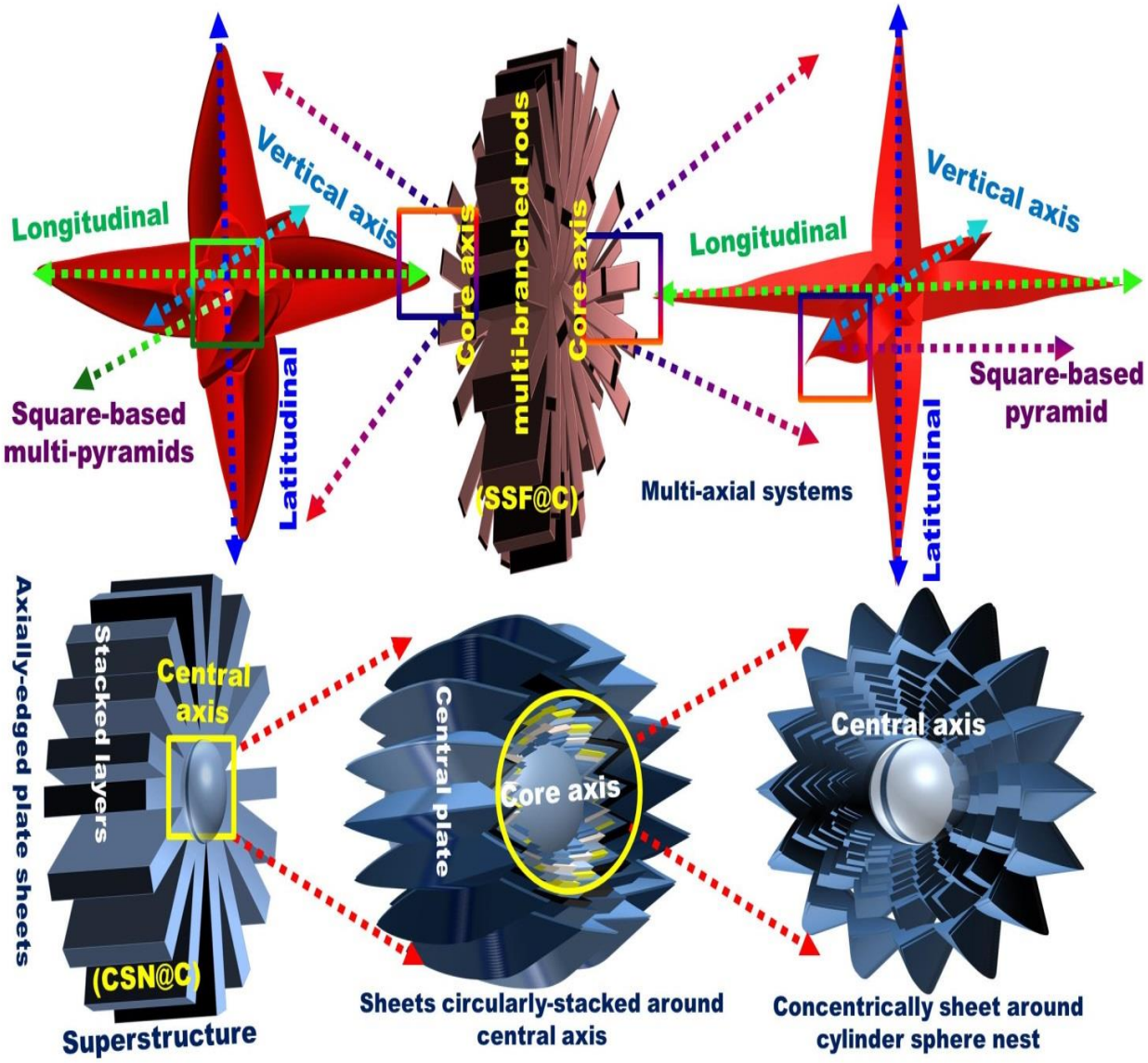
Longitudinal
Vertical axis
Square-based multi-pyramids
Latitudinal
Core axis
multi-branched rods
Core axis
(SSF@C)
Multi-axial systems
Longitudinal
Vertical axis
Square-based pyramid
Latitudinal
Axially-edged plate sheets
Stacked layers
Central axis
(CSN@C)
Superstructure
Central plate
Core axis
Sheets circularly-stacked around central axis
Central axis
Concentrically sheet around cylinder sphere nest

Scheme 2

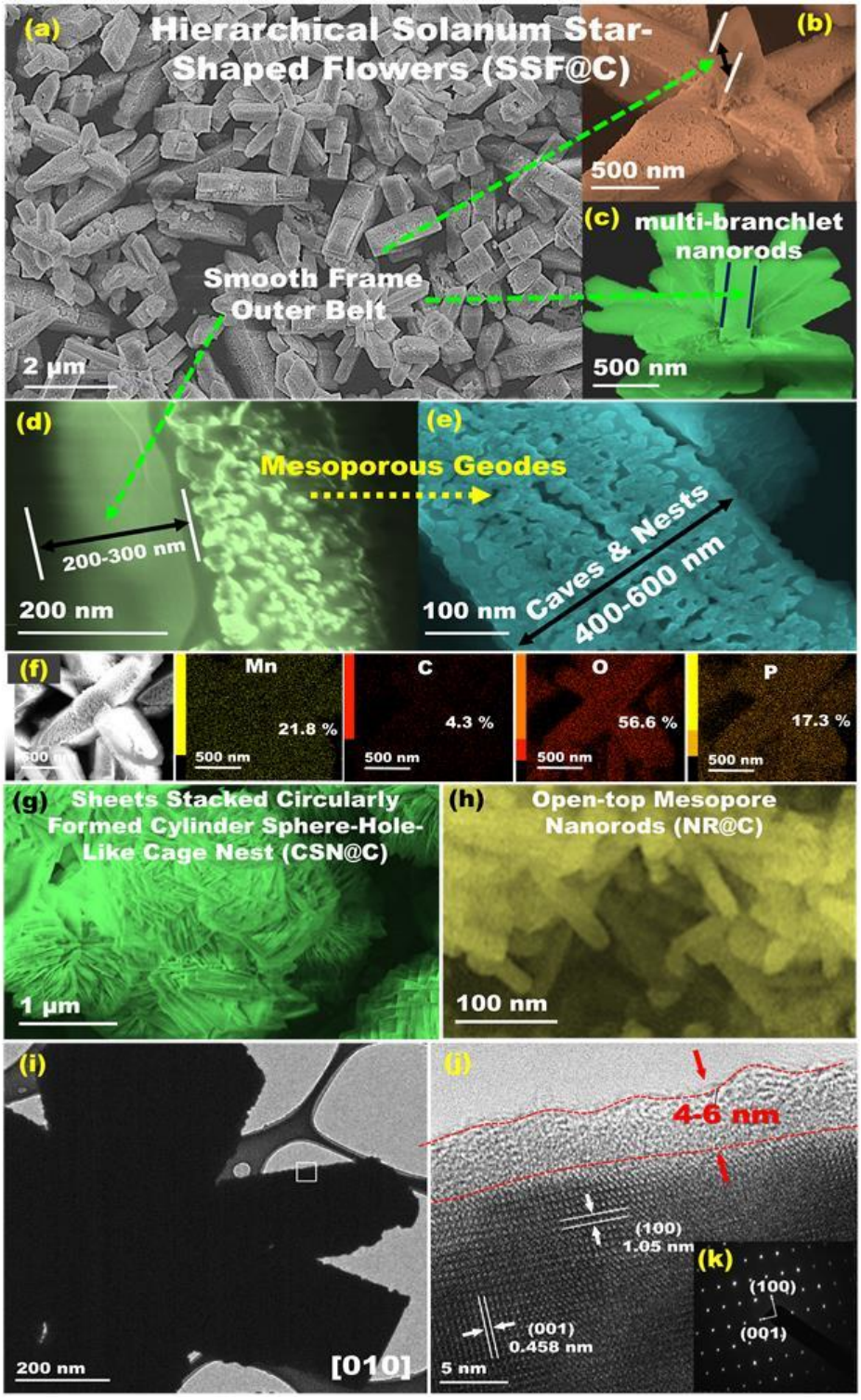
(a)
Hierarchical Solanum Star-Shaped Flowers (SSF@C)
(b)
500 nm
(c) multi-branchlet nanorods
500 nm
Smooth Frame Outer Belt
2 μm
(d)
Mesoporous Geodes
200-300 nm
200 nm
(e)
100 nm
Caves & Nests
400-600 nm
(f)
Mn
21.8 %
C
4.3 %
O
56.6 %
P
17.3 %
500 nm
(g) Sheets Stacked Circularly Formed Cylinder Sphere-Hole-Like Cage Nest (CSN@C)
1 μm
(h) Open-top Mesopore Nanorods (NR@C)
100 nm
(i)
200 nm
[010]
(j)
4-6 nm
(100)
1.05 nm
(001)
0.458 nm
5 nm
(k)
(100)
(001)

Fig.1

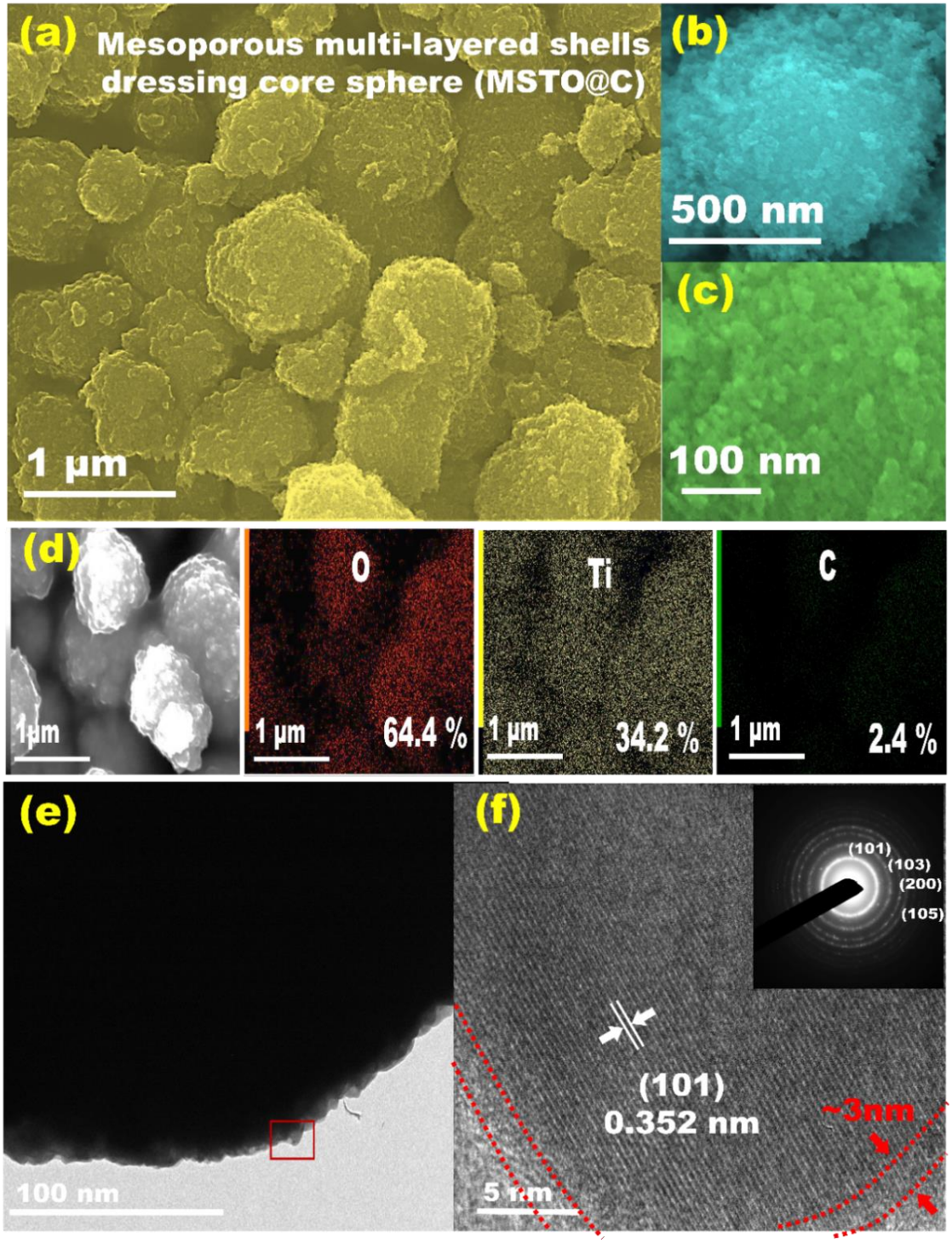
(a)
Mesoporous multi-layered shells dressing core sphere (MSTO@C)
1 μm
(b)
500 nm
(c)
100 nm
(d)
1μm
O
1 μm
64.4 %
Ti
1 μm
34.2 %
C
1 μm
2.4 %
(e)
100 nm
(f)
(101)
(103)
(200)
(105)
(101)
0.352 nm
~3nm
5 nm

Fig.2

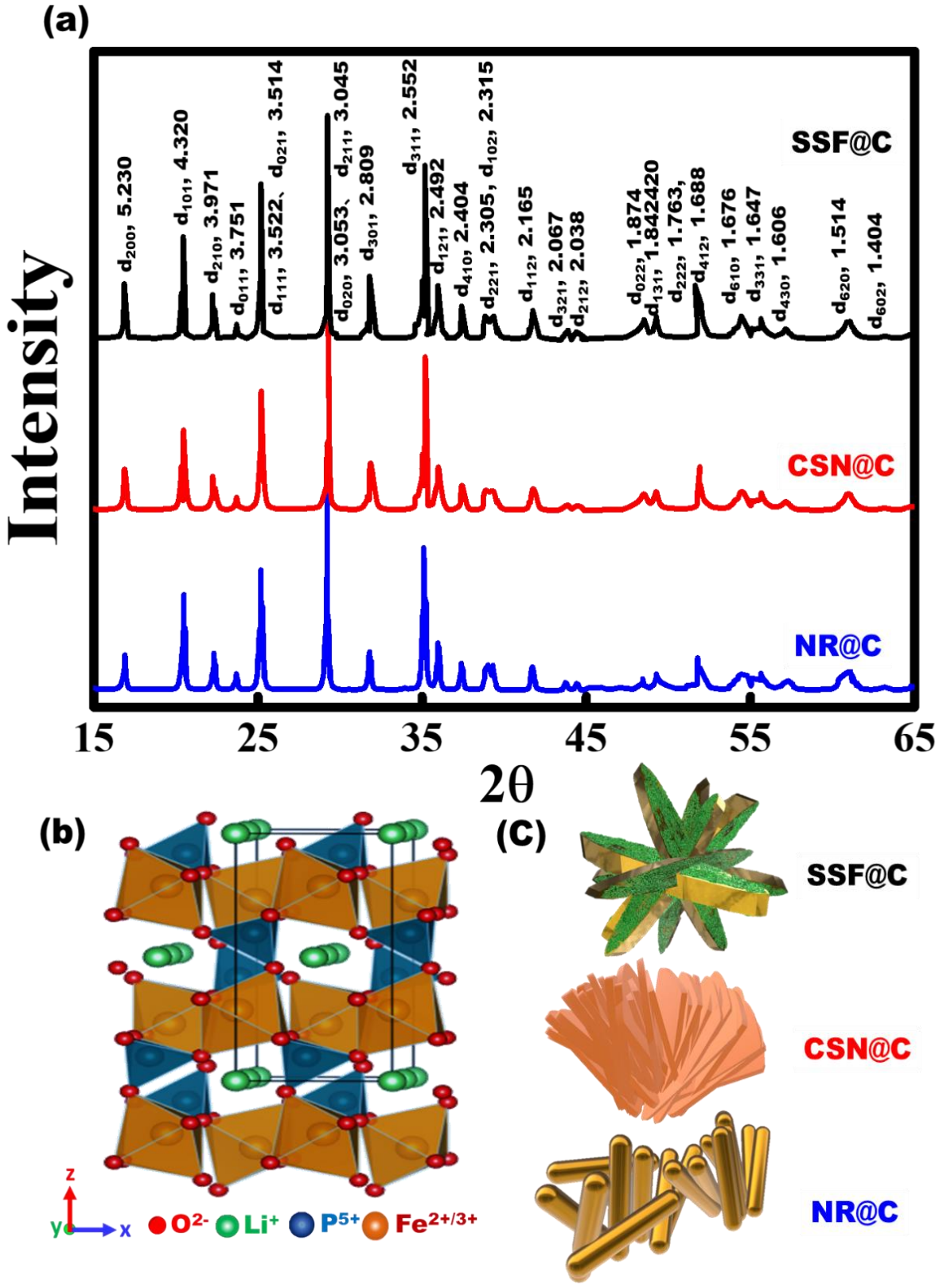
(a)
Intensity
SSF@C
CSN@C
NR@C
15
25
35
45
55
65
2θ
(b)
(C)
z
y
x
O2-
Li+
P5+
Fe2+/3+
SSF@C
CSN@C
NR@C

Fig. 3

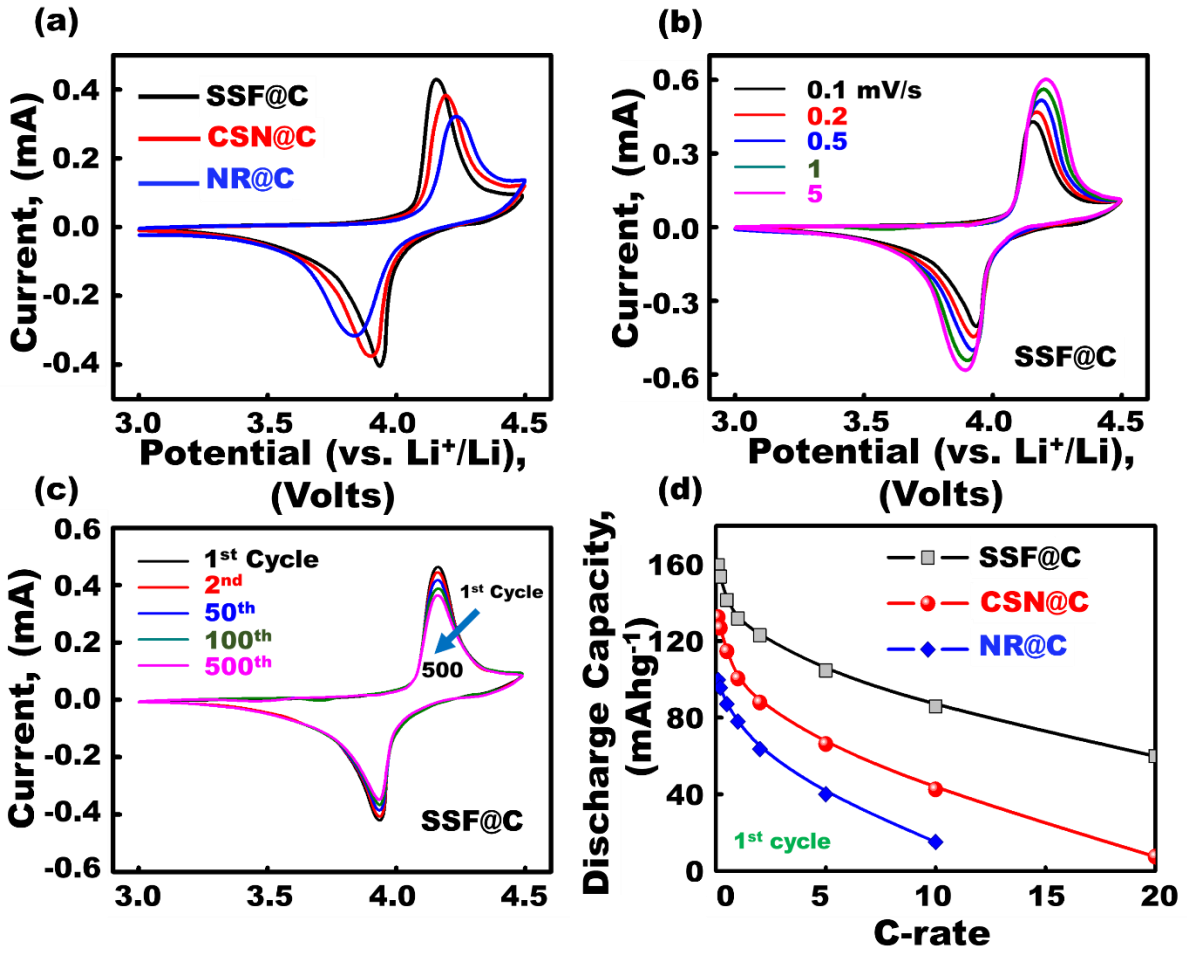
(a)
SSF@C
CSN@C
NR@C
Current, (mA)
Potential (vs. Li+/Li), (Volts)
(b)
0.1 mV/s
0.2
0.5
1
5
SSF@C
Current, (mA)
Potential (vs. Li+/Li), (Volts)
(c)
1st Cycle
2nd
50th
100th
500th
1st Cycle
500
SSF@C
Current, (mA)
(d)
SSF@C
CSN@C
NR@C
1st cycle
Discharge Capacity, (mAhg-1)
C-rate

Fig. 4

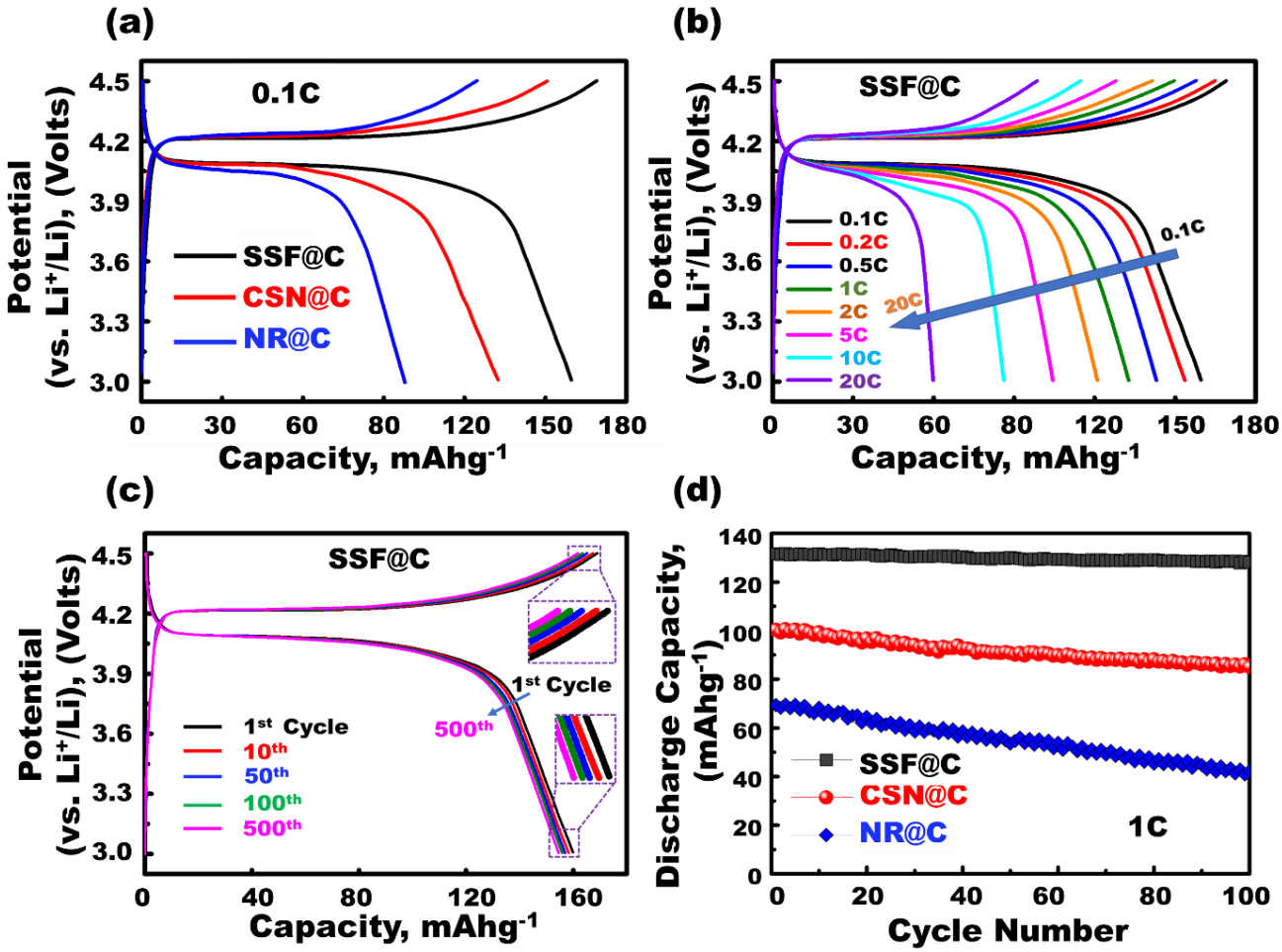
(a)
0.1C
SSF@C
CSN@C
NR@C
Potential (vs. Li+/Li), (Volts)
Capacity, mAhg-1
(b)
SSF@C
0.1C
0.2C
0.5C
1C
2C
5C
10C
20C
0.1C
20C
Potential (vs. Li+/Li), (Volts)
Capacity, mAhg-1
(c)
SSF@C
1st Cycle
10th
50th
100th
500th
1st Cycle
500th
Potential (vs. Li+/Li), (Volts)
Capacity, mAhg-1
(d)
SSF@C
CSN@C
NR@C
1C
Discharge Capacity, (mAhg-1)
Cycle Number

Fig. 5

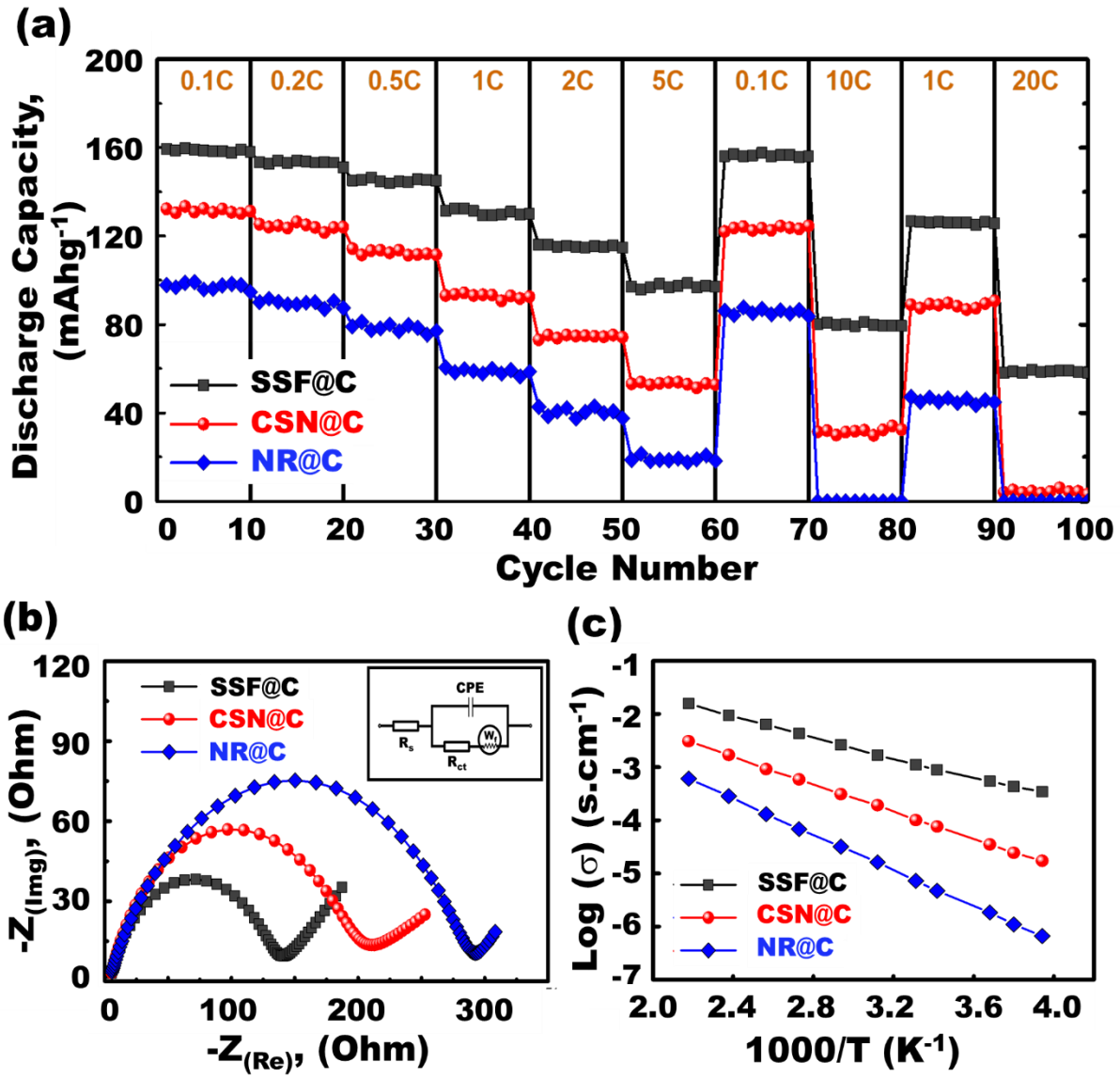
(a)
0.1C
0.2C
0.5C
1C
2C
5C
0.1C
10C
1C
20C
SSF@C
CSN@C
NR@C
Discharge Capacity, (mAhg-1)
Cycle Number
(b)
SSF@C
CSN@C
NR@C
CPE
Rs
Rct
W1
-Z(Img), (Ohm)
-Z(Re), (Ohm)
(c)
SSF@C
CSN@C
NR@C
Log (σ) (s.cm-1)
1000/T (K-1)

Fig. 6

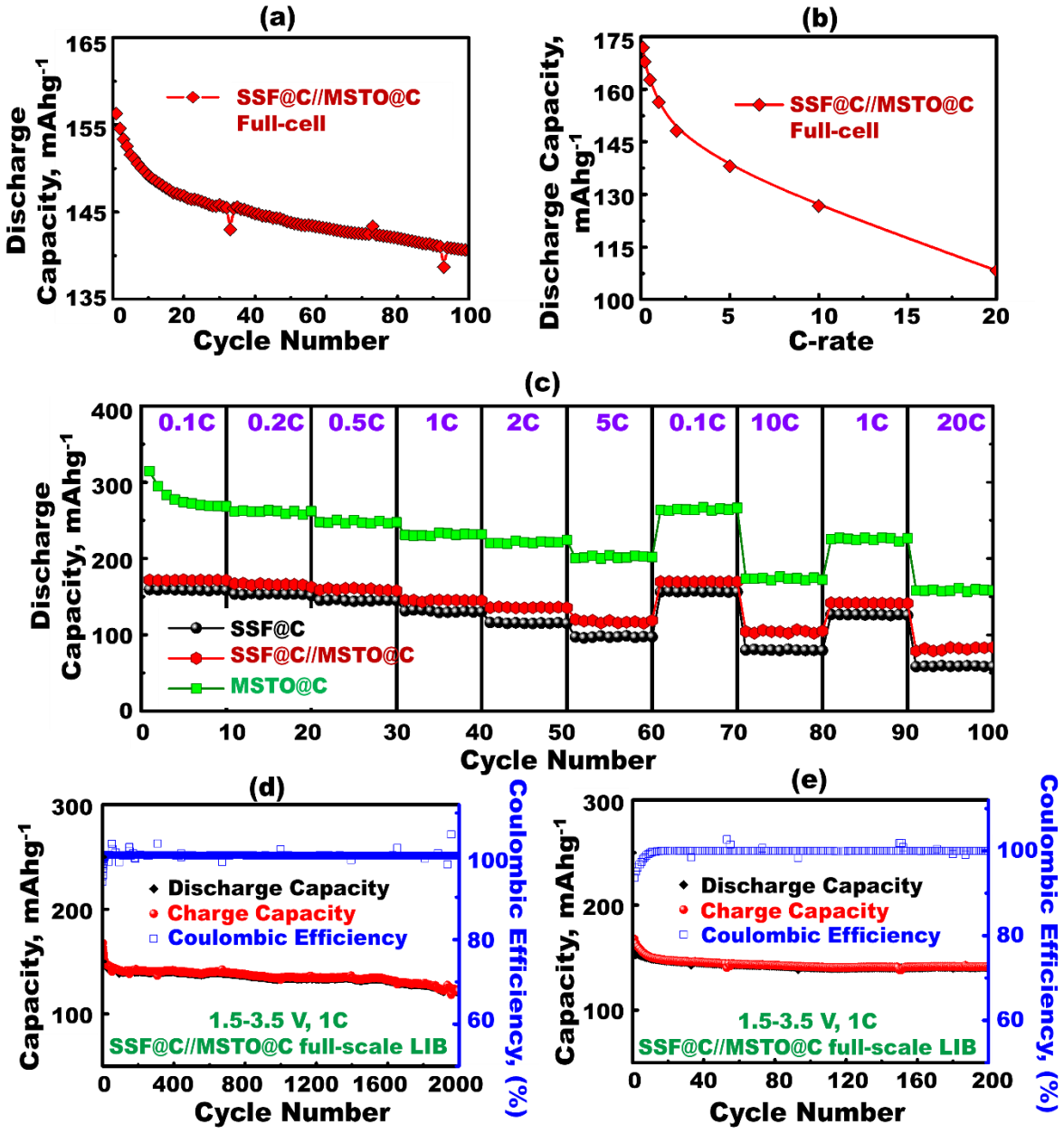
(a)
Discharge Capacity, mAhg-1
Cycle Number
SSF@C//MSTO@C
Full-cell
(b)
Discharge Capacity, mAhg-1
C-rate
SSF@C//MSTO@C
Full-cell
(c)
Discharge Capacity, mAhg-1
Cycle Number
0.1C
0.2C
0.5C
1C
2C
5C
0.1C
10C
1C
20C
SSF@C
SSF@C//MSTO@C
MSTO@C
(d)
Capacity, mAhg-1
Coulombic Efficiency, (%)
Cycle Number
Discharge Capacity
Charge Capacity
Coulombic Efficiency
1.5-3.5 V, 1C
SSF@C//MSTO@C full-scale LIB
(e)
Capacity, mAhg-1
Coulombic Efficiency, (%)
Cycle Number
Discharge Capacity
Charge Capacity
Coulombic Efficiency
1.5-3.5 V, 1C
SSF@C//MSTO@C full-scale LIB

Fig. 7

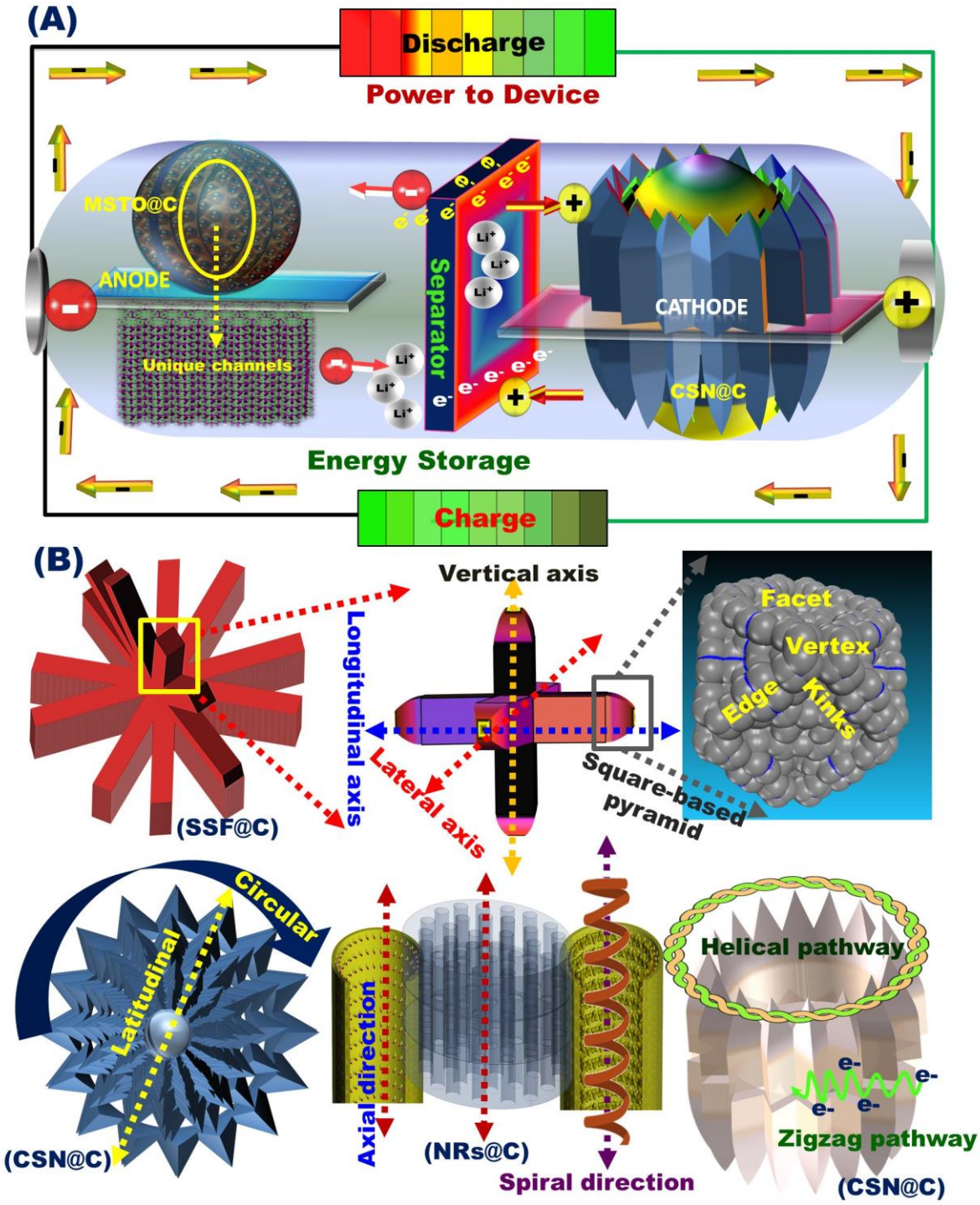
(A)
Discharge
Power to Device
MSTO@C
ANODE
Unique channels
Separator
CATHODE
CSN@C
Energy Storage
Charge
(B)
Vertical axis
Longitudinal axis
Lateral axis
(SSF@C)
Facet
Vertex
Edge
Kinks
Square-based pyramid
Circular
Latitudinal
(CSN@C)
Axial direction
(NRs@C)
Spiral direction
Helical pathway
Zigzag pathway
(CSN@C)

Scheme 3

- **Declaration of competing interests policy**

The authors declare that they have no competing interests that might be perceived to influence the results and/or discussion reported in this paper.

- **Declaration of competing financial interests**

The authors declare that they have no known competing financial interests or personal relationships that could have appeared to influence the work reported in this paper.